Past oxygen minimum zone in the Bay of Bengal reconstruction from sedimentary particulate manganese: Implications to productivity variability

A Thesis submitted to Goa University for the Award of the Degree of

DOCTOR OF PHILOSOPHY

In

Marine Sciences

By

Sarathchandraprasad. T

Under the guidance of

Dr. Virupaxa Banakar

Goa University
Taleigao, Goa
2019

DEDICATED TO
MY PARENTS AND TEACHERS

STATEMENT OF CANDIDATE

As required under the University ordinance OB-9.9 (v-vi), I state that the present thesis entitled "***Past oxygen minimum zone in the Bay of Bengal reconstruction from sedimentary particulate manganese: Implications to productivity variability*****"** is original contribution and the same has not been submitted on any previous occasion. To the best of my knowledge, the present study is the first of its kind for the area mentioned. The literature related for the study has been clearly cited. Due acknowledgements have been made as required.

Place: Vasco Da Gama
Date: 18th June 2019

Sarathchandraprasad T

Project Scientist-B,
National Center for Polar and Ocean Research,
Head land Sada,
Vasco Da Gama.

CERTIFICATE OF GUIDE

This is to certify that the thesis entitled "***Past oxygen minimum zone in the Bay of Bengal reconstruction from sedimentary particulate manganese: Implications to productivity variability*",** submitted by **Mr. Sarathchandraprasad T** for the award of the degree of Doctor of Philosophy in the department of Marine Sciences, GU, is based on his original studies carried out by him under my supervision. The thesis or any part thereof has not been previously submitted for any other degree or diploma in any university or institution.

Place: Dona Paula

Date: Date: 18th June 2019

Dr. Virupaxa K. Banakar

Chief Scientist (retired)

Zeib Castle, La Oceana
Beside International Centre,
Dona Paula, 403 004

ACKNOWLEDGEMENTS

First of all, I wish to thank the National Institute of Oceanography for providing me an opportunity and for extending all analytical facility to work for the thesis while I was working as a project assistant under Cobalt Crust Project funded by the Ministry of Earth Sciences. The support of the Director, Dr. S. R. Shetye, to students at NIO are highly appreciated and acknowledged.

I am grateful to Dr. Virupaxa Banakar, for introducing me to this fascinating research subject and guiding me. From the beginning of the work, his guidance is the source of inspiration and thought evoking. His own zeal for perfection, unflinching courage and integrity always inspired me to challenge any situation. I thank Dr. B N Nath, FRC Member, for his continuous and constructive suggestions for this research and also for providing sediment cores for this study. I extend my gratitude to Co-Guide- Prof. H.B Menon for supporting me throughout. I thank other FRC Members Prof. Rivonkar and Prof. Janarthanam for providing their valuable time to evaluate my progress and for making productive comments and suggestions. I would like to thank Mr. Naik and Mrs. Johnina- the office staffs of the Marine Science Department, GU for administrative assistance. Mr. Krishnakumar, HRD-NIO, helped me to fulfill administrative requirements at NIO.

I express my thanks Mrs. Anita Garg, and Dr. Parthiban who helped me to generate the data for the present study. Dr. Alex Piotrowski of Cambridge University helped me to obtain radiocarbon and oxygen isotope measurements of one sediment core from the Arizona University and Cambridge University respectively.

I am also thankful to my colleagues Drs. Mahesh, Swetha, Rosaline, Puja, Sneha, Govind, and Rajasree who were working with my guide for making my working environment pleasant.

I am thankful to Dr. Yatheesh who offered his friendly support and Dr. Akhil, Arindam Sarkar, Prajith, Tyson Linsy, Vijith, Haris, Charles, and Kartik for discussions.

I am very grateful to Drs. Renjith, Glejin, Bajish, Nidheesh, Suhail, Vipin, Nikhil, Subeesh, Seemanth, Rajeev, Rao, George, Robin, Elaine, Remya, Dr. Vivek, Sreejith, Zakaria, Ajmal, Jishad, John, Anzal, Ajay, Binson and Rev. Fr. Tony for rendering unconditional support during my doctoral work.

Last but not least, the love and blessing of my Late Father, Mother, Brother Bhagath, my wife Deepa and my daughter Madhuparna gave me required energy to accomplish this work. Finally, I thank *Almighty* for providing me what I deserved.

SARATHCHANDRAPRASAD T

CONTENTS

LIST OF TABLES

LIST OF FIGURES

PREFACE

The earth system has been undergoing exceptionally rhythmic climatic changes since beginning of the Pleistocene (2.6 Ma) in the form of alternating cold-dry glacial and warm-wet interglacials. These climatic cycles have been shown to have profound impact on the Indian monsoon system and in turn the properties of the upper water column of the northern Indian Ocean (NIO). The biogeochemical changes in the NIO are associated with the monsoon variability. One of the upper water column characteristics of NIO is existence of a perennial Oxygen Minimum Zone (OMZ), i.e. the subsurface zone where the dissolved Oxygen (DO) concentration is the least.

The factors responsible for the formation and sustainment of OMZ are primary productivity, ventilation at thermocline depth, and mixed layer dynamics. The ventilation at OMZ depth in NIO is largely comprises of a mixture of Persian Gulf Water (PGW), Red Sea Water (RSW) and Subantarctic Mode Water (SMW). These water masses remain unchanged through the Holocene. Secondly, the deepening of the mixed layer depth due to turbulent wind-forced mixing during the summer monsoons is expected to weaken the OMZ. The modern OMZ in NIO is primarily governed by primary productivity, as the sources of ventilated waters remain constant throughout the year. However, the glacial-interglacial OMZ changes cannot be expected to be forced only by the productivity alone, because, the water masses ventilating the OMZ have also changed. The ventilation changes are mainly due to significantly decreased sill-depth at the outflow of PGW and RSW waters in to the NIO during the glacial time.

In general the Arabian Sea OMZ is more intense (<10 µM of DO) between ~200 and 700 depth than the BoB-OMZ (> 10-15 µMol). A seasonal contrast in the dynamics of OMZ in these two basins has also been observed. During March to August (spring-summer) the core of Arabian Sea OMZ thickens by ~150 m, while the BoB-OMZ thins by ~70 m. On the other hand, during September to February (fall-winter) the thicknesses of the cores of both OMZs remain nearly unchanged at ~700 m in Arabian Sea and at ~400 m in BoB. The BoB-OMZ appears to have significantly deeper organic matter reminerlization depth unlike the Arabian Sea hence has distinct control on the OMZ.

A recent study suggested that the BoB-OMZ has reached a tipping point. However, evidences for presence of PGW in its core, extensive eddy mixing in BoB and unlikely de-oxygenation of the interior of BoB even after 2100 AD, together argue against the suggested ‘tipping point’ or its further intensification. Although, it is known that the OMZ in the NIO has shown dramatic variation from the LGM to Holocene, it is not clearly known yet whether the BoB-OMZ in the Holocene (present warm period) has remained as observed today or it has changed. Such information may be of necessity for developing predictive models. The natural variation of OMZ in absence of anthropogenic forcing can be obtained from reconstruction of the past OMZ by extracting appropriate redox-sensitive element

signals buried in the sediments. Therefore, my doctoral research aims to reconstruct the past OMZ of the BoB. The objectives for the present study are: a) To understand the OMZ variation during the LGM and Holocene Periods in the waters of the eastern continental margin of India, and b) To assess the possible contributing factors such as productivity, ventilation and detritus input to its variation, which are largely connected to the summer monsoon intensity.

Reconstruction of changes in the dimension of OMZ through glacial-interglacial times is of palaeoclimatic significance, because the intensity and depth of OMZ may have varied in accordance with the interglacial (warm) and glacial (cold) climates as a result of concurrent monsoon variability. The expansion of the Arabian Sea OMZ was shown to have extended beyond the Equator at around Miocene-Pliocene Boundary apparently associating with extremely high productivity. The last 250 kyr OMZ reconstructions for the NIO have indicated that there have been times with weakest or non-existent OMZ coinciding with lowest productivity, while the intensified OMZ was found associated with periods of high productivity. These palaeo-productivity studies demonstrate a potential link between OMZ and palaeo-monsoons via the productivity.

The redox sensitive elements such as Mn, Co etc. in the sediments having multiple oxidation states in solution and solids are promising proxies for tracking changes in the DO of palaeo-oceans through sediment repository. If the oxygen demand by settling organic matter overwhelms the oxygen supply in intermediate waters then the secondary oxidants in underlying sediments such as Mn-oxides and -oxyhydroxides (MnOx) are utilized as source of oxygen for the decay of organic matter. It means, the oxic-suboxic boundary condition seems to define the Mn- oxidation and reduction boundary in the oceanic water. Hence the accumulation of Mn is susceptible to OMZ fluctuation. Whenever DO falls below a critical level (2 ml/l), the Mn starts reducing (Dickens and Owen, 1994), and gets diffused to deeper depths or redirects to more oxygenated region and reprecipitate. The reprecipitated MnO_2 colloidal particulates efficiently adsorb variety of dissolved cations and carry to the sediment and bury along with other sedimentary particles of diverse origin. Under the influence of an OMZ below the suboxic level, the concentration of Mn in the underlying sediments decreases as a result of its removal to the surrounding water as reduced (dissolved) -Mn as soon as the preformed Mn-oxide particulates in the sediment are reduced due to oxidation of decaying organic matter. The available dissolved Mn in the water column re-precipitates as Mn-oxide particulate as soon as it comes in contact with waters having DO above sub-oxic level. Therefore, Mn variation in the sedimentary column can be used as a qualitative proxy to reconstruct intermediate water oxygenation. The concentration of redox sensitive Mn, U, Mo, and Re which have ability to precipitate as particulate oxides and sulfides under variable oxygenation conditions and few bivalent cations such as Co, Cu, Ni, and Cr, which are sensitive to surface adsorption (scavenging) from water column hence can be used as tracers of the redox

variability.

To understand past variation of oxygenation in the intermediate waters flooding the OMZ in BoB, a pair of sediment cores underlying most intense region of modern OMZ (core) and the base of the same OMZ off Chennai coast are utilized. One sediment core (SSK50-GC14A) is from a water depth of 325 m (core of OMZ) and second sediment core (SSK50-GC13) is from ~1474 m (base of the OMZ, where there is higher oxygen than in the core of OMZ). The sediment column at these water depths can serve as archives of palaeo-OMZ variability in both intensity and vertical extent, and closely associated productivity, terrigenous detritus input, and ventilation. Using elemental proxies of representing these processes it is feasible to understand the past OMZ variability and its connection to climate driven biogeochemistry of the basin via the monsoon variation.

For bulk geochemistry the solutions prepared from HF + $HClO_4$ digested sediment, and for oxide fraction analysis the leachates from acid reductive leaching techniques have been adopted and analyzed on simultaneous ICP-OES and ICP-MS. The $\delta^{18}O_{formainifera}$, and C_{org} and $\delta^{13}C_{org}$, were measured on continuous flow IR-MS coupled with gas bench and element analyzer at the National Institute of Oceanography, Goa. The quality of analytical results was assessed by analyzing international reference material. The statistical analysis of the data was carried out utilizing Microsoft Excel software. Three sections from these sediment cores were subjected to AMS-radiocarbon dating at Arizona University, USA.

With the help of radiocarbon dates and $\delta^{18}O_{\textit{G. sacculifer}}$ and other published radiocarbon $\delta^{18}O$ data from the same region a reliable chronology for studied sediment cores has been developed. The OMZ sediment core (SSK50-GC14) covers the last ~40 kyr and OMZ-base Sediment core (SSK50-GC13) covers the last 16 kyr climate history. The well recognized global climate events are clearly evident in these sediment cores. The past variation of BoB-OMZ as reflected by sediment composition has been assessed in light forcing parameters.

The thesis is divided in to seven chapters. The background information on climate variability and present day OMZ dynamics and associated biogeochemical processes in particular with respect to BoB and working hypothesis are presented in Chapter 1 – Introduction. The Chapter 2- Study area comprises brief description of regional tectonic setting, hydrography, sediment sources, climatology, and seasonal fluctuation in the OMZ etc. A detailes of sediment cores, sample processing and analytical protocols are given in Chapter 3 – Material and methods. The Chapter 4 – Results contains all the analytical results of elemental and isotopic composition in the form of tables and figures. The discussion and interpretation of the data in light of the published literature is presented in Chapter 5. The conclusions and references are provided in Chapters 6 and 7 respectively.

ABBREVATIONS USED IN THE THESIS

AIW	Antarctic Intermediate Water
AS	Arabian Sea
ASHSW	Arabian Sea High Salinity Water
BA	Bølling-Ållerød
BoB	Bay of Bengal
DO	Dissolved Oxygen
EAS	Eastern Arabian Sea
EICC	East Indian Coastal Current
ICW	Indian Central Water
ISM	Indian Summer Monsoon
ITF	Indonesian Throughflow Water
KGK	Krishna, Godavari and Kaveri rivers
LGM	Last Glacial Maximum
MIS	Marine Oxygen Isotope Stage
NIO	Northern Indian Ocean
OM	Organic Matter
OMZ	Oxygen Minimum Zone
PGW	Persian Gulf Water
RSW	Red Sea Water
SMW	Sub Antarctic Mode Water
YD	Younger Dryas

1. INTRODUCTION

The solar energy received at the Earth's surface (insolation) varies geographically due to its shape and different physical setups (land and ocean configuration). The insolation variation from place to place results in systematic gradient in warmth of the Earth-Ocean surface causing atmospheric and oceanic circulations, which bring about inter-hemispheric energy-balance. This energy-balancing processes along with Earth's astronomical elements result in regionally characteristic weather and climate systems. The oceans play a vital role in dictating weather and climate, which involve pumping-in and -out a vast amount of heat energy between different physical spheres of the planet, viz. atmosphere, hydrosphere, cryosphere, and lithosphere. Amongst the entire Earth's surface, the tropical region acts as the heat-generator while the polar regions as heat absorbers. The global thermohaline circulation redistributes the tropical heat-energy across the hemispheres via the oceans (Figure 1), and plays a decisive role in climate system (Broecker, 1997). Thus, the hydrosphere largely governs the global climatic state, wherein the solar energy acts as the fuel for this engine.

The Earth's climate is continuously and rhythmically changed since its formation. A climate change can be considered as the result of perturbations induced by variation in the insolation activity (i.e., continuously changing Earth's orbital parameters), volcanic activity, changes in atmospheric composition of greenhouse gases, etc. The paleoclimatology deals with climate dynamics through the evolutionary history of earth. This branch of science aims to track climatic episodes that happened in the past on various time-scales such as decadal, centennial and millennial scale. The climate linkage with other processes on the planet encompassing biosphere, atmosphere, hydrosphere, cryosphere and lithosphere is an important component of the paleoclimate research. In a nutshell, the paleoclimate can be considered as a systematic study of the Earth System and intricate relationships between various components of this system in the past.

The physicochemical and biogeochemical imprints preserved in various repositories can be used as paleo-records. As the paleoclimate is concerned only with the changes occurred prior to the instrument era (geological time-scales), it cannot measure the components of the climate system directly. Therefore, the ice cores, tree-rings, marine and lake sediment cores, stalactites and stalagmites, etc are utilized as reliable repositories of past climate, because their deposition is progressive through the time. The evidences for paleoclimatic variation are extracted from the above repositories through chemical, isotopic, mineralogical, biological, physical etc signatures which are known as proxies.

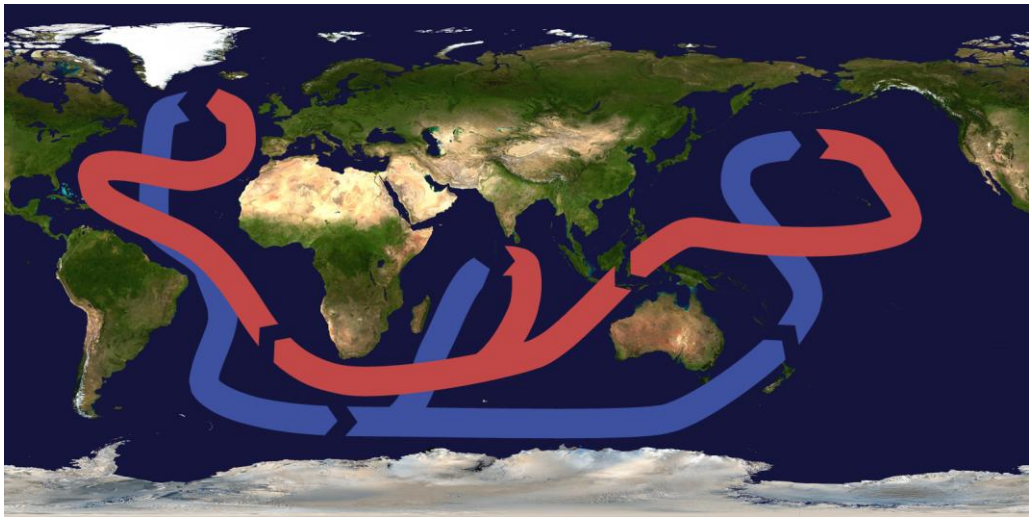

Figure1. Schematic diagram of the deep ocean thermohaline circulation. Blue arrows indicate cold deep-water currents originating in North Atlantic and red arrows indicate warm returning surface current to the origin. This circulation scheme is also termed as Atlantic Meridional Overturning Circulation (AMOC). This figure represents resultant structure of circulation loop on long time-scale of few hundreds of years (500-800 years) (Rahmstorf, 2003). Therefore, it is a highly simplified long-term average pattern of a complex deep current system. Figure source: Wikipedia (February 2018).

Almost all the major components of the Earth System can be reconstructed via the paleoclimate proxies. The time-series of these proxy data provide substantial evidences to reconstruct earth's climate over millions of years (Bradley, 1999). Through the paleoclimate reconstructions one can provide baseline natural variability of different components of the climate system over which the anthropogenically forced climate changes are imprinted. This baseline information in fact is a necessity to unscramble natural changes and human induced changes from the overall resultant climate we experience and to assist in developing reliable predictive climate models.

1.1. Astronomical forcing of the Earth's climate.

In the last few decades the cyclic changes in the geometry of the Earth's orbital parameters have been found to be closely associated with Earth's natural climate. These parameters are, the degree of ellipticity in the Earth's orbit around the Sun (eccentricity), tilt angle in the rotation axis of the Earth (obliquity), and wobbling or orientation of the rotation axis (precession) (Figure 2) having periodicities of roughly 100000, 40000 and 20000 years respectively (Milankovitch, 1941). These changes in the orbital parameters results in continuously changing insolation (W/m^2) received at the earth surface through time, which is the basic fuel or fundamental driver of the climate or weather systems. Therefore, in paleoclimate records the above periodicities have been recognized and evaluated (see Hays et al., 1976; Shackleton, 1987; 2000).

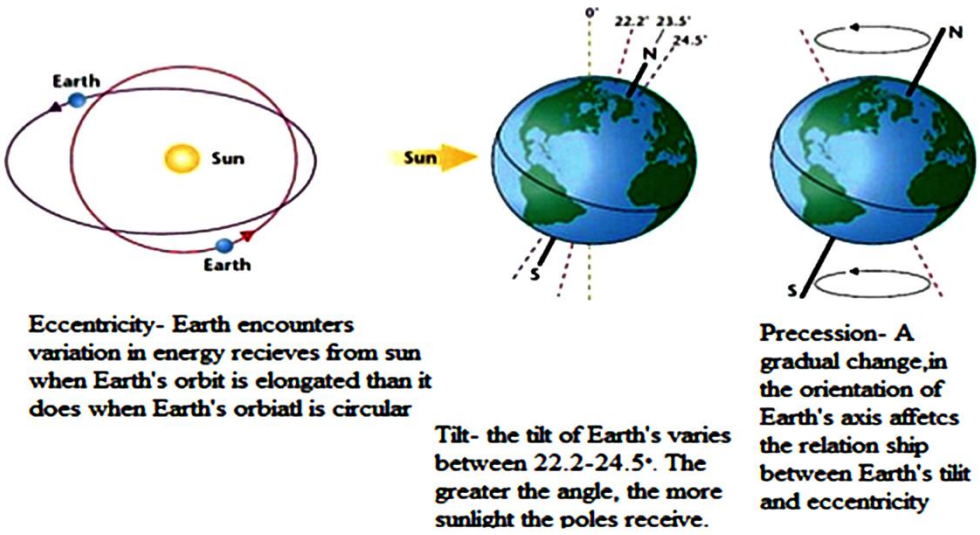

Figure 2. Milankovitch pace maker of climate which explains earth's orbital variations that affect the insolation received at the surface of the earth. Figure source: www.frontiersofsci.org

The Quaternary climate records show rythemic perturbations in climate as a result of changes in the Earth's orbital parameters. Within the last two glacial cycles at around 100 ky cyclicity, twenty-six well expressed temperature oscillations termed as Dansgaard-Oeschger cycles (DOC) have been recorded in the Greenland ice-cores (Dansgaard et al., 1993; Grootes et al., 1993), with alternate warm inter-stadials and cold stadials occurring on an average interval of 1470 years (Bond et al., 1997), and ice rafting events known as Heinrich events (Bond et al., 1992). The glaciation in the northern hemisphere is terminated by rapid de-glaciation at Bølling- Alleord warm period at 14.5 ka BP, which is terminated by rapid cooling at Younger Dryas (YD) at 12.5 ka BP that extends for about 1000 years and ended abruptly at the commencement of present warm period Holocene (11.8 ka BP).

The Holocene, a latest interglacial phase of the Quaternary witnessed a remarkable stability in global temperature and sea level. The climatic variation within the Holocene although appears stable includes millennial scale temperature oscillations as medieval warm period and succeeding little ice age with 2°C temperature drop (Miller et al., 2012) and significant cooling in the northern hemisphere at 8.2 ka (Alley and Augustsdottir, 2005). Several previous reports suggest a close link between the global climate and regional weather systems.

The Indian monsoon system is one of such regional weather system affecting the biogeochemistry of the northern Indian Ocean comprising two highly dynamic basins viz.,

Arabian Sea (AS) and the Bay of Bengal (BoB). In a recent study, the changes in inter-hemispheric heat transfer associated with changing intensity of the Indian Monsoon System (ISM) have been shown to have caused reversals in the polar climates during the last deglacial transition (Banakar et al., 2017). Therefore, the ISM may not be simply a passive follower of the global climate as thought previously, but it has potential to contribute to the global climate variation. It is well known that this monsoon system has definite bearing on the biogeochemistry of the northern Indian Ocean in the modern times (Dileep Kumar, 2009). This particular aspect is important in the present study that deals with the changes in the past Oxygen Minimum Zone (OMZ) in BoB.

1.2. Oxygen minimum zone.

The surface oceans have very high dissolved oxygen (DO) as they continuously interact with the atmosphere. As one moves away from the equator (tropics) towards polar-regions, the surface water DO increases progressively with increasing latitudes (Figure 3). This is because, a) the miscibility of gases in water increases with decreasing temperature and b) the water temperature decreases with increasing latitudes caused by progressively decreasing insolation. Below such highly oxygenated surface water the OMZs occur. In this subsurface zone of few ocean basins the DO concentration reaches a lowest level <5 µM, particularly in the intermediate depths of coastal seas and land locked bays. The OMZ can be defined as a depth range in which the settling organic matter decomposes or remineralizes (breakdown) to yield inorganic carbon and the nutrients back into the water column. The AS and BoB have been shown to host nearly half of the world's OMZ regions (Helly and Leven, 2009). However, the OMZ in the AS is most intense leading to basin-wide dentirification (Codispoti et al., 2001; Naqvi et al., 2010). When the primary oxidant, the DO, is exhausted due to remineralization of organic matter (respiration), the secondary oxidants such as dissolved nitrates (primary nutrient) and Mn-oxides particulates at the seafloor provide a source of oxygen by breaking-down in to free oxygen, nitrous oxide (N_2O) and inorganic carbon in case of former oxidant, and Mn^{2+} in case of latter oxidant. The nitrous oxide is considered as a highly potent greenhouse gas. Therefore, OMZs play an important role in regulating global warming and oceanic carbon- and nitrogen- cycling.

The primary productivity in the surface and renewal of intermediate and deep water DO (ventilation) has been considered to be the primary drivers of the OMZs (Olson et al., 1993). The primary productivity in the AS and BoB is very high (>500 mgC/m^2; Kabanova, 1963) due to monsoon forced upwelling and strong mesoscale eddies in the northern Indian

Ocean. As far as the BoB-OMZ is concerned, a third parameter viz., terrigenous silicate (or mineral grains derived from land) also play a vital role in its dynamics (Azhar et al., 2017). Therefore, OMZ variation in the past BoB is not as straightforward as in the AS. Thus a combination of three primary factors, viz., primary productivity, thermocline ventilation, and the terrigenous detritus input determine the past variation in the OMZ of the bay.

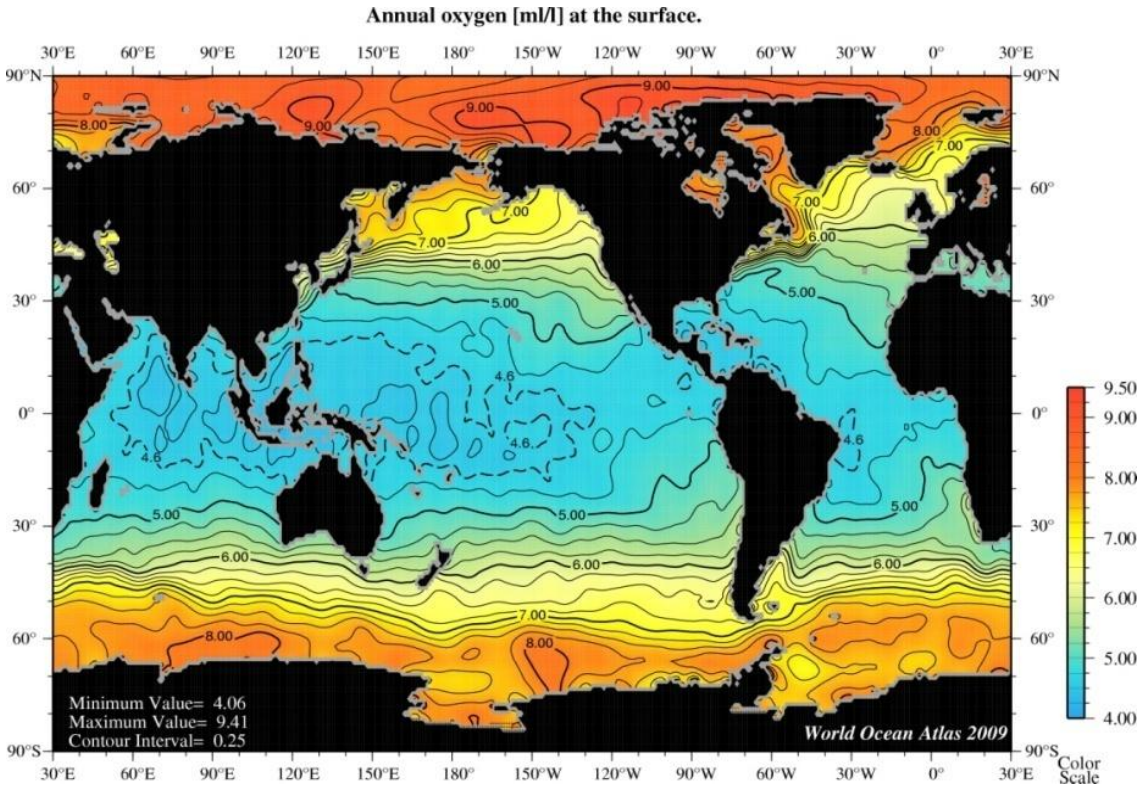

Figure 3. Annual surface water dissolved oxygen concentration of World Ocean. Due to low temperature high latitude waters have high concentration of dissolved oxygen compared to low latitude oceans. Source: World Ocean Atlas, 2009 (www.nodc.noaa.gov).

The oceanic surface waters (mixed layer) is oxygen saturated and in equilibrium with atmospheric oxygen, which is the source of DO in the ocean. The temperature of the surface water has two roles to play with respect to OMZ. Firstly, if the source water that ventilates a given OMZ is warm, then its oxygen holding capacity is less; secondly, the density of the water at its source region is also reduced. Both these together can intensify a given OMZ. Contrastingly, if the salinity of surface water at the source region is high then there shall be increased production of intermediate water that ventilates a given OMZ due to increased density that can result in weakening of the OMZ. Thus, the salinity and temperature of remote regions where the ventilating water mass/s is/are formed are important for development and sustainability of an OMZ. Under normal conditions the oxygen minima conditions are

localized to intense upwelling regions, which result in high primary productivity. The organic matter from highly productive surface water column that rains into the intermediate or thermocline waters undergoes bacterial degradation (remineralization or oxidation) consuming the DO. This process leads to rapid depletion of DO in the intermediate depths resulting in OMZ. Therefore, the ventilation of intermediate depths and the surface productivity in a given region are mainly responsible for the development of OMZ in that region.

The re-mineralization is also responsible for the formation of OMZ. The re-mineralization or nutrient recycling is one of the prerequisite for continuation of primary productivity (Cavan et al., 2017). Most of the organic matter (~80 %) gets oxidized within upper 1000 m water. Therefore, the well sustained OMZ regions are normally found in the continental margins where only aged waters (low DO waters) fill the intermediate regions of the oceans (Olson et al., 1993). Below the mixed layer the atmospheric oxygen cannot penetrate vertically downward and hence the source of DO at intermediate depths is only from ventilation by oxygenated waters formed elsewhere. The seafloor at about 300 m depth receives only a half of the total organic matter produced in the upper 100 m of photic zone, suggesting very high rate of remineralization or oxygen consumption below the mixed layer. The organic matter produced at surface decreases exponentially with depth and at the most only 10 % of it would reach 1000 m depth and deposit. This in turn suggests that the rate of DO consumption is extremely high in water depths from the base of mixed layer up to around 300 m, which normally is the depth zone covered by most intense (least DO) part of the OMZ known as ‘Core of the OMZ’ in highly productive regions (for example, see Figure 4). Hence, the anoxia is absent below 1500 m water depth (Kamykowski and Zentara, 1990). When the oxygen demand by oxidizable organic matter cannot be met by the DO, the formation of OMZ is initiated, and when the adequate replenishment of DO is not done at these depths, the OMZ is sustained (Wyrtki, 1962; Kamykowski and Zentara 1990; Olson et al. 1993; Sarma, 2002; Paulmier and Ruiz-Pino 2009).

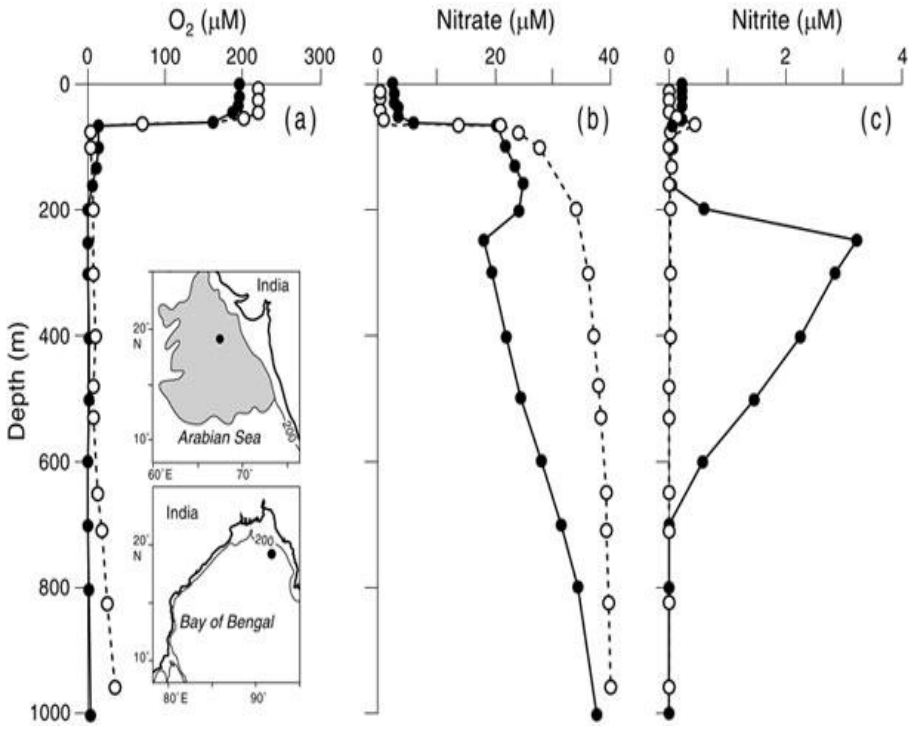

Figure 4. Vertical distribution of dissolved oxygen (a) shown along with NO_3^- (b) and NO_2^- (c) in the Arabian Sea (filled circles) and in Bay of Bengal (open circles). The insets show the station locations. Grey shaded area of the inset indicates perennial denitrification region. Note: Extremely intense OMZ in the Arabian Sea as compared to the Bay of Bengal is indicated by near zero concentration of DO. Figure source: Naqvi *et al.* (2006)

The OMZ regions are important because, a) worlds 80 % of petroleum deposits have been formed from ancient organic-rich sediments of continental margins suggesting their formation in oxygen-depleted, b) they are the primary regions of nitrogen cycling (Codispoti et al., 2001), c) they are the regions which sequester significant amount of atmospheric CO_2 burying it in the sediment as organic matter (Cavan et al., 2017; van der Weijden et al., 2001), and d) they are known for rich microbial communities (Kiene and Bates, 1990). The OMZ are considered as analogous of primitive anoxia in which life is widely thought to have first appeared (Zumft, 1997), because there are similarities between primitive life (Archea) and bacteria inhabiting in OMZ. Thus, the OMZ regions are not only important in terms of economic importance but also in academic and climate perspective.

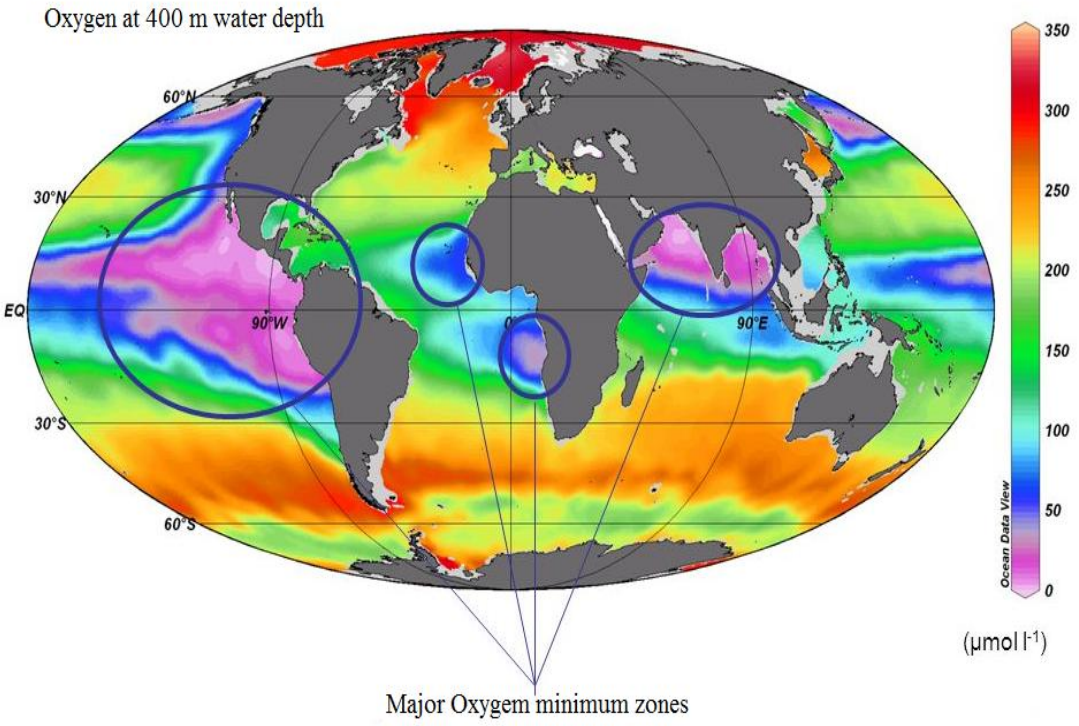

Figure 5. Global distribution of dissolved oxygen concentration at 400 m water depth exhibiting locations of perennial OMZ. Note the extremely depleted dissolved oxygen (pink band) in coastal and enclosed basins. (Cover page Figure) Figure source: www.slideplayer.com

The vast expanses of highly depleted DO (<25 µmol/l) and nitrite-rich waters in interiors of the world ocean define the intense OMZ (Ulloa et al., 2012) (Figure 5), also known as marine dead zones. Around 400 such marine dead zones have been reported worldwide which closely match with human footprints (Diaz and Rosenberg, 2008); while very few of them are permanently anoxic (Paulmier and Ruiz-Pino, 2009). The permanent OMZ (Figure 5) are seen in continental margin waters hosting very high primary productivity (Wyrtki, 1962). Such permanent OMZs are characteristic of both the basins (AS and BoB) of the northern Indian Ocean and in the tropical eastern Pacific margins (Karstensen et al., 2008; Olson et al., 1993). The anoxic OMZs are mostly found in the AS and Pacific. Some researchers term these regions as AMZ (anoxic marine regions) (see Ulloa et al., 2012). The AMZs are characterized by sulfate reduction at the sediment surface swept by anoxic waters (Figure 6). The global OMZ covers an area of around 32 million sq. km. and a volume of around 110 million cubic km, which account for over 7 % of the total area and volume of all the oceans together (Paulmier and Ruiz-Pino, 2009). The less intense OMZ (within suboxic levels) is found in the BoB (Figure 6).

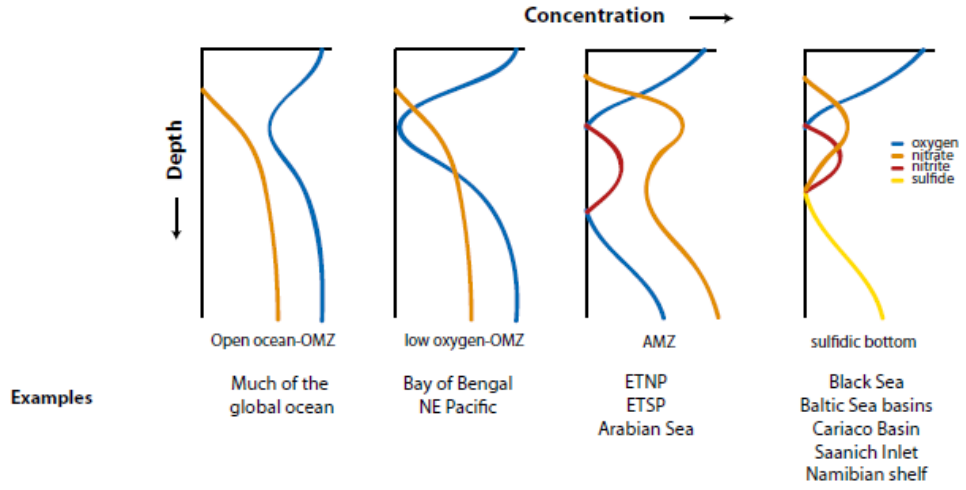

Figure 6. Schematic diagrams of the different types of OMZs in the World Oceans and the vertical profile of important dissolved species.

The dynamics of OMZ largely depends on variation in productivity and ventilation (Olson et al., 1993). However, recent studies have also indicated importance of detrital silicate particles in remineralization of settling organic matter (see Azhar et al., 2017). The changes in OMZ can cause wide-scale alteration in marine ecosystem (Diaz and Rosenberg, 2008). Recent studies indicate a severe oxygen depletion and vertical expansion of the OMZ in the tropical northeast Atlantic wherein nearly 15 % of habitat loss during 1960 - 2010 (Stramma et al., 2011). The OMZ in the northern Indian Ocean is highly dynamic and undergoes seasonal changes in thickness and oxygen concentration in the core (Dileep Kumar, 2009). During the spring summer transition (June - July) or during the onset of summer monsoon the AS witnesses rapidly enhanced primary productivity (Dileep kumar, 2009). As a result the OMZ shows a 20 % thickening and severe depletion in DO in the core of OMZ. During the intensification of the summer monsoon the BoB OMZ also undergoes a horizontal contraction of ~10 %. The increase in core thickness was found to be associated with shoaling of the upper limit of the core to ~20 - 30 m in the AS and extreme depletion of DO in the core without any effect on the horizontal extension of the OMZ. The limitation on the depth of the upper limit of the OMZ core is further associated with the depth of mixed layer. In other words, with amplified depth of mixed layer the upper limit of the OMZ deepens. Therefore, the OMZs are controlled by seasonal changes in the wind intensity. Thus, the summer monsoon season in the northern Indian Ocean that is associated intense wind mixing results in deepening of the OMZ and reverse happens during the winter monsoon season that is associated with strong stratification and thinning of the mixed layer.

The primary components of the OMZ dynamics in the northern Indian Ocean basins (productivity and ventilation, and also the organic matter remineralization depth) must have been affected by climate change from the glacial to interglacial type via the seasonal changes in the monsoon intensity. Hence, the strength of palaeo-OMZ of AS and BoB are expected to show differences between glacial and interglacial climates. Changes in the benthic foraminifera assemblages of California Basin (Cannariato and Kennett, 1999), laminated sediments off Pakistan (Von Rad et al., 1999; Schulte et al., 1999), and proxies of surface water productivity, changes in aragonite compensation depth (Reichart et al., 1998) etc clearly suggest climate dependent fluctuations in the OMZ of the AS, which must hold good also for BoB.

1.3. Biogeochemical effect of OMZ

A perennial OMZ can cause wide ranging effects in the biotic and abiotic components in the marine system. The DO concentration affects all the ecological processes in the marine environments. Based on the DO concentration, the OMZs and their main ecological and environmental characters are tabulated below.

Table 1. Classification of physical and biological facies on different oxygenation levels (Tyson and Pearson, 1991).

Oxygen (ml/L)	Oxygenation regime Environmental facies	Biofacies	Physiological regime
8.0-2.0	Oxic	Areobic	Normoxic
2.0-0.2	Dysoxic	Dysaerobic	Hypoxic
2.0-1.0	Moderate		
1.0-0.5	Severe		
0.5-0.2	Extreme		
0.2-0.01	Suboxic	Quasi-Anaerobic	
<0.01	Anoxic	Anaerobic	Anoxic

As the variable concentrations of DO in the OMZ regions lead to the formation of different types of ecological and physiological environments, the chemical processes are also expected to differ accordingly. The main chemical process within the OMZ is the reduction of different type of inorganic substances present in the water column as well as in sediment in

contact with OMZ waters. A series of molecular reduction occurs once DO in the water column begins to decline. They are de-nitrification, oxide-reduction, sulphate-reduction and methanogenesis. The respiratory decomposition of the organic matter leads to the release of photosynthetically fixed CO_2 back into the water and hence CO_2 maxima are seen in the OMZ depths (Paulmier et al., 2010), reducing the pH of waters through the formation of carbonic acid, i.e., developing zones of acidification (Gobler and Baumann, 2016). It is well known that the acidification of oceanic waters promote dissolution of carbonate skeletons of various phyto-zoo-planktons deposited in the continental and slope regions and also coral reefs, in turn increasing the climatically very important pCO_2 of the ocean surface. The chemical processes involved in such conditions are shown in the following equations.

Respiration

$$(CH_2O)_{106}(NH_3)_{16}H_3PO_4 + 138O_2 \rightarrow H_3PO_4 + 16HNO_3 + 106CO_2 + 122H_2O$$

Nitrate Reduction

$$NO_3^- + 6H^+ + 6e^- \rightarrow N_2$$

$$(CH_2O)_{106}(NH_3)_{16}H_3PO_4 + 94.4HNO_3 \rightarrow H_3PO_4 + 55.2N_2 + 106CO_2 + 177.2H_2O$$

Mn-Reduction

$$MnO_2 + 4H^+ + 2e^- \rightarrow Mn^{2+} + 2H_2O$$

$$(CH_2O)_{106}(NH_3)_{16}H_3PO_4 + 236\ MnO_2 + 472H^+ \rightarrow H_3PO_4 + 236\ Mn^{2+}\ 16\ NH_3 + 106\ CO_2 + 366\ H_2O$$

Fe-Reduction

$$Fe(OH)^3 + 3H^+ + e^- \rightarrow Fe^{2+} + 3H_2O$$

$$(CH_2O)_{106}(NH_3)_{16}H_3PO_4 + 212\ Fe_2O_3 + 848\ H^+ \rightarrow H_3PO_4\ 424Fe^{2+}16\ NH_3 + 106\ CO_2 + 530\ H_2O$$

Sulfate Reduction

$$SO_4^{2-} + 10H^+ + 8e^- \rightarrow H_2S + 4H_2O$$

$$(CH_2O)_{106}(NH_3)_{16}H_3PO_4 + 53\ SO_4^{2-} \rightarrow H_3PO_4 + 53\ S^{2-} + 16\ NH_3 + 106\ CO_2 + 106\ H_2O$$

Methanogenesis

$$CO_2 + 8H^+ + 8e^- \rightarrow CH_4 + 2H_2O$$

$$(CH_2O)_{106}(NH_3)_{16}H_3PO_4 \rightarrow H_3PO_4 + 16\ NH_3 + 53\ CO_2 + 53\ CH_3$$

Immediately after utilizing free-DO by respiration (oxidation/remineralization), the next targets of the organic matter for oxygen (electron acceptor) is nitrate, which is achieved by converting NO_3^- to gaseous nitrogen (Codispoti et al., 2001) and particulate MnO_2. At the same time, the anaerobic oxidation- annamox- of NO^{3-} also happens in OMZ using NO_2^- (Murray et al., 2005; Kuypers et al., 2004; Kalvelage et al., 2013). The increased demand for electron acceptors (oxygen ion) by the oxidizable organic matter leads to a series of reduction reactions once DO drops down to a critical level normally defined as suboxic. The order of these reactions is nitrate reduction, MnO_x reduction, FeO_x reduction, SO_x reduction and finally

methanogenesis. Hence, the concentration of reduced chemical species in the aqueous form (N_2, Mn^{2+}, Fe^{2+}, H_2S, and CH_4) would be very high in an intense and well sustained OMZ.

1.4. Behavior of redox sensitive elements in the OMZ

The seafloor sediments in contact with OMZ waters is prone to develop severe reducing environment, where several redox-sensitive element species are subjected to reduction induced mobility. The OMZ intercepts in continental margin and creates permanent hypoxia that could persist for thousands of years (Reichart et al., 1998). The interaction of OMZ waters with sediment promotes reduction of oxides at sediment water interface. This may lead to the depleted concentrations of leachable redox sensitive elements such as Mn and Fe in sediment. The dispersed particulate Mn and Fe in the sediment can undergo complete reduction in suboxic environments. The leached elements exit from the sediment and migrate to more oxygenated deeper regions and re-precipitates as their oxides and hydroxides (Dickens and Owen, 1994). The re-precipitating Mn and Fe oxide colloids subsequently act as host (carrier) phase for several cations present in the ambient seawater through surface adsorption (Koschinsky and Halbach, 1995).

The elements which undergo changes in their oxidation states according to redox variability are known as redox sensitive elements, which undergo partitioning between solid and solution phases. These elements (major or minor) have multiple valancy (oxidation) states with significantly differing solubility in seawater. Hence, the behavior of redox sensitive elements in both water and sediment could be reliable tools for understanding the redox variability in the water that impinges over sediment (Calvert and Pedersen, 1993).

As already mentioned in above paragraphs the increased oxygen demand for the decay of organic matter continues even after the consumption of free-DO. From previous studies it is now known that there are two types of redox sensitive elements, viz., those who change the valancy state during reduction and those which won't (Calvert and Pederson, 1993). The Mn, which is soluble in suboxic to anoxic condition and insoluble in oxic condition, and Cr, U, and Re, which are soluble in oxic and insoluble in anoxic are the elements which undergoes change in valance under different redox conditions. While Cu, Ni, Zn and Cd is soluble in oxic as chloride ions and adsorb to sulfates in anoxic condition to precipitate without changes in their valancy (Bertine, 1972; Breit and Wanty, 1991; Emerson, 1998; Emerson and Huested, 1991; Colodner et al., 1993; Crusius et al., 1996; Crusius & Thomson, 2000; Calvert and Pedersen, 1993; Tribovillard et al., 2006; Bruland, 1980). Therefore, the enrichment or depletion of certain elements in sediment renders them useful to track the paleo-redox status of

the water in contact. The Table 2 presents the state (soluble/insoluble or aqueous/solid) of few elements in the oxic and anoxic environments.

Table 2. Principal redox sensitive element species in oxic and anoxic environments

Element	Oxic	Anoxic
Mn	$MnO_{2\ (s)}$	Mn^{2+}; $MnCl^{+}$ (aq);$MnCO_3$ (s)
Cr	$CrO_4^{2-}{}_{(aq)}$	$Cr(H_2O)_4\ (OH)^{2+}{}_{(aq)}$; $Cr(OH)_{3\ (s)}$
Mo	$MoO_4^{2-}{}_{(aq)}$	$MoO_2^{+}{}_{(aq)}$; $MoS_{2\ (s)}$
U	$UO_2(CO_3)3^{4-}{}_{(aq)}$	$UO_{2\ (s)}$
Re	$ReO^{4-}{}_{(aq)}$	$ReO_{2\ (s)}$; $ReS_{2\ (s)}$; $ReS_{7\ (s)}$
Cu	$CuCl^{+}{}_{(aq)}$	$CuS_{\ (s)}$; $Cu_2S_{\ (s)}$
Ni	$NiCl^{+}{}_{(aq)}$; Ni^{2+}	$NiS_{\ (s)}$
Zn	$ZnCl^{+}{}_{(aq)}$; Zn^{2+}	$ZnS_{\ (s)}$

Among the above element species the chemically dynamic characteristics of Mn may be due to its higher crustal abundance (~600 ppm: McLennan, 2001), as well as its ability to exist in several oxidation states (Mn^{2+} to Mn^{6+}) compared to other elements. The Mn is the only redox sensitive element, which exists in solid phase in oxic environment along with Fe. Their oxy-hydroxides can act as a host for minor elements present in the ambient sea water during their precipitation as colloidal oxides and hydroxides (Koschinsky and Halbach, 1993). Hence, hydrogenous (or authigenic Mn-oxide) plays vital role in the transfer of trace elements to the sediments. The dominant species of Mn in sea water are Mn^{2+} and $MnCl^{+}$. Its thermodynamic instability leads to its precipitation as Mn oxides and oxyhydroxides, i.e., MnO_2 and MnOOH (together MnO_x). The source of Mn to the oceanic water is the weathered continental crust transported by rivers and winds, hydrothermal activity and halmyrolysis (submarine alteration of basalts and sediment). The latter along with several sheet silicates carrying Mn can readily undergo chemical transformation in seawater and release several minor elements to the surrounding water. The fourth source of Mn to seawater is its diffusion from sediments which take place in reducing conditions nearly similar to halmyrolysis but specific to Mn-oxides. All these together enrich the seawater with primary redox sensitive elements, which have ability to readily re-precipitate as oxides and hydroxides as soon as they come in contact with waters having DO above suboxic level. Thus, the suboxic water roughly defines the boundary between dissolved and particulate Mn or Fe phases. The hydrothermal input of Mn is rather highly localized to mid-ocean ridges and is removed quickly from the

water as oxide in the vicinity of hydrothermal plumes hence an insignificant contributor to the OMZ regions. Below the oxic anoxic interface the reductive dissolution of oxy-hydroxide particles release soluble Mn (Mn^{2+}) that may diffuse upward and downward (Rajendran et al., 1992) without forming any organometallic or sulfidic complexes like other several trace elements (i.e., Cu, U, Mo etc) (Algeo et al., 2012). However, Mn can form carbonates in seawater (rhodochrosite) under high carbonate-ion saturation conditions (Pedersen and Price, 1982; Thomson et al., 1986; Calvert and Pedersen, 1993).

1.5. Scope and significance of reconstructing paleo-OMZ

In the geological past OMZs have probably expanded and contracted in the interglacial (warm) and glacial (cold) periods respectively (Cannariato and Kennett, 1999). There are evidences to show that the past ISM variation has influenced the productivity in northern Indian Ocean and also the redox conditions in sediments (Banakar et al., 2005; Chodankar et al., 2005; Finney and Lyle, 1988; Pattan et al., 2017; Punyu et al., 2014). The OMZ in the AS has completely disappeared during Heinrich events and YD probably due to changes in the pattern of thermohaline circulation (Schulte et al., 1999). The last 250 kyr OMZ reconstructions for the northern-AS (Makhran Coast) has indicated that there have been times with weakest or non-existent OMZ coinciding with lowest productivity and *vice versa* (Reichart et al., 1998).

The OMZ perturbations can adversely affect the marine ecosystem. The primary drivers of OMZ such as productivity and ventilation are shown to have influenced by the local climatology. The past-OMZ reconstruction can be useful to understand the biogeochemical responses of a basin to the past climate in general and productivity and ventilation in particular. The OMZs are the potential regions to sequester atmospheric CO_2 via the enhanced burial of the photosynthetically synthesized organic matter by phytoplankton communities, which are one of the largest reservoirs of atmospheric CO_2 and provide a strong negative feedback mechanism for global warming (Cavan et al., 2017). Thus, paleo-OMZ reconstruction is an important study in climate perspective.

The long-term real-time modern observations suggest that the frequency of dysoxia (2-0.2 ml/l DO) has increased in time over last few decades (Officer et al., 1984; Stramma et al., 2011) and resulted in intensification of modern OMZ. This may be due to various reasons like increase in productivity, higher nutrient loading, metal input, riverine discharge, atmospheric dust fallout, volcanic activity, etc (Keeling et al., 2010). The deoxygenation is regarded as a near ubiquitous feature of all oceanic basins that is indicative of the effect of global warming.

Modern OMZs have expanded in the last 50 years and are expected to expand further more with global warming due to raise in temperature and slowdown in ventilation (Stramma et al., 2010; Cabre et al., 2015) leading to an boost up organic carbon transfer by means of biological pump and accumulate in the deep ocean. The future expansion of OMZ is likely to increase the biological ocean carbon storage and act as a negative feedback to climate warming (Cavan et al., 2017). Thus, it is apparent that a good understanding of the past OMZ dynamics controlled naturally is of necessity to address the issues related to modern climate change.

1.6. Working hypothesis and objectives

Manganese in sediments can be broadly classified in to lithogenic and non lithogenic fractions (Chester and Hughes, 1967; Manjunatha and Shankar, 1996). The lithogenic fraction includes elements in the resistant phase (crystal lattice of minerals), and the non-lithogenic fraction includes particle adsorbed, carbonates and oxide particulates. The Mn in the non-lithogenic fraction (oxides) starts reducing whenever DO level falls below 2 ml/l (Dickens and Owen, 1994) and reduces completely within the suboxic environment. Hence, Mn deposition within the OMZ is not feasible that leads to decreased concentration in sediment deposited within conditions below suboxic. Sediment deposited within or swept by the core of OMZ therefore contains less Mn as compared to the sediment deposited out of the OMZ, where waters are oxic. The Mn from sediment located within OMZ undergoes Mn-oxide/hydroxide reduction and exits the sediment reservoir. Thus, measuring the Mn associated with sedimentary oxide particulates can provide clues about the changes in past OMZ. This working hypothesis is depicted schematically in Figure 7. By quantifying the concentration of Mn within a sediment core that represents a time-in-past it is possible to qualitatively asses the fluctuation of OMZ in a given region. This hypothesis forms the basis for the present study.

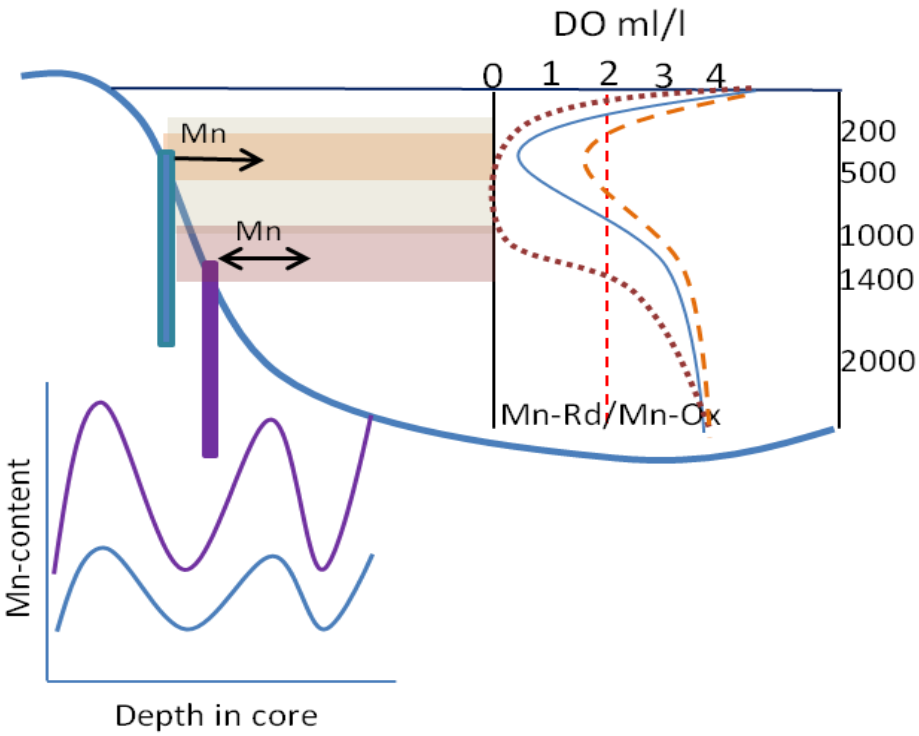

Figure 7. The schematic diagram to elucidate the working hypothesis. The bottom thick blue line indicates the sediment water interface. The right side of the schematic diagram shows the depth Vs dissolved oxygen curves in the different oxygen levels. The blue line represents the modern OMZ while the orange dashed line shows a weakened OMZ with minimal core and the brown dotted line indicates an intensified OMZ with an extended core. All the three hypothetical OMZs have the same core (least DO concentration). Below 2 ml DO level is taken as the Mn reduction starting zone (Dickens and Owen, 1994) and above 2 ml/l is taken as the Mn oxidation level. This Mn_{Rd}/MnOx boundary is indicated with straight red dashed line at 2ml/l in DO scale. The left side of the panel indicates the location of the core with respect to the presented OMZs. The first sediment core which is located ~400 m water depth is from the core of the modern OMZ of the BoB. While the sediment core from the base of the modern BoB-OMZ (~1400 m water depth) is indicated by the purple bar. The shallow water sediment core is well located in the core of the OMZ where the precipitation of Mn is not feasible. Hence, undergoes reductive redirection of Mn from the depositional site. While the deep water core (~1400 m) is influenced mostly by Mn deposition and influenced by reductive dissolution only during an extended OMZ period. The bottom panel indicates the expected Mn profile of shallow and deepwater cores under above two conditions of the OMZ.

Objectives of the present study

1. To understand the variation in past-OMZ in the waters of eastern continental margin of India (western Bay of Bengal).
2. To reconstruct terrigenous- and organic- matter input changes to the study region and qualitatively assess their influence on the palaeo-OMZ.
3. To evaluate various parameters forcing OMZ changes in BoB in light of established climate dependent monsoon variability.

2. STUDY AREA

2.1. General introduction

The Indian subcontinent divides the Northern Indian Ocean (NIO) into two basins, the AS in west and the BoB in east. The NIO is characterized by existence of half of the world OMZ (Helly and Levin, 2004; Paulmier and Ruiz-Pino, 2009). The present study region, BoB, is a semi-enclosed basin extending between 6° and 24° N latitudes and between 80° and 92° E longitudes. The average depth of the bay is 2600 m. A unique feature of the bay is the huge freshwater influx it receives from one of the world's largest perennial drainage system viz., Ganga and Brahmaputra and also several seasonal peninsular rivers. The BoB also receives a large amount of freshwater by overhead precipitation. The estimated annual freshwater input to BoB by rivers is of the order of 1.6 trillion m^3 (Subramanian, 1993), in addition to overhead precipitation of ~2000 mm/y (Prasad, 1997). The majority of freshwater input to the basin occurs mostly during the Summer Monsoon and following inter-monsoon period (June-October). Because of such huge freshwater input the evaporation minus precipitation in BoB is always negative in contrast to its counterpart - the AS.

2.2. Local climatology

The monsoon currents regulate climatology of the entire NIO (Dileepkumar, 2009). During November to March continental high pressure system is developed in the north leads to northeast monsoon. During this period the cold dry north easterlies brings cold climate to the subcontinent. During April to September the peninsular India bears the low pressure belt and winds flow from ocean to land known as the southwest monsoons, which are much stronger than northeast monsoons and bring over 90 % of the rains to the subcontinent. The moisture charged summer monsoons together with the presence of imposing Himalaya in north result in highest rainfall on the subcontinent that mostly drains in to BoB. The open ocean water of BoB is oligotrophic and is characterized by the chlorophyll concentration less than 0.30 mg/m^3 (Ramaiah et al., 2010). However, the bay has a subsurface chlorophyll maximum (Sarma and Aswanikumar, 1991).

The BoB salinity is strongly influenced by freshwater runoff from the Ganga and Brahmaputra at the northern end of the bay. Hence, the surface water become progressively fresher or less saline from south to north of the bay (from ~35 psu in south to ~30 psu at the mouth of Ganga-Brahmaputra in north). This overall low salinity surface water virtually creates a strong near surface stratification or freshwater plug over the bay. Below a

depth of about 100 m, the stratification is dominated by thermocline dynamics. Over most of the continental shelf the salinity varies from 34.5 to 34.9 psu (Levitus and Boyer, 1994). The overall sea surface temperature (SST) distribution in the BoB is highly influenced by the prevailing monsoon system with annual mean of ~27 °C. During the winter (northeast) monsoons the SST ranges from ~26 °C in northern bay to ~29 °C at the southern end of the bay. During the summer monsoons, in contrast, the temperature decreases from north to south because of the heavy freshwater input. However, during the summer monsoon period the SST structure in the bay is complex due to existence of several warm and cold cells across the bay.

The circulation in the BoB is characterized by reversal of clockwise currents during southwest (summer) monsoons to anticlockwise during northeast (winter) monsoons. The bay is characterized by frequent cyclones and gyres. Intense tropical storms of high winds and torrential rains occur in April–May and during October–November. These processes develop turbulent eddies across the bay causing injection of deep nutrients in to the photic zone and also ventilate the OMZ (Sarma et al., 2017) by locally mixing the atmospheric oxygen with the OMZ beyond the depth of its core. The seasonally reversing western boundary currents which is known as the East Indian coastal current (EICC) in the BoB drives most of the exchange of water masses between the AS and the bay (Akhil et al., 2014; Shankar et al., 2003). The southward flow of this current transfer the low salinity water from the bay in to the AS (Chaithanya et al., 2014)

2.3. Water masses

The intermediate and deep waters in BoB are ventilated by cold and oxygen rich waters formed in distant open oceans (Sverdrup et al., 1942). The dominant water-mass below the mixed layer up to around 1000 m depth is Indian Central Water, which is a mixture of several waters originating in Persian Gulf, Red Sea, Sub-Antarctic Region and Indonesian Sea (Emery and Meincke, 1942; You and Tomczak, 1993). The dynamics of this mixed character water mass is most important with respect to OMZ in the bay. As already mentioned huge input of freshwater to the BoB results in strongly stratified low salinity surface plug over the bay and creates a surface barrier layer (Shetye 1993; Vinayachandran et al., 2002). The Arabian Sea high salinity water (ASHSW), Persian Gulf water (PGW), Red Sea water (RSW) can be traced in the bay with increasing depths (Jain et al., 2017). The summer monsoon currents carry ASHSW in to the BoB (Murty et al.,1992; Shankar et al., 2002; Vinayachandran, 2013) that slides below the surface low salinity plug (Jain et al., 2017). The intermediate depths (thermocline) of the BoB also receive Sub-Antarctic mode water (SMW).

These water masses govern the ventilation of the BoB at depth where the OMZ exists.

2.4. Sediment sources to BoB

The Himalaya, Indo-Burma, and Southern Peninsular India are the main sources of terrigenous sediment to the BoB (Colin et al.,1999). The Nd -Sr isotopes of sediments from the study region (eastern continental margin) closely resemble the Nd -Sr systematics of the Deccan basalts and peninsular granites (Colin et al., 1999). The clay mineral assemblage of the margin and fan sediments suggested a significant amount of sediment in the BoB is derived from Precambrian Indian Shield and Deccan basalts (France-Lanord et al.,1993; Aoki et al.,1991). Further, these isotopic characters of several sediment samples from the Central Indian Ocean fall within the mixing region between High Himalayan Crystalline and Deccan Basalt (Fagel et al., 1994), suggesting the influence of pensinsular lithology on the sedimentation in BoB. Therefore, the Krishna, Godavari and Kaveri rivers (KGK) which drain the peninsular India must have delivered the peninsular characteristic sediment not only to the present study area, but also contributed to the Bengal Fan sedimentation. As the study area is located close to the mouth of KGK river system, the present sediment cores are expected to reflect changes in terrigenous matter supply by the monsoon dependent peninsular rivers.

2.5. Characteristics of BoB - OMZ

The BoB mixed layer variability is largely depends on the regional oceanographic characteristics and atmospheric forcing. During summer monsoon period the BoB has a shallow mixed layer than in AS (Shenoi, 2002; Vinayachandran et al., 2002). This is primarily controlled by the combination of weaker winds and strong near surface stratification associated with the entrainment restriction and increased barrier layer thickness in BoB (Han, et al., 2001). Although the physical and biological oceanographic parameters in NIO remain more or less similar, the high overhead precipitation in BoB results in shallow mixed layer. This low salinity lens restricts vertical mixing within the upper 100 m water depth (Sarma, 2002). Hence, the organic matter production in BoB is lesser compared to AS. This relatively less productive surface waters in BoB results in the formation of a relatively weaker OMZ as compared to the OMZ in AS. However, the measurements of vertical fluxes of the particulate organic matter suggested that the organic fluxes at depths in BoB are higher than at similar depths in AS (Gauns et al., 2005; Ittekkote et al., 1992). This enhanced particulate organic matter flux in low productive BoB waters are found to be due to aggregation of organic matter with mineral particles, which increases the settling speed by reducing the rate of

remineralization by providing a protection to the organic matter against oxidation (Rao et al., 1994; Howell and Doney, 1997). Productivity is the key factor which determines the formation of OMZ in any ocean. The episodic events like meso-scale cool eddies and cyclones are capable of enhancing productivity, but, these are inconsistent events of short time-scale and hence difficult to identify in long time-scale palaeo-records.

In contrast to perennially anoxic OMZ in the AS, the BoB-OMZ is a nearly suboxic and hence absence of large scale de-nitrification (Rao et al., 1994; Howell and Doney, 1997). The BoB-OMZ extends up to a depth of ~700 m (Figure 4). Further downwards the DO gradually increases due to the advection of oxygenated water from the south (Sardessai et al., 2007). The formation and sustainment of BoB-OMZ are regulated by physical and biological processes with insignificant seasonal variability and the residence time of intermediate water (Sarma, 2002). The strong surface stratification not only inhibits nutrient injection in to the surface waters leading to oligotropic conditions (<0.30 mg/m^3 chlorophyll: Ramaiah et al., 2010), but also restricts oxygen exchange leading to the formation of intense OMZ (Sarma et al., 2013). In addition, the OMZ depth in BoB is ventilated by a complex mixture of inherently oxygen depleted aged water (Sengupta et al., 2013). Thus, the overall oxygen minimum condition is sustained throughout the year by combination of complex physical and biological processes specific to this basin (Sarma, 2002).

2.6. Paleoclimatology of the BoB

The SSTs were depleted by ~3 °C and $\delta^{18}O_{SEAWATER}$ was enriched by ~0.6 ‰ during the Last Glacial Maximum (LGM) as compared to Holocene (Rashid et al., 2011). A drastic change in precipitation over BoB appears to have taken place during the early Holocene (Rashid et al., 2007; 2011), which is consistent with the ISM intensification in the AS (see Fleitmann et al., 2004). The deglacial ISM records from BoB showing intensification during Bølling-Allerod warm event and weakening during Younger Dryas (YD) cold event (Rashid et al., 2011) are also consistent with AS records (Banakar et al., 2004; 2017; Kesserkar et al., 2013). Therefore, paleomonsoon records extracted from sediments of both these basins are nearly consistent.

The above review of modern and paleoclimatological studies from the NIO indicate that, a) the modern and palaeomonsoon forcing on the biogeochemistry of BoB and AS appear to be nearly similar, b) the terrigenous sediment differs significantly between these two basins, c) the modern hydrographic set-up, nutrient dynamics and organic matter remineralization depths are quite different in these two basins hence significant differences in export production

and OMZ status, d) although the surface circulations connect both these basins very well, a significant differences in freshwater budgets render the basins highly contrasting with respect to mixed layer dynamics, e) the water masses ventilating the modern OMZ depth in both basins are the same except for more aged in BoB. As there are both similarities and dissimilarities in bio-geo-physico-chemical characteristics of these two basins, the palaeo-OMZ of the BoB needs to be understood separately from that of the palaeo-OMZ of the AS.

3. MATERIAL AND METHODS

3.1. Sediment cores

Two sediment cores are utilized for the present work and were collected using a cylindrical gravity corer during the 50th cruise of R.V Sindhu Sankalp under GEOSINKS project funded by the Ministry of Earth Sciences. The SSK50-GC14A is retrieved from a water depth of 325 m, which is presently swept by the most intense core of the OMZ. This sediment core (hereafter referred as 'OMZ- core' or GC14) is 282 cm long. The SSK50-GC13 sediment core (hereafter referred as 'Base-OMZ core' or GC13) is from a water depth of 1474 m, which is out of the modern OMZ. This core is 200 cm long. Further details of these two sediment cores are presented in Table 3 and Figure 8. The Figure 8 also shows the modern DO conditions at the locations of these two sediment cores. The sub-sampling was done at 1 cm intervals using PTFE knife to avoid metal contamination. The sub-samples were dried at low temperature (~40 °C) in oven and transferred to clean labeled plastic vials for further analysis.

The sediment record contains indirect fingerprints of past climatic and biogeochemical processes. To understand those processes it is necessary to focus on particular component from multi-component sedimentary system. Such particular component/s must have well known natural behavior and capable to record and preserve the changes of that known natural processes. Different types of analytical procedures are required for qualitative and quantitative measurement of those components which are called as 'proxies'. In the following paragraphs the analytical procedures followed in the present study are briefly explained.

Table 3. Details of the sediment core utilized for the present study

Sediment core	Water depth	core length	Location
SSK50 GC14A	325 m	282 cm	13^{o} 39' 58"N 80^{o} 34 ' 30" E
SSK50 GC13	1474 m	200 cm	13^{o} 31'31" N 80^{o} 39' 24" E

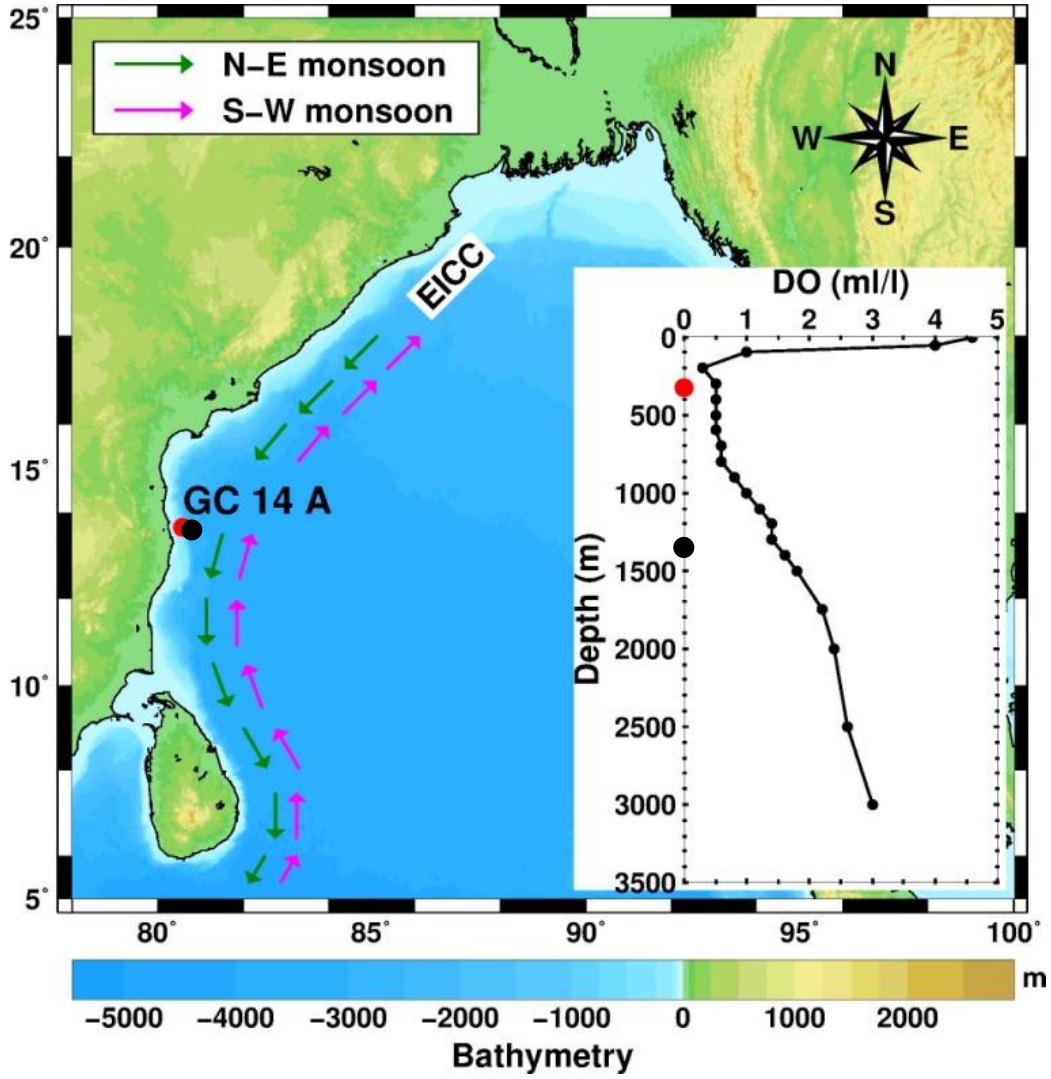

Figure 8. Location details of the sediment cores SSK50-GC14A (red filled circle) and SSK50-GC13 (black filled circle. The inset shows sediment core locations with respect to present-day depth profile of dissolved oxygen. The modern OMZ (DO < 1 ml/l) occurs between 200 and 700 m. The seasonally reversing coastal currents are shown with colored arrows.

3.2. Coarse fraction extraction

The coarse fraction (+63 µ size fraction) analysis was carried out to extract foraminifera skeletons for oxygen isotopes and radiocarbon measurements. About 5 g of freeze dried sediment sample was dispersed in RO-water in presence of 10 % of sodium hexa-metaphosphate for overnight. The dispersed sediment was wet sieved over 63µ standard sieve using gentle water jet to wash off fine fraction (< 63 µ). The separated coarse fraction was oven dried. When observed under the microscope the tests of foraminifera did not show any indications of dissolution as evident by absence of *G. menardii* keels and translucent patches on chamber walls of most of the species including *O. universa* that is considered to be most prone to dissolution (Hemleben, 1996).

3.3. Oxygen isotope measurement

The oxygen isotopic ratio (expressed as $\delta^{18}O$) is the ratio of abundance of a heavy (^{18}O) and light oxygen (^{16}O) isotopes present in natural system. These isotopes have played a crucial role in unraveling the past climatic history of the Earth. The evaporation and precipitation are the two primary factors which fractionate the water molecules ($H_2{}^{16}O$ and $H_2{}^{18}O$) having different molecular weights (18 and 20 respectively) in the oceanic reservoir. As per the Rayleigh's fractionation law, the lighter water molecules (18) preferentially go in to vapor phase and heavier water molecules (20) preferentially stay in the liquid phase (ocean water). Thus, the evaporation leads to relative enrichment of heavier oxygen isotopes in the oceans when evaporated ocean water locks in to ice in high latitudes and mountains instead of returning to oceans in the form of rains or precipitation. Therefore, the ice formed at the polar regions and mountains invariably is enriched with ^{16}O or depleted with ^{18}O as compared to the ocean water at a given time because the vapor evaporated from the oceans itself is the source of water for the formation of polar and continental ice. If the oceans receive more freshwater than evaporated at a given point of time by melting of continental ice and polar ice-caps, then the oceans get relatively enriched with light water molecules (18) or depleted with heavy water molecules (20), because the melt-water is invariably depleted with ^{18}O as compared to the ocean water. The formation or expansion of ice-caps and continental ice is typical of cold glacial climates and the melting of ice-caps and continental ice is typical of warm interglacial conditions. Accordingly, the $^{18}O/^{16}O$ of the ocean water exhibit different patterns of ratios depending upon the type of climate prevailed in the past. The foraminifera secreting their tests in equilibrium with the composition of the ambient ocean water therefore preserve the above described climate dependent ratios of oxygen isotopes during their short life-time of few weeks. After the death of the organism the oxygen isotope signatures embedded in the tests during their life-time are preserved. Thus foraminifera provide a powerful proxy to understand the past climate change via the oxygen-isotopic ratios (expressed as $\delta^{18}O$). This forms the fundamental aspect of utilizing oxygen isotope ratio as a proxy for palaeoclimatology. The oxygen isotopic ratio is expressed with delta notation - $\delta^{18}O$ where;

$$\delta^{18}O_{Foraminifera} = [(^{18}O/^{16}O_{Foraminifera} - ^{18}O/^{16}O_{Standard}) \times ^{18}O/^{16}O_{Standard}] \times 10^3$$

The $\delta^{18}O$ changes are expressed in permill unit (‰), as a change with respect to international reference standard Pee-Dee Belemnite (PDB). Urey (1947) for the first time recognized the climate dependent behavior of these isotopes. Later, Epstien (1953), Emiliani (1954), and Shackleton (1974) developed this method and made it an integral part of the

paleoclimate research.

Around 20 clean tests of upper mixed layer dwelling planktonic foraminifera *Globigerinoides sacculifer* (*G. sacculifer*) of 250-355µ size were picked from the coarse fraction. The tests were gently crushed and sonicated in presence of 10 % H_2O_2 to remove adhering and chamber filling fine particles of clay and organic matter, and washed and dried over night in specific glass vials. The sample was reacted with 100 % orthophosphoric acid at 90°C in a gas-bench coupled with an in-house Thermo Delta$^+$ Isotopic Ratio Mass Spectrometer. The relative abundance of molecules with mass discriminator at $^{46}CO_2$ ($^{12}C^{18}O^{16}O$) and $^{44}CO_2$ ($^{12}C^{16}O^{16}O$) were measured.

The deep water core (GC13) was totally devoid of planktonic foraminifera hence benthic foraminifera *Uvigerina peregrina* were used for $\delta^{18}O$ measurement following the procedure described above. The precision of $\delta^{18}O$ measurements is ±0.1 ‰.

3.4. Radiocarbon dating

The radiocarbon dating is used to determine the absolute age of a sample which contains measurable activity of ^{14}C (radiocarbon). This isotope of carbon has a half life of 5568 ± 30 years (Libby, 1949). The ^{14}C is continuously formed in the atmosphere by the interaction of cosmic ray neutrons on ^{14}N atoms. Then it oxidizes in air forming ^{14}C-dioxide in a way similar to stable carbon-dioxide and enters in carbon cycle through metabolism. When an organism dies the intake of ^{14}C by that organism is ceased. From that moment the ^{14}C begins to decay at a rate dictated by its half-life. By measuring the residual ^{14}C activity in fossilized organism and considering its production rate as constant, the lapsed number of years from its death until the time of measurement (age) can be obtained. Thus, the radiocarbon dating provides absolute age of the samples. Around 1000 tests of mixed planktonic foraminifera were handpicked from the coarse fraction under binocular microscope. Two sub-sections were used for radiocarbon dating of GC14 (shallow-water core). As the coarse fractions from the upper 200 cm sections of GC13 (deep-water core) did not contain sufficient number of tests required for radiocarbon measurements only one bottom section is dated to know the maximum age of this sediment core.

3.5. Organic matter analysis

Sedimentary organic matter holds substantial information on environmental conditions under which it was synthesized by the organisms. The biological paleoproductivity can be inferred from quantifying the sedimentary organic matter if preserved quantitatively (Meyers, 1997). The photosynthetic production in the photic zones is the primary source of organic matters. The proper combination of C, H, N, O and P in accordance with the Redfield Ratio defined (Redfield, 1942) for different types of organic matter is the key to understand the past climate, whether dry or wet. The photosynthetic pathways for fixing CO_2 in the synthesized chlorophyll (organic matter) are different for different ecosystem. For example, higher order plants such as in tropical rain forests and phytoplanktons in the marine environment follow C-3 pathway while the grass and arid climate plants normally follow C-4 pathway, which have very distinct fractionation of CO_2 with ($^{12}CO_2$ or $^{13}CO_2$) molecules in the atmosphere while incorporating in to their photosynthetic matter. Also, the organic matters synthesized through different pathways have different C/N ratios. Redfield (1942) summarized this photosynthetic process for diatom as:

$$106CO_2 + 16HNO_3 + H_3PO_4 + 122H_2O \rightarrow (CH_2O)\ 106(NH_3)_{16}\ H_3PO^4 + 138O_2$$

The subsamples of the sediment cores were rendered salt-free by repeated washing with de-ionized water and freeze dried. Finely ground alternative depth subsamples were decarbonized by treating with 0.1N HCl until the effervescence ceased. The decarbonated sediment was repeatedly washed with DI water, centrifuged, and dried overnight at 50°C. Around 10µg of the decarbonated sediment aliquots were packed in tin-cups and analyzed for C_{org} and total-N in an Elemental Analyzer. Isotopes of C and N were also measured simultaneously by using Thermo Delta$^+$ IRMS coupled to the Element Analyzer. The measurement accuracy of C_{org} is ±2 % and ±0.2 ‰ for $\delta^{13}C$.

3.6. Sediment composition measurement

In order to track the paleo-OMZ dynamics it is necessary to understand the variation in chemical composition of both the sediment cores. The redox-sensitive element concentrations in dispersed Mn-oxide particulates and coatings, which are precipitated as the authigenic oxides, were extracted using acid-reductive procedure. The bulk sediment compositional variation to understand variation in terrigenous matter supply to the core location was measured in bulk sediment digested using strong acid mixture.

The particulate oxides are authigenic Fe-Mn particulates in the sediment column which also scavenge several divalent cations from the water. As explained in introductory section the solubility of redox sensitive elements varies according to the redox variability of the ambient water column. As the terrigenous silicates are the dominant mineral phases in margin sediment potentially subdue the signals of very low concentration of authigenically precipitated oxides. Therefore, it is necessary to extract only the oxides from the sediment using leaching methods capable of leaving behind the silicates without reacting with them. The leaching method adopted in the present study is well established procedure followed by several researchers in the past (see Rutberg et al., 2000; Bayon et al., 2004; Piotrowski et al., 2002; 2012; Wilson et al., 2013).

Step 1 – Carbonate removal

1. Take exactly 1gm of sample in the extraction vial.
2. Add 10 ml of 10 % (v/v) acetic acid.
3. Place the above mixture on rotor for 5 minutes after initial effervescence.
4. Decant the clear solution (without losing the sediment particles from the vial) after centrifuging the mixture at 6000 rpm for 5 minutes.
5. Repeat above steps till the completion of CO_2 release as evident from total absence of effervescence.
6. Washing the residue two times with 30 ml of DI-water after centrifuging and dried.

Step 2 – Oxide leaching

1. Add 10 ml of 0.02M hydroxyl amine hydrochloride in 25 % of acetic acid to the extraction vial containing the residue after decarbonation.
2. Place the above mixture on the rotor disk and rotate for 2 hours.
3. Centrifuge the vials for 7 minutes at 6000 rpm.
4. Transfer the clear leachate to 50 ml acid cleaned and dried beakers.

Step 3 – Pre-concentration

1. Place the vials containing above leachates on hot plate at temperature of 80 °C and evaporate completely the solvent. The residue remaining is the extracted oxide-fraction.
2. Dilute the residue with 5ml of 0.05 M supra-pure HNO_3.
3. The above concentrate of oxide fraction is ready for the analysis.

The salt-free dried sub-samples were ground, and accurately weighed sediment was digested in open PTFE beakers in presence of HF and $HClO_4$. The incipiently dried digest was dissolved in 5 ml of supra-pure 0.5 M HNO_3 and diluted to 20 ml with DI-water for analysis. The USGS nodule reference standards A-1 and P1 were used as reference material to assess the recovery of oxide fraction (Fe-Mn oxide/hydroxide) by the adopted oxide-leaching method. The Japanese sediment standard (JMS-1) was used to assess the accuracy of bulk-sediment composition of acid digested total sample. The solutions were analyzed on Perkin-Elmer Optima 7300 DV ICP-OES calibrated with 5 matrix-matched multi-element calibration standards. The measured and reported values for reference standards are given in Tables 10 and 13 in the next section.

4. RESULTS

4.1. Age of the sediment cores

Two depth-sections (0.5 cm and 281.5 cm) of the GC14A (OMZ sediment core) and one depth section (200 cm) of GC13 (Base-OMZ sediment core) were dated by radiocarbon as described in Section 3. The measured radiocarbon ages were corrected for reservoir age of 331 years estimated for western BoB, north of Sri Lanka (Dutta et al., 2001). The reservoir corrected ages are converted into calendar ages using online CalPal-7 radiocarbon calibration program with reference year of 1950 CE (Dangzelocke et al., 2007). The radiocarbon ages along with lab reference numbers (Arizona University's AMS Facility) are presented in Table 4

Table 4. Radiocarbon ages for dated sections of the two sediment cores

Radiocarbon ages					
Sediment core	Section (cm)	Lab reference Number	^{14}C age y BP	± y	Calibrated age (y BP)
SSK 50 GC 14 A	0.5	AA106592 X29195	2159	35	1770
	281.5	AA106595 X29198	38560	980	42806
SSK 50 GC 13	200	AA106596 X29199	12926	53	15705

From the Table 4 it is evident that the OMZ core (GC14) covers the redefined LGM (~29 ka BP to ~18 ka BP: Clark et al., 2008), last deglaciatin (18 – 12 ka BP) and Holocene (12 – 1.8 ka BP). This core extends back in to later part of the Marine Isotope Stage-3. Whereas, the Base-OMZ core (GC13) covers only later part of the last deglaciation (15.7 – 12 ka BP). For the former sediment core (GC14), the well expressed deglacial climate events in $\delta^{18}O_{G.sacculifer}$ record (Bolling and YD: Figure 9) are used as tie points along with two radiocarbon ages to assign the ages for intermediate sections, which will be described in detail in subsequent section. On the other hand, only the bottom-most section of the latter sediment core (GC13) was dated, hence, it is not possible to assign the actual age for the core-top. However, based on the $\delta^{18}O_{Uvigerina}$ record, which is presented later as Figure 10, I speculate that complete Holocene is represented by this sediment core. This speculation is also based on the presence of semisolid thin peneliquid layer at the core-top observed when the core was collected, which indicates that the core-top is intact. Therefore, the core-top is assumed to be of 'Zero' age. The ages for other intermediate sections are estimated based on the calculated sedimentation rates considering core-top to correspond to "Today or Zero year' and '15.7 ka BP' for core bottom', i.e., a total of 200 cm deposited in 15.7 kilo years.

4.2. Oxygen isotopes and chronology of the OMZ sediment core

The fidelity of a sediment core as palaeoclimate repository depends upon how best that core is intact and deposited continuously over a time period without undergoing any post-depositional disturbances such as internal sediment mixing or slumping or presence of turbidites. Such disturbances in the OMZ sediment core (GC14) may be ruled out based on progressively increasing radiocarbon ages with depth in the sediment core and occurrence of prominent past climatic events. Further, the oxygen isotopic events in this sediment core are closely comparable with other published records from the same region (e.g. see Govil and Naidu, 2011).

Two distinct climate events (YD at 12.3 ka BP and Bølling warm event at 14.5 ka BP) identified in $\delta^{18}O_{G.sacculifer}$ record of the OMZ sediment core (GC14) are exactly similar with those recorded in a nearby sediment core (SK218/A) having eight radiocarbon dates (Govil and Naidu, 2011). Therefore, these events are used as tie-points between two radiocarbon ages (top and bottom sections of the sediment core) for establishing chronology for this sediment core. The core covers a time span of ~42 kyr. The $\delta^{18}O_{G.sacculifer}$ for all the measured sections along with their calculated ages is presented in Table 5 and its depth-profile as Figure 9.

Table 5. Variations of $\delta^{18}O_{G.\ sacculifer}$ extracted from OMZ sediment core (GC14)

Depth cm	Age ka BP	$\delta^{18}O_{G.sacculifer}$ ‰ vPDB	Depth cm	Age ka BP	$\delta^{18}O_{G.sacculifer}$ ‰ vPDB
0.5	1.77	-2.582	139.5	22.40	-1.26
4.5	2.47	-2.35	144.5	23.12	-0.83
8.5	3.17	-2.61	152.5	24.27	-0.51
12.5	3.87	-2.52	160.5	25.42	-1.06
16.5	4.57	-2.17	164.5	25.99	0.21
20.5	5.26	-1.92	168.5	26.57	-0.70
24.5	5.96	-1.55	172.5	27.14	0.61
28.5	6.66	-1.77	176.5	27.72	0.06
32.5	7.36	-2.36	180.5	28.29	-0.32
36.5	8.06	-2.48	188.5	29.44	0.59
44.5	9.46	-1.81	192.5	30.02	0.24
48.5	10.15	-1.95	196.5	30.59	0.54
52.5	10.85	-1.01	200.5	31.17	-0.13
56.5	11.55	-0.52	204.5	31.74	-0.40
60.5	12.25	0.00	212.5	32.89	-0.59
64.5	12.60	-0.74	214.5	33.18	-0.54
68.5	12.95	-0.92	216.5	33.47	-0.50
72.5	13.29	-0.59	220.5	34.04	-0.69
76.5	13.64	-1.24	224.5	34.62	-0.96
80.5	13.99	-0.77	228.5	35.19	-0.77
84.5	14.50	-2.21	232.5	35.77	-0.41
88.5	15.07	-1.85	236.5	36.34	0.60

92.5	15.65	-1.86	240.5	36.91	0.01
96.5	16.22	-1.00	244.5	37.49	0.01
99.5	16.66	-0.88	248.5	38.06	0.54
108.5	17.95	-0.71	256.5	39.21	-0.26
112.5	18.52	-0.10	260.5	39.79	-0.18
116.5	19.10	-0.84	264.5	40.36	-0.48
120.5	19.67	-0.35	268.5	40.94	-0.39
124.5	20.25	-0.42	272.5	41.51	-1.08
128.5	20.82	-0.85	276.5	42.09	-0.90
132.5	21.40	-1.09	280.5	42.66	-0.31
136.5	21.97	-0.62			

Figure 9. Depth-series of $\delta^{18}O_{G.\ sacculifer}$ for OMZ sediment core (GC14)

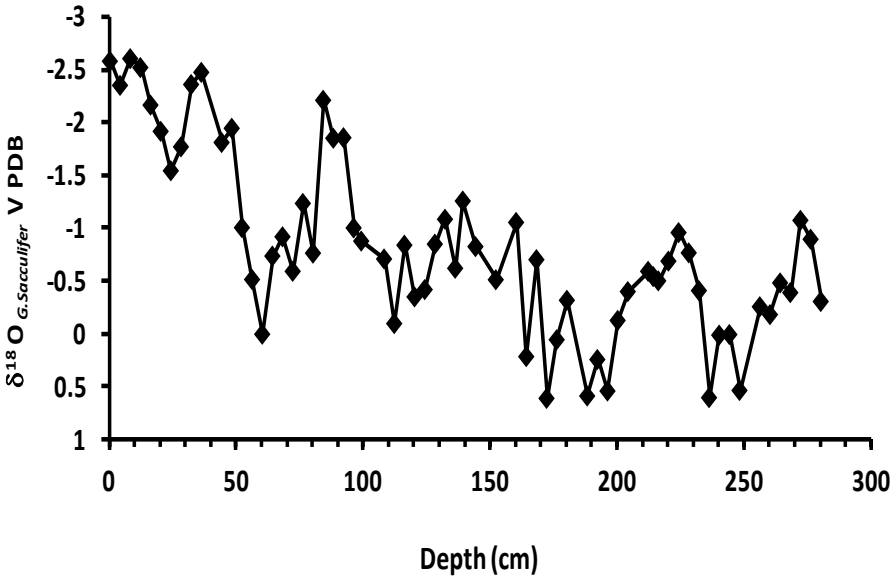

From Figure 9, it is evident that the range of variation in the $\delta^{18}O_{G.\ sacculifer}$ is between 0.5 ‰ and – 2.5 ‰. The enriched values occur between 250 and 150 cm depth intervals and between 70 and 40 cm depth intervals corresponding to 38 – 24 ka BP and 13 – 9 ka BP (Table 5). While most depleted values are found in the upper 40 cm sections and at around 85 cm depth. The former trend is characteristic of cold and dry climate and the latter is for warm and wet climate. There is ~2 ‰ difference between the maximum and minimum $\delta^{18}O_{G.\ sacculifer}$, which is nearly similar to the LGM to Holocene $\delta^{18}O_{G.\ sacculifer}$ contrast found in the AS sediments (Banakar et al., 2005; 2010; Chodankar et al., 2005).

4.3. Time-series of $\delta^{18}O_{U.Perigrina}$ from the Base-OMZ sediment core (GC13)

The Base-OMZ sediment core, which was collected from a water depth of 1474 m is not only devoid of planktonic foraminifera, but also contains very few tests of benthic foraminifera tests. Only in the bottom section (200 cm depth section) abundant number of foraminifera tests were available for radiocarbon dating. Hence, the chronology of this sediment core is based on only one radiocarbon date. The calibrated age for the bottom section (Table 4) indicates that this sediment core covers a time span of last 16 kyr and the $\delta^{18}O_{U. perigrina}$ are presented in Table 6 and Figure 10. The reason for the scarcity of foraminifera is not clear. However, few carbonate test present in the sediment core are intact and hence loss due to dissolution may be ruled out. The possibility of terrigenous matter diluting the carbonate fraction is likely, but could not be confirmed. All the available benthic foraminifera tests of *U. peregrina* (10-15 Nos.) from each section were utilized for $\delta^{18}O$ measurement. The standard precision of the $\delta^{18}O$ measurement is 0.1‰.

Table 6. Variations of $\delta^{18}O_{U.Perigrina}$ with depth/age in Base-OMZ sediment core (GC13)

Depth cm	Age ka BP	$\delta^{18}O_{U. perigrina}$ ‰ vPDB	Depth cm	Age ka BP	$\delta^{18}O_{U. perigrina}$ ‰ vPDB
0.5	0.33	3.11	76.5	6.17	3.12
4.5	0.64	3.08	80.5	6.48	3.11
8.5	0.95	3.13	84.5	6.79	3.11
12.5	1.25	3.03	88.5	7.10	3.15
20.5	1.87	3.05	92.5	7.40	3.07
24.5	2.18	3.11	96.5	7.71	3.18
28.5	2.48	3.09	100.5	8.02	3.03
32.5	2.79	3.01	108.5	8.63	3.19
36.5	3.10	3.12	116.5	9.25	3.09
40.5	3.41	3.10	124.5	9.86	3.16
44.5	3.71	3.06	128.5	10.17	3.12
48.5	4.02	3.07	152.5	12.02	3.20
52.5	4.33	3.00	160.5	12.63	3.18
56.5	4.64	3.12	168.5	13.25	3.15
60.5	4.94	3.11	176.5	13.86	3.35
64.5	5.25	3.10	184.5	14.48	3.16
68.5	5.56	3.05	192.5	15.09	3.45
72.5	5.87	3.07	200.5	15.71	3.33

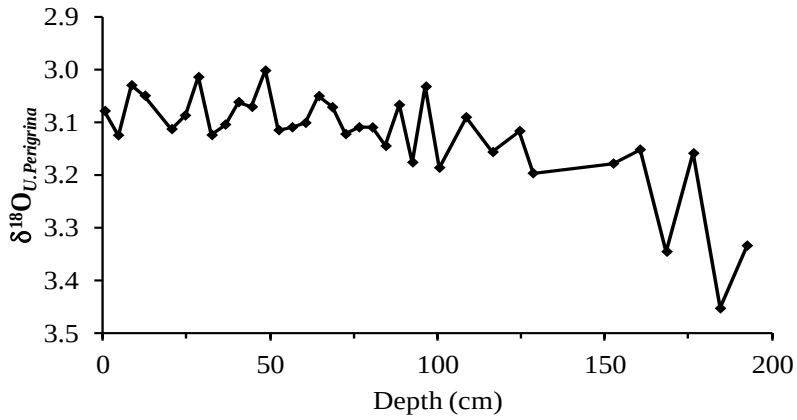

Figure 10. Depth-series of $\delta^{18}O_{U.Perigrina}$ in deep-water sediment core (GC13)

The consistently depleted $\delta^{18}O_{U.perigrina}$ is evident from 150 cm depth up to the core-top with values around 3.1‰, whereas, the sections below 150 cm exhibit slightly enriched values (Figure 10). The former interval corresponds to 15.7 ka BP to 12.8 ka BP and the latter sections represent the period older than12 ka BP (Table 6). Although, the $\delta^{18}O_{U.perigrina}$ contrast between these two intervals is small (~0.4 ‰), it in fact, indicates a kind of transitional climate from cold to warm.

4.4. Organic matter measurements

The down core variations of the marine organic matter and its nature can reveal environmental changes in the past. The present dataset of sedimentary organic matter comprises organic carbon (C_{org}), total nitrogen (N_{tot}), and carbon isotopes (δ^{13} C_{org}). The accuracy of the measurements is assessed by reference standards analyzed along with samples and presented as Table 7 and 8

Table 7. Concentration ranges, range, and analytical errors associated with measured components of the organic matter in two sediment cores

			BBOT		Sucrose
			C_{org} %	N %	$\delta^{13}C_{org}$ ‰
Reference standards		Reported	72.53±0.26	6.51±0.15	-10.45
		Analyzed	71.8	6.95	-10.59
		% Error	1.05	6.82	-1.31
Present sediments Cores	GC14	Lowest	1.70	0.08	-19.80
		Highest	6.92	0.81	-17.27
		Mean	2.67	0.23	-18.51
	GC13	Lowest	1.56	0.13	-20.71
		Highest	2.88	1.13	-18.67
		Mean	2.24	0.25	-19.69

Table 8. Variations of C_{org}, and $\delta^{13}C_{org}$ with depth/age in OMZ sediment core (GC14)

Depth cm	Age ka BP	$\delta^{13}C_{org}$ ‰ vPDB	C_{org} %	Depth cm	Age ka BP	$\delta^{13}C_{org}$ ‰ vPDB	C_{org} %
0.5	1.8	-18.1	1.8	134.5	21.7	-19.0	2.4
2.5	2.1	-17.6	1.7	140.5	22.5	-19.0	2.4
4.5	2.5	-18.3	1.8	142.5	22.8	-18.8	2.7
6.5	2.8	-17.6	1.8	144.5	23.1	-19.0	2.6
8.5	3.2	-17.6	1.8	146.5	23.4	-19.1	2.4
10.5	3.5	-17.5	1.8	148.5	23.7	-18.9	2.7
12.5	3.9	-17.4	1.8	150.5	24.0	-18.6	4.8
14.5	4.2	-17.6	2.0	152.5	24.3	-19.0	2.7
16.5	4.6	-17.4	2.1	154.5	24.6	-18.8	2.5
18.5	4.9	-17.9	2.1	156.5	24.8	-18.8	2.1
20.5	5.3	-17.7	2.1	158.5	25.1	-18.9	2.8
22.5	5.6	-17.5	2.2	160.5	25.4	-18.7	2.6
24.5	6.0	-17.8	2.2	162.5	25.7	-18.8	2.4
26.5	6.3	-17.4	2.2	164.5	26.0	-18.7	3.7
28.5	6.7	-17.7	2.2	166.5	26.3	-18.8	2.3
30.5	7.0	-17.8	2.3	170.5	26.9	-18.7	2.3
32.5	7.4	-17.9	2.2	172.5	27.1	-18.8	2.8
34.5	7.7	-17.8	2.3	176.5	27.7	-18.8	2.3
36.5	8.1	-17.8	2.3	178.5	28.0	-18.6	2.2
38.5	8.4	-17.5	2.2	180.5	28.3	-18.8	2.1
40.5	8.8	-17.9	2.2	182.5	28.6	-19.2	4.8
42.5	9.1	-18.1	2.4	184.5	28.9	-18.7	2.1
44.5	9.5	-18.4	2.2	186.5	29.2	-19.2	2.6
46.5	9.8	-18.4	2.4	188.5	29.4	-18.7	2.3
48.5	10.2	-18.3	2.2	190.5	29.7	-18.8	2.5
50.5	10.5	-18.7	2.6	192.5	30.0	-18.7	2.3
52.5	10.9	-18.6	2.4	194.5	30.3	-18.4	2.4
54.5	11.2	-18.7	2.4	196.5	30.6	-18.6	2.4
56.5	11.6	-19.7	2.4	200.5	31.2	-18.1	1.8
58.5	11.9	-19.4	2.6	202.5	31.5	-18.5	2.3
60.5	12.3	-19.3	2.6	204.5	31.7	-18.5	1.9
62.5	12.4	-19.1	2.8	206.5	32.0	-18.3	2.2
64.5	12.6	-18.8	2.8	208.5	32.3	-18.4	2.3
66.5	12.8	-19.0	2.7	210.5	32.6	-18.5	2.3
68.5	12.9	-18.4	2.6	212.5	32.9	-18.6	6.9
70.5	13.1	-18.3	2.5	214.5	33.2	-18.1	6.9
72.5	13.3	-18.3	2.6	216.5	33.5	-18.1	5.2
74.5	13.5	-18.8	2.0	218.5	33.8	-18.2	5.8
76.5	13.6	-18.4	2.3	220.5	34.0	-18.4	2.9
78.5	13.8	-19.3	2.3	222.5	34.3	-18.3	3.4
80.5	14.0	-19.2	2.5	228.5	34.6	-18.5	3.5
84.5	14.5	-19.1	2.3	230.5	35.5	-18.0	2.8
86.5	14.8	-19.7	3.2	232.5	35.8	-17.9	1.8

88.5	15.1	-19.8	2.3	234.5	36.1	-18.0	4.2
90.5	15.4	-19.5	2.3	236.5	36.3	-18.1	2.3
92.5	15.6	-19.3	2.2	238.5	36.6	-18.0	5.4
94.5	15.9	-19.4	2.4	240.5	36.9	-17.9	2.4
96.5	16.2	-19.3	2.2	242.5	37.2	-18.0	4.3
98.5	16.5	-19.2	2.0	244.5	37.5	-18.1	2.9
100.5	16.8	-19.3	2.0	246.5	37.8	-18.2	3.7
102.5	17.1	-19.2	2.1	248.5	38.1	-17.9	4.5
104.5	17.4	-19.2	1.9	250.5	38.4	-18.0	3.9
106.5	17.7	-19.4	2.2	252.5	38.6	-18.2	3.6
108.5	17.9	-19.6	2.3	254.5	38.9	-17.9	4.1
110.5	18.2	-19.7	2.2	256.5	39.2	-17.8	2.3
112.5	18.5	-19.7	2.2	258.5	39.5	-17.8	2.4
114.5	18.8	-19.5	2.1	260.5	39.8	-17.8	5.1
116.5	19.1	-19.3	1.9	262.5	40.1	-18.0	2.1
118.5	19.4	-19.3	2.2	264.5	40.4	-17.5	3.3
122.5	20.0	-18.9	2.3	266.5	40.7	-18.0	3.3
124.5	20.2	-19.3	2.2	268.5	40.9	-17.8	3.0
126.5	20.5	-19.1	2.1	270.5	41.2	-18.2	6.0
128.5	20.8	-19.0	2.1	272.5	41.5	-17.8	2.5
130.5	21.1	-19.1	2.3	274.5	41.8	-17.3	2.0
132.5	21.4	-19.1	2.3	276.5	42.1	-17.5	2.0

Figure 11. Depth-series of C_{org}, and $\delta^{13}C_{org}$ of the OMZ sediment core (GC14).

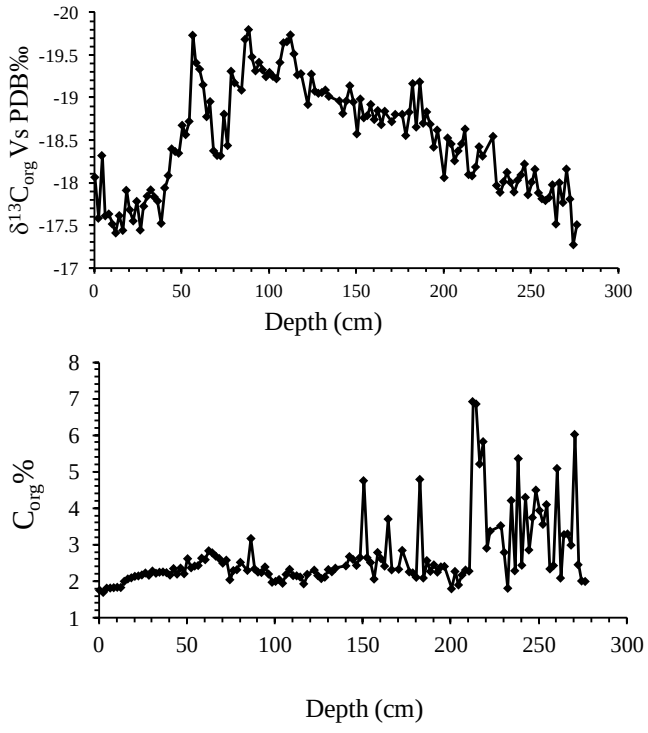

Table 9. Variations of total organic carbon and $\delta^{13}C_{org}$ in Base-OMZ core (GC13)

Depth (cm)	Age KyBP	$\delta^{13}C_{org}$ ‰	C_{org} %	Depth (cm)	Age KyBP	$\delta^{13}C_{org}$ ‰	C_{org} %
0.5	0.3	-20.0	1.7	86.5	6.9	-19.5	2.5
2.5	0.5	-19.4	1.6	90.5	7.2	-19.6	2.6
4.5	0.6	-19.4	1.6	94.5	7.6	-19.9	2.6
8.5	0.9	-19.3	1.6	96.5	7.7	-20.1	2.7
10.5	1.1	-19.2	1.7	98.5	7.9	-19.6	2.6
12.5	1.3	-19.1	1.6	102.5	8.2	-19.9	2.7
14.5	1.4	-19.7	1.8	106.5	8.5	-20.1	2.6
16.5	1.6	-19.1	1.8	110.5	8.8	-20.2	2.7
18.5	1.7	-19.1	1.7	114.5	9.1	-20.1	2.6
20.5	1.9	-18.8	1.7	116.5	9.2	-20.1	2.7
22.5	2.0	-19.0	1.8	118.5	9.4	-20.2	2.6
24.5	2.2	-19.0	1.9	120.5	9.6	-20.3	2.4
26.5	2.3	-19.3	1.9	122.5	9.7	-20.4	2.6
28.5	2.5	-18.8	1.7	124.5	9.9	-20.7	2.4
30.5	2.6	-19.0	1.9	126.5	10.0	-20.1	2.4
32.5	2.8	-19.1	1.8	128.5	10.2	-20.4	2.1
34.5	2.9	-18.7	1.9	150.5	11.9	-20.3	2.4
36.5	3.1	-18.7	1.9	154.5	12.2	-20.1	2.3
38.5	3.3	-19.0	1.9	156.5	12.3	-19.9	2.2
40.5	3.4	-18.9	1.9	158.5	12.5	-20.1	2.3
42.5	3.6	-19.0	2.0	160.5	12.6	-20.3	2.2
44.5	3.7	-19.4	1.9	162.5	12.8	-20.1	2.3
46.5	3.9	-19.0	2.1	164.5	12.9	-20.5	2.2
48.5	4.0	-19.2	2.1	166.5	13.1	-20.2	2.4
50.5	4.2	-20.3	2.1	168.5	13.2	-20.6	2.2
52.5	4.3	-19.2	2.2	170.5	13.4	-20.3	2.4
54.5	4.5	-19.1	2.2	172.5	13.6	-20.5	2.2
56.5	4.6	-18.7	2.0	174.5	13.7	-20.0	2.3
58.5	4.8	-19.5	2.3	176.5	13.9	-20.4	2.4
60.5	4.9	-19.3	2.3	180.5	14.2	-20.4	2.5
62.5	5.1	-19.4	2.3	182.5	14.3	-20.0	2.4
64.5	5.3	-19.7	2.4	184.5	14.5	-20.5	2.4
66.5	5.4	-19.4	2.3	186.5	14.6	-20.0	2.5
68.5	5.6	-19.5	2.3	187.5	14.7	-20.2	2.4
70.5	5.7	-19.4	2.3	190.5	14.9	-19.9	2.6
72.5	5.9	-19.2	2.4	192.5	15.1	-20.4	2.4
74.5	6.0	-19.8	2.6	194.5	15.2	-19.4	2.6
78.5	6.3	-19.8	2.6	196.5	15.4	-20.0	2.5
82.5	6.6	-19.9	2.6	198.5	15.6	-19.3	2.9
84.5	6.8	-19.6	2.5				

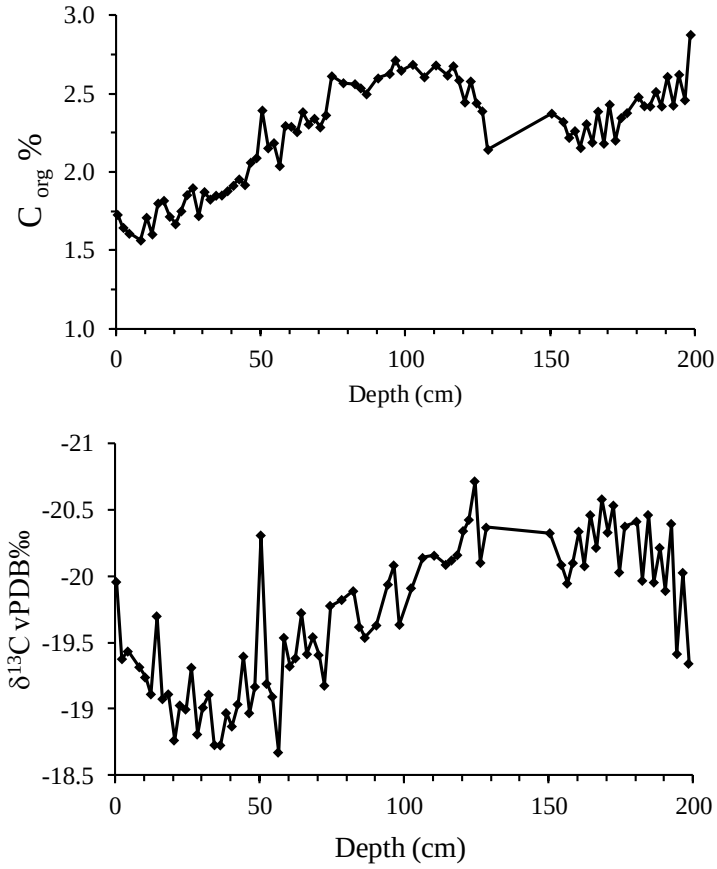

Figure 12. Depth-series of C_{org} and $\delta^{13}C_{org}$ in Base-OMZ sediment core (GC13).

4.5. Variations in elemental composition

Several major and minor elements in marine sediment provide clues about their source and pathways, which are normally dependent of monsoon variations. The terrigenous silicate detritus entering the marine regime also determines the remineralization depth of organic matter (Azhar et al., 2018). For this purpose the down-core elemental distribution of a set of index elements are measured in both bulk sediment, as well as in authigenically precipitated oxide (hydrolysate or leachable) component of the sediment. A complete recovery of authigenic component by any adopted leaching methods is important for reliable interpretations, hence, needs to be validated. The Table 10 below helps to assess the extraction-efficiency of the leaching method adopted in this study.

Table 10. Recovery details of primary elements with respect to authigenic oxide fraction. Two ferromanganese nodule (Fe-Mn oxide) reference standards having genetic and compositional similarity to the authigenic-oxide particles in the sediment are utilized.

Element	Fe-Mn nodule standard (element oxide in %)				Present sediment cores (element in ppm)					
	USGS A1		USGS P1		GC 14 A			GC 13		
	Measured	Reported	Measured	Reported	Average	Lowest	highest	Average	lowest	highest
Mn	24.2	23.9	38.71	37.6	23	13	39	139	93	226
Fe	16.4	15.6	8.43	8.3	1545	102	3438	2963	1836	4043

From Table 10 it is evident that the recovery of elements associated with the Fe-Mn oxide fraction of the reference material is nearly complete (> 95 %). Therefore, the elemental composition of authigenic components of the present sediment cores presented in Tables 10, 11, and 12 may be considered as reliable.

Table 11. Composition of authigenic oxide fraction leached from OMZ sediment core (GC14)

Depth	Ka BP	Mn (ppm)	Fe (ppm)	Ti (ppm)	Co (ppm)	Cr (ppm)	V (ppm)	Mo (ppb)	U (ppb)	Re (ppb)
0.5	1.8	17	301	0.3	1.0	1.4	6.0	8.0	0.4	0.3
8.5	3.2	17	379	0.3	1.1	1.4	7.2	5.4	0.5	0.2
16.5	4.6	18	552	0.3	1.4	1.8	6.2	4.5	0.6	0.4
24.5	6.0	19	704	0.4	1.7	1.7	8.0	4.1	0.5	0.4
32.5	7.4	26	1007	0.5	2.5	2.1	6.8	4.3	0.6	0.4
40.5	8.8	24	1104	0.8	2.7	2.0	6.6	3.5	0.7	0.6
48.5	10.2	26	1199	1.2	3.1	1.8	5.2	3.3	0.8	0.5
56.5	11.6	35	1132	4.6	3.4	1.7	4.0	4.0	1.8	0.6
64.5	12.6	27	913	9.8	3.1	2.2	3.3	5.0	3.7	0.8
72.5	13.3	16	1132	3.6	2.2	1.8	3.5	4.0	1.1	0.5
80.5	14.0	18	102	0.1	1.6	0.6	3.2	3.7	0.0	0.4
88.5	15.1	26	1991	2.1	3.4	1.6	4.3	3.6	1.1	0.6
96.5	16.2	26	1710	0.4	2.2	1.3	5.1	4.1	0.6	1.1
104.5	17.4	14	1319	0.5	2.0	0.8	3.2	2.6	0.4	0.6
112.5	18.5	21	2013	0.8	2.1	1.5	7.0	4.0	0.8	0.3
120.5	19.7	13	846	0.5	1.0	0.7	2.4	2.0	0.6	0.2
128.5	20.8	21	1617	0.7	2.0	1.3	6.6	2.5	0.5	0.3
136.5	22.0	24	2089	0.4	2.4	1.5	7.1	3.2	0.4	0.4
145.5	23.3	20	2023	0.6	2.1	1.8	6.7	2.9	0.8	0.3
152.5	24.3	21	2007	0.5	2.1	1.6	8.1	4.4	0.5	0.4
168.5	26.6	22	2373	0.6	2.3	2.0	8.6	6.5	0.7	0.6
176.5	27.7	32	1852	1.1	2.8	1.9	6.4	5.0	2.0	0.4
184.5	28.9	26	2052	1.8	2.3	2.0	7.6	6.5	3.3	0.5
194.5	30.3	20	2278	0.5	2.4	2.1	7.0	4.8	1.4	0.5
200.5	31.2	29	1999	0.7	3.3	2.3	9.8	5.4	0.8	0.7

208.5	32.3	14	4758	0.5	1.8	2.1	6.1	5.0	1.0	0.8
216.5	33.5	39	1291	5.6	3.4	2.4	6.9	6.1	2.1	0.7
224.5	34.6	24	2071	1.1	2.0	2.6	8.0	8.9	1.3	0.6
232.5	35.8	14	3438	0.4	2.1	1.8	6.7	8.5	0.7	0.5
240.5	36.9	23	2167	0.5	2.3	2.2	8.1	5.3	0.8	0.7
248.5	38.1	29	1777	0.8	1.9	3.0	10.7	11.7	0.9	1.3
256.5	39.2	25	1942	0.5	2.5	1.9	7.5	2.4	0.4	0.6
265.5	40.5	18	1893	0.3	2.0	2.3	8.4	4.7	0.4	0.6
273.5	41.7	23	1562	0.5	2.0	1.6	9.1	6.8	0.6	0.4
280.5	42.7	25	2432	0.7	2.6	2.1	9.3	5.1	0.8	0.6

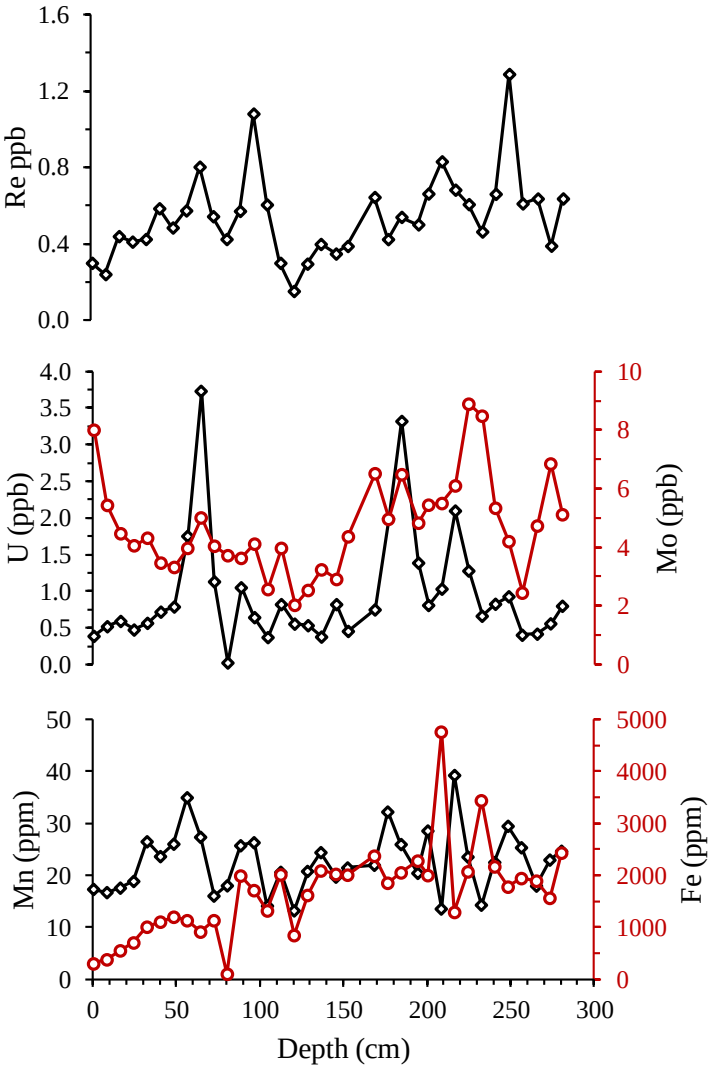

Figure 13. Depth profile of elements in the leachable fraction of OMZ sediment core (GC14).

Table 12. Composition of authigenic oxide fraction leached from Base-OMZ sediment core (GC13).

Depth (cm)	Ka BP	Mn (ppm)	Fe (ppm)	Ti (ppm)	U (ppm)	Re (ppb)	Mo (ppb)	Co (ppm)	V (ppm)	Cr (ppb)
0.5	0.3	170	1284	0.2	0.4	0.0	1.2	9.4	5	949
8.5	0.9	164	1987	0.3	0.5	0.1	2.3	9.8	6	1394
16.5	1.6	175	2012	0.4	0.7	0.1	2.3	9.8	7	1398
24.5	2.2	148	2468	0.4	0.8	0.2	2.4	8.9	7	1487
32.5	2.8	119	2204	0.2	0.8	0.2	2.3	7.9	7	1404
40.5	3.4	121	2047	0.2	0.6	0.2	2.4	7.4	7	1429
48.5	4.0	120	2748	0.2	0.8	0.3	2.4	7.6	7	1642
56.5	4.6	99	2819	0.3	1.1	0.4	3.5	6.8	8	1901
64.5	5.3	84	2827	0.3	1.1	0.5	3.1	6.6	8	1794
72.5	5.9	75	2406	0.2	1.0	0.4	3.3	5.7	6	1583
80.5	6.5	72	2411	0.2	1.0	0.3	3.0	5.8	6	1638
88.5	7.1	95	2378	0.3	1.1	0.7	5.3	5.6	6	1743
96.5	7.7	82	1948	0.3	1.3	0.4	5.5	6.3	6	1753
104.5	8.3	91	2449	0.3	1.8	0.6	7.4	5.5	7	2057
112.5	8.9	92	2059	0.3	1.4	0.4	7.7	5.1	6	1788
120.5	9.6	91	2016	0.3	1.4	0.4	7.1	5.5	6	1855
128.5	10.2	122	1920	0.3	1.1	0.5	6.4	5.2	6	1759
152.5	12.0	84	1883	0.2	1.0	0.3	7.0	4.8	6	1593
160.5	12.6	104	1925	0.5	1.0	0.2	7.8	5.4	6	1531
168.5	13.2	83	1667	0.3	0.9	0.2	8.7	4.0	5	1510
176.5	13.9	104	1777	0.3	1.0	0.8	8.8	5.7	6	1546
181.5	14.2	88	1316	0.2	0.8	0.3	7.5	4.7	5	1307
192.5	15.1	109	1877	0.3	0.8	0.3	9.8	6.5	6	1616
200.5	15.7	104	1303	0.3	0.7	0.7	6.8	5.3	5	1571

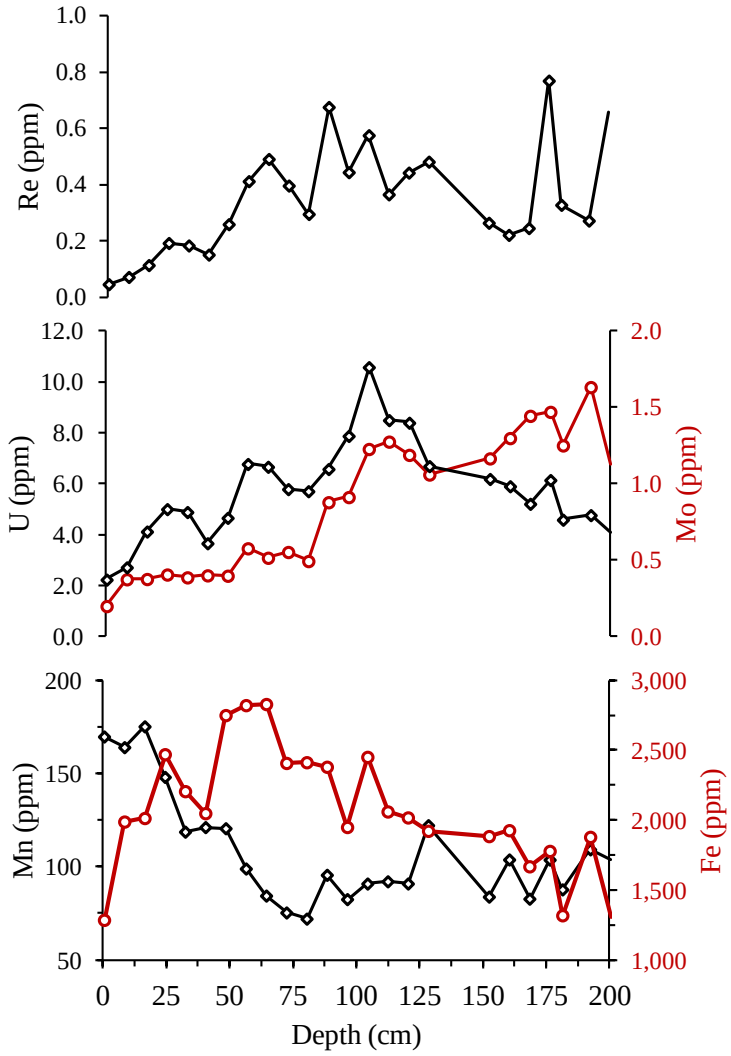

Figure 14. Depth profile of elements in the leachable fraction from Base-OMZ sediment core.

4.6. Bulk sediment composition

The bulk sediment composition is nothing but the total-sediment composition, which is cumulative result of all fractions together, forming the sediment. As the continental shelf sediment in the vicinity of river discharge points can capture the changes in terrigenous silicate supply, the present OMZ sediment core (GC14) is suitable for understanding the monsoon dependent variation in river discharge of silicate matter derived from the land they drain. To assess the accuracy of analytical results one reference standards (Japanese Marine Sediment-1: JMS1) is used and the percent error associated with the results are presented in Table 13. This table also contains range of variation of the analyzed elements. The Tables 14 and 15 present the down-core variation of a set of elements utilized in the present study and their depth-series are presented as Figures 15 and 16.

Table 13. Analytical errors estimated from the sediment reference standards

##	*JMS-1 standard (Deviation in % of the reported values)*	Sediment cores (concentration units given in first column are applicable to all other columns)					
		GC14 (Shallow-water core)			GC13 (deep-water core)		
		Lowest	Highest	Average	Lowest	Highest	Average
Fe	*8*	0.50 (%)	7.64	4.83	5.17	7.82	6.35
Mg	*7*	0.84 (%)	1.97	1.43	1.46	2.34	1.87
Zn	*2*	44 (ppm)	129	75	97	157	118
Ti	*3*	0.03 (%)	0.58	0.42	0.32	0.57	0.44
V	*7*	39 (ppm)	134	98	112	195	148
Mn	*6*	0.01 (%)	0.04	0.03	0.03	0.05	0.04
Ca	*8*	2.17 (%)	20.19	9.04	NA	NA	NA
Al	*7*	3.26 (%)	7.86	6.12	7.14	9.22	8.22
Co	*11*	0 (ppm)	24	9	20	35	27
Ni	*5*	35 (ppm)	94	72	67	110	83
Cr	*NA*	55 (ppm)	130	95	NA	NA	NA

NA – Not available (analyzed values are very close to blank level, hence rejected).
- The element variations in the time-series larger than the above estimated percent deviation (1σ error) only are considered as significant for interpretations.

Table 14. Depth-distribution of major and minor elements in OMZ sediment core (GC14)

Age KaBP	Al %	Ti %	Fe %	Mn %	Mg %	Bulk-Ca %	Co ppm	Zn ppm	Cr ppm	V ppm	Carb-Ca %	Ba ppm	Sr ppm	Sc ppm	Cu Ppm
1.77	6.65	0.55	4.85	0.043	1.57	4.15	25	79	96	117	1.98	196	215	12	67
2.47	6.84	0.55	5.04	0.040	1.60	4.31	24	78	104	120	2.14	198	213	13	68
3.17	6.99	0.56	5.21	0.037	1.59	4.84	24	81	102	124	2.67	20	220	12	69
3.87	6.94	0.55	5.25	0.037	1.62	5.36	23	80	107	118	3.19	168	240	11	69
4.57	6.69	0.53	4.93	0.033	1.58	6.19	22	77	93	112	4.02	185	225	11	60
5.96	5.55	0.45	4.32	0.025	1.36	6.91	17	70	83	103	4.74	203	228	10	69
6.66	5.79	0.43	4.02	0.024	1.31	6.57	15	65	77	90	4.40	211	236	11	63
8.06	5.27	0.37	3.63	0.020	1.12	8.06	12	71	81	80	5.89	227	238	12	64
8.76	5.12	0.36	3.51	0.019	1.07	8.68	11	75	93	77	6.51	234	255	11	63
9.46	5.19	0.36	3.55	0.017	1.09	9.54	11	73	83	73	7.37	261	309	9	53
10.85	4.92	0.31	3.21	0.017	1.02	10.27	8	67	70	60	8.10	271	349	9	52
11.55	4.67	0.29	3.10	0.016	0.99	12.07	6	53	76	55	9.90	234	409	8	49
12.25	3.49	0.23	2.45	0.013	0.84	15.57	4	44	65	42	13.40	27	538	6	40
12.60	3.33	0.23	2.44	0.013	0.88	19.22	3	54	76	42	17.05	240	659	4	33
12.95	3.26	0.22	2.62	0.011	0.90	20.19	2	57	76	39	18.02	309	702	4	32
13.29	3.93	0.26	3.14	0.013	0.97	17.30	4	52	75	52	15.13	277	759	3	35
13.64	4.27	0.28	3.30	0.014	1.02	15.84	5	52	86	54	13.67	260	707	2	24
13.99	4.41	0.29	3.56	0.015	1.02	15.80	5	52	73	60	13.63	240	607	4	32
14.50	4.87	0.33	3.60	0.017	1.13	15.97	7	62	76	67	13.80	32	556	4	37
15.07	5.28	0.36	3.76	0.017	1.10	13.10	9	60	73	70	10.93	300	538	3	38
15.65	6.06	0.43	3.94	0.025	1.45	9.26	13	69	87	93	7.09	271	501	6	40

16.22	6.49	0.46	4.19	0.027	1.53	7.35	14	75	92	98	5.18	277	433	5	41
16.66	6.31	0.43	3.99	0.025	1.46	8.86	14	70	90	93	6.69	274	456	9	57
16.80	6.20	0.45	5.31	0.028	1.63	10.58	6	74	98	96	8.41	265	468	8	63
17.95	5.95	0.45	5.17	0.028	1.72	10.21	6	69	93	105	8.04	250	641	8	60
18.52	6.39	0.48	5.28	0.030	1.79	9.08	5	73	98	107	6.91	237	623	7	55
19.10	6.77	0.48	5.17	0.028	1.80	9.21	4	75	103	107	7.04	270	587	10	66
19.67	6.29	0.46	5.06	0.028	1.68	9.71	5	78	99	102	7.54	25	522	8	53
20.25	6.12	0.44	5.68	0.031	1.60	8.27	5	71	55	100	6.10	251	437	9	44
20.82	7.06	0.52	5.59	0.030	1.77	7.15	7	81	107	115	4.98	251	470	9	61
21.40	7.15	0.49	6.01	0.031	1.74	8.82	5	83	110	107	6.65	353	360	10	63
21.97	7.76	0.58	7.09	0.037	1.97	8.00	11	106	130	134	5.83	250	443	9	60
22.55	7.28	0.54	6.78	0.037	1.86	8.29	9	103	130	124	6.12	268	334	9	64
23.12	6.86	0.51	6.09	0.036	1.86	8.83	7	87	114	116	6.66	247	504	9	62
23.70	6.47	0.48	5.91	0.032	1.77	10.79	5	78	99	110	8.62	242	387	9	63
24.27	6.88	0.48	5.89	0.030	1.71	7.67	10	78	101	119	5.50	231	427	9	64
24.85	6.53	0.47	5.88	0.032	1.63	10.01	6	88	105	106	7.84	245	539	9	54
25.42	6.75	0.48	5.55	0.029	1.71	9.21	5	78	103	107	7.04	256	522	8	58
25.99	6.05	0.42	7.10	0.027	1.60	9.39	2	75	97	98	7.22	248	555	7	59
26.57	6.83	0.48	5.96	0.032	1.76	10.84	7	83	112	122	8.67	238	648	6	56
27.14	6.08	0.41	7.64	0.028	1.58	9.70	2	74	98	98	7.53	241	562	8	60
27.72	6.17	0.42	5.13	0.027	1.60	10.91	3	69	94	102	8.74	228	586	7	64
28.87	5.46	0.37	4.94	0.026	1.50	13.49	0	60	79	89	11.32	221	562	6	53
29.44	5.15	0.35	6.46	0.025	1.41	12.63	0	66	85	86	10.46	246	549	7	53
30.02	5.56	0.39	5.73	0.025	1.46	10.74	1	66	81	98	8.57	289	543	6	51
30.59	6.16	0.40	4.87	0.027	1.42	8.87	1	66	86	95	6.70	311	475	6	54
31.17	6.15	0.40	4.33	0.023	1.45	9.12	1	62	87	96	6.95	306	309	8	59
31.74	5.30	0.33	3.99	0.020	1.27	10.83	4	58	74	84	8.66	265	323	8	59
32.32	5.86	0.37	5.87	0.024	1.37	7.30	7	77	93	102	5.13	329	678	7	56
32.89	6.86	0.42	4.91	0.023	1.40	5.92	9	79	93	106	3.75	343	328	6	60
33.47	6.31	0.39	4.86	0.024	1.44	10.38	8	68	86	104	8.21	224	248	7	53
34.33	4.99	0.31	5.64	0.018	1.09	8.10	4	59	71	85	5.93	310	414	7	46
35.19	7.62	0.46	5.25	0.026	1.38	9.31	10	85	109	106	7.14	283	464	4	48
35.77	6.28	0.35	5.26	0.020	1.14	7.25	6	82	82	88	5.08	283	431	8	56
36.91	4.11	0.25	3.17	0.016	0.86	5.24	1	51	68	63	3.07	290	618	5	58
37.49	6.36	0.40	4.34	0.024	1.34	7.85	10	82	125	109	5.68	279	241	9	57
38.06	6.88	0.42	4.77	0.028	1.46	6.35	9	90	110	125	4.18	288	341	7	53
38.64	7.14	0.44	5.01	0.027	1.45	5.01	10	97	106	121	2.84	277	257	7	54
39.21	7.30	0.44	5.07	0.028	1.40	6.57	12	93	107	112	4.40	269	237	7	55
39.79	7.09	0.44	4.14	0.024	1.41	5.48	10	81	112	111	3.31	275	172	7	53
40.36	7.67	0.46	4.91	0.023	1.53	4.01	13	104	122	123	1.84	264	107	9	64
41.51	7.55	0.45	4.92	0.24	1.53	2.17	16	100	118	121		270	99	9	55
42.81	7.35	0.45	5.23	0.025	1.44	6.40	13	94	120	123	4.23	231	216	3	59

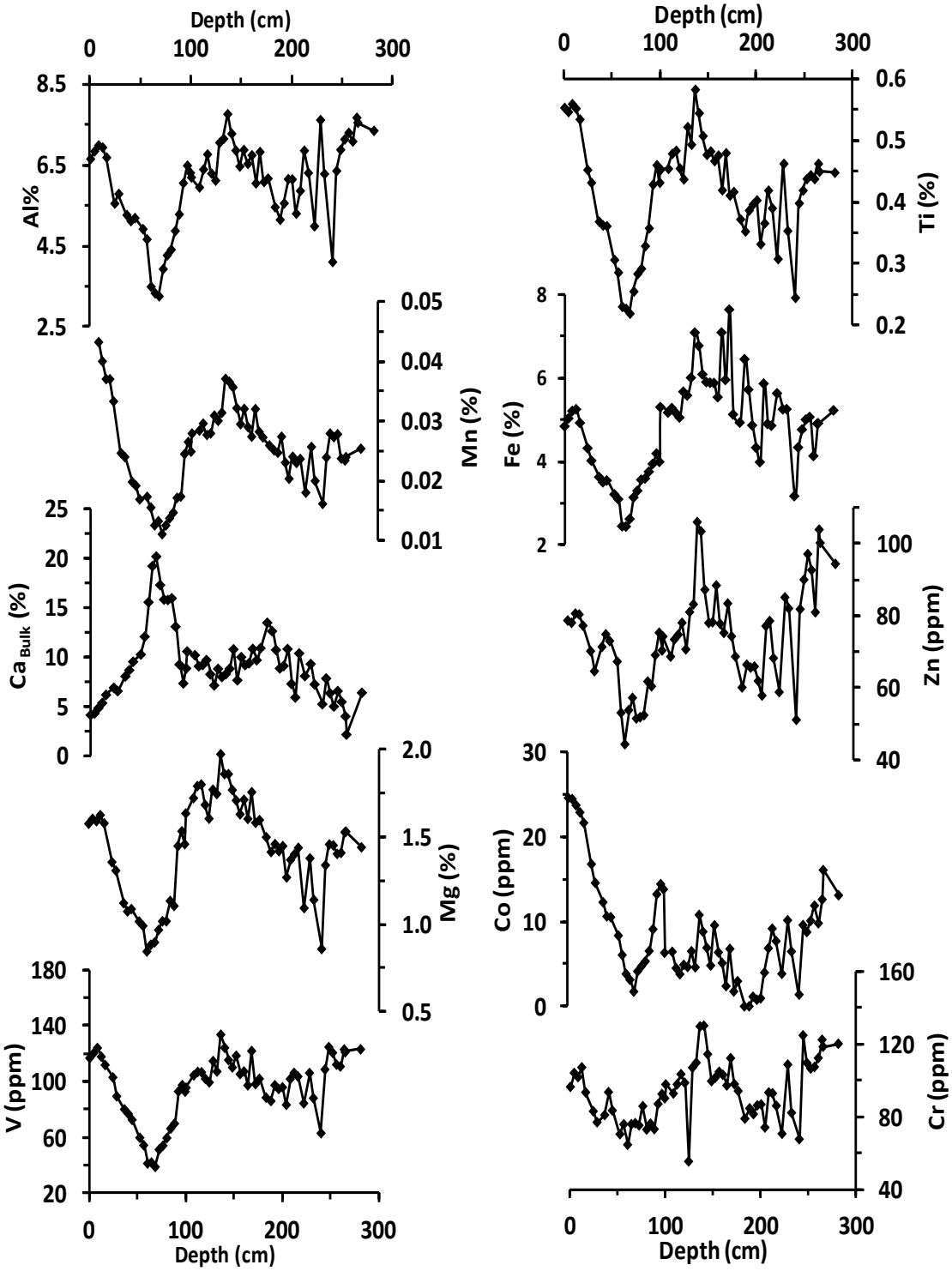

Figure 15. Depth distribution of elements in bulk sediment of GC14 (OMZ sediment core)

Table 15. Depth-distribution of major and minor elements in Base-OMZ sediment core (GC13)

Age ka	Al %	Ti %	Fe %	Mn %	Mg %	Co ppm	Zn ppm	V ppm	Sr Ppm	Cu ppm	Ni ppm
0.33	8.24	0.49	6.92	0.05	2.16	32	115	170	97	82	87
0.64	8.12	0.53	6.82	0.05	2.14	33	114	175	97	84	87
0.95	8.25	0.52	7.20	0.05	2.16	33	117	178	34	85	90
1.25	8.30	0.49	7.00	0.04	2.15	31	120	172	93	82	87
1.56	8.81	0.56	7.42	0.05	2.25	35	129	187	100	86	96
1.87	8.81	0.45	7.65	0.04	2.31	32	130	179	79	86	96
2.18	8.64	0.53	7.13	0.05	2.18	32	123	177	103	78	91
2.48	9.08	0.53	7.82	0.05	2.34	33	157	190	94	97	99
2.79	8.75	0.56	7.64	0.05	2.33	34	134	195	103	94	97
3.10	8.48	0.52	7.31	0.04	2.25	32	126	187	93	85	110
3.41	8.27	0.57	7.09	0.05	2.14	33	132	186	100	85	98
3.71	8.08	0.56	6.91	0.04	2.09	31	122	178	101	81	89
4.33	8.30	0.51	6.71	0.04	2.01	29	120	169	100	76	86
4.94	8.51	0.52	6.51	0.04	1.91	29	123	164	107	71	87
5.25	8.66	0.51	6.57	0.04	1.91	28	123	164	109	70	87
5.56	9.22	0.40	6.95	0.03	2.12	26	129	162	76	73	92
5.87	8.44	0.47	6.14	0.04	1.85	26	113	146	103	62	81
6.17	8.35	0.41	6.18	0.03	1.84	25	120	141	94	63	83
6.48	7.74	0.42	5.63	0.03	1.76	24	119	134	106	57	80
6.79	8.04	0.41	5.96	0.03	1.81	24	119	137	94	59	83
7.10	8.16	0.43	5.98	0.03	1.81	25	117	137	100	58	82
7.40	7.89	0.40	5.90	0.03	1.80	23	115	133	95	59	79
7.71	8.45	0.44	6.17	0.04	1.86	27	120	142	115	64	83
8.02	8.35	0.42	6.05	0.03	1.83	26	124	133	112	60	81
8.33	8.23	0.39	5.89	0.03	1.77	24	120	126	109	58	77
8.63	8.54	0.42	6.12	0.03	1.82	25	124	130	115	60	81
8.94	8.59	0.42	6.20	0.04	1.81	26	128	131	123	62	82
9.56	8.28	0.44	5.95	0.03	1.76	26	115	127	131	57	78
9.86	8.45	0.40	6.07	0.03	1.78	25	114	130	119	58	77
12.32	8.43	0.40	6.16	0.04	1.68	25	112	129	114	57	79
12.63	8.51	0.39	6.24	0.04	1.74	26	114	133	114	59	79
12.94	7.94	0.38	5.96	0.03	1.62	25	113	130	128	58	76
13.25	7.78	0.37	5.68	0.03	1.55	24	106	123	122	57	73
13.55	7.73	0.35	5.17	0.03	1.49	20	97	112	124	51	68
13.86	7.14	0.34	5.26	0.03	1.49	22	106	115	217	56	71
14.17	7.98	0.38	6.07	0.03	1.64	25	116	137	155	63	79
14.48	7.88	0.36	5.82	0.03	1.59	24	111	126	154	61	74
14.78	7.71	0.34	5.84	0.03	1.57	23	110	124	164	57	77
15.09	7.41	0.34	5.54	0.03	1.49	23	103	118	165	57	72
15.40	7.32	0.33	5.41	0.03	1.52	23	101	115	200	55	70
15.71	7.18	0.32	5.25	0.03	1.46	21	99	117	230	54	68

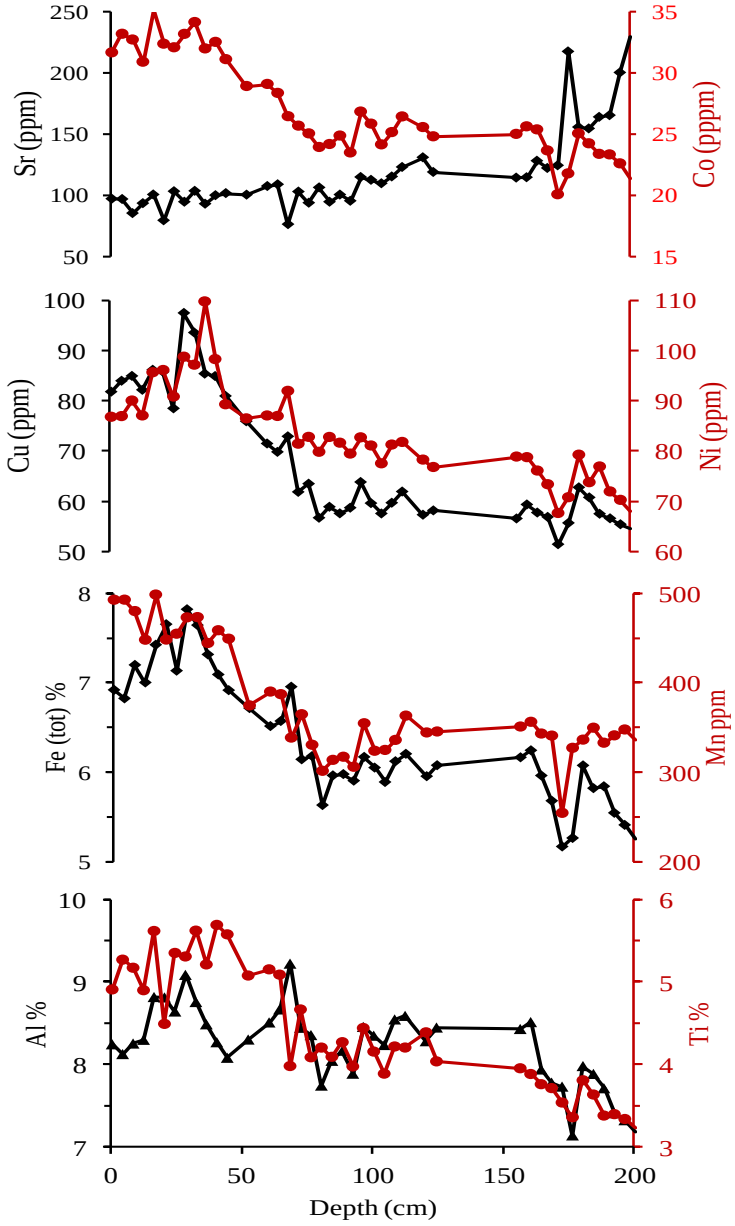

Figure 16. Depth-distribution of elements in bulk sediment of Base-OMZ sediment core (GC13).

5. DISCUSSION

As already described in the introduction chapter, the OMZ is a subsurface zone of lowest DO concentration, which occurs as a result of high surface productivity and poor ventilation of the intermediate waters (Olson et al., 1993). In this chapter, the interpretation based on variations observed in the time-series of compositional parameters with respect to past changes in OMZ, productivity, thermocline ventilation and terrigenous matter supply are presented.

5.1. Sedimentation rate

The changes in marine sedimentation rates at continental shelves and slopes provide preliminary indications about variations in terrigenous material input as these sediments are dominated by land-derived silicates. The sedimentation rates for the identified Holocene Period are 5.7 and 13 cm/ky respectively in OMZ and Base-OMZ sediment cores. The LGM sedimentation rate is 6.9 cm/ky in the farmer sediment core. Other well dated sediment cores from deep-water BoB (>3000 m) (Pavan and Govil, 2011; Pattan et al., 2013) have yielded further higher mean sedimentation rates of ~15 cm/ky. These observations suggest that the sedimentation rate in Indian eastern continental margin increases with depth probably due to increased influence of fan sediment with water-depth.

5.2. Climate and monsoon variations as depicted by $\delta^{18}O$

The $\delta^{18}O$ of foraminifera encodes the $\delta^{18}O$ of the ambient seawater in which it has accreted its calcite skeleton (Emiliani and Ericson, 1991). The $\delta^{18}O_{SEAWATER}$ response to past climate change has been shown to be globally uniform, which is forced by the global ice volume extent (Shackleton, 2000). Therefore, the calcite secreting organisms such as planktonic and benthic foraminifera are well suited to delineate the past climate stages (Imbrie et al., 1973). The $\delta^{18}O$ of the *G. sacculifer* (a planktonic species), is used for identifying the climate stages in OMZ sediment core (GC14) that was retrieved from the seafloor swept presently by most-intense (core) OMZ. The $\delta^{18}O_{G.\ sacculifer}$ time-series of OMZ sediment core (GC14) reflects the changes in global ice-volume, which had changed dramatically according to the climate prevailed at the time of sediment deposition.

The $\delta^{18}O$ of the benthic foraminifera *U. peregrina* was used for the Base-OMZ sediment core (GC13) which was retrieved from the seafloor that is presently swept by the base of the OMZ. Although not of significance, both these sediment cores are from nearby

locations, hence fall under the influence of same vertical extent of the OMZ. This minimizes the effect of spatial differences in oceanographic parameters responsible for OMZ dynamics. The reason for selecting different species for $\delta^{18}O$ measurement has already been presented in the 'material and methods' section. In addition to global ice-volume changes, the $\delta^{18}O_{G.sacculifer}$ is also a function of local surface - salinity and -temperature changes (Labeyrie et al., 1996; Lea et al., 2000; Chodankar et al., 2005; Banakar et al., 2005; 2010). However, these aspects are out of scope of the present thesis and only the total variation in the $\delta^{18}O$ is presented and discussed.

The overall $\delta^{18}O_{G.sacculifer}$ variation in the depth-series in the OMZ sediment core (GC14), which is located right within the depth range of most intense OMZ (150 - 400 m), is between -2.5 ‰ (at 8.5 cm) and 0.5 ‰ (at 196.5 cm) (Figure 9 and 17), i.e., a contrast of ~3 ‰. In the Base-OMZ sediment core (GC13), which is located at water depth that corresponds to the base of modern OMZ, the $\delta^{18}O_{U.\ perigrina}$ variation is ~3.4 ‰ (at 192.5 cm) to 3.0 ‰ (at 8.5 cm) (Figure 10), i.e., a contrast of only 0.4 ‰.

As per the ice-volume based estimates of global $\delta^{18}O$ contrast between the coldest LGM and the warmest Holocene is ~1 ‰ (Shackleton, 2000; Imbrie et al., 1973; Bassinot et al., 1994) and can be accounted in the OMZ sediment core (GC14). But, this contrast is significantly lower in the Base-OMZ sediment core (GC13) than the expected 1‰. This observation, at the outset, suggests that, the former sediment core covers both climate extremities (LGM and Holocene), while the latter sediment core does not cover the LGM. This observation becomes clearer when the $\delta^{18}O$ variation is plotted against the time based on the radiocarbon ages (Figure 17).

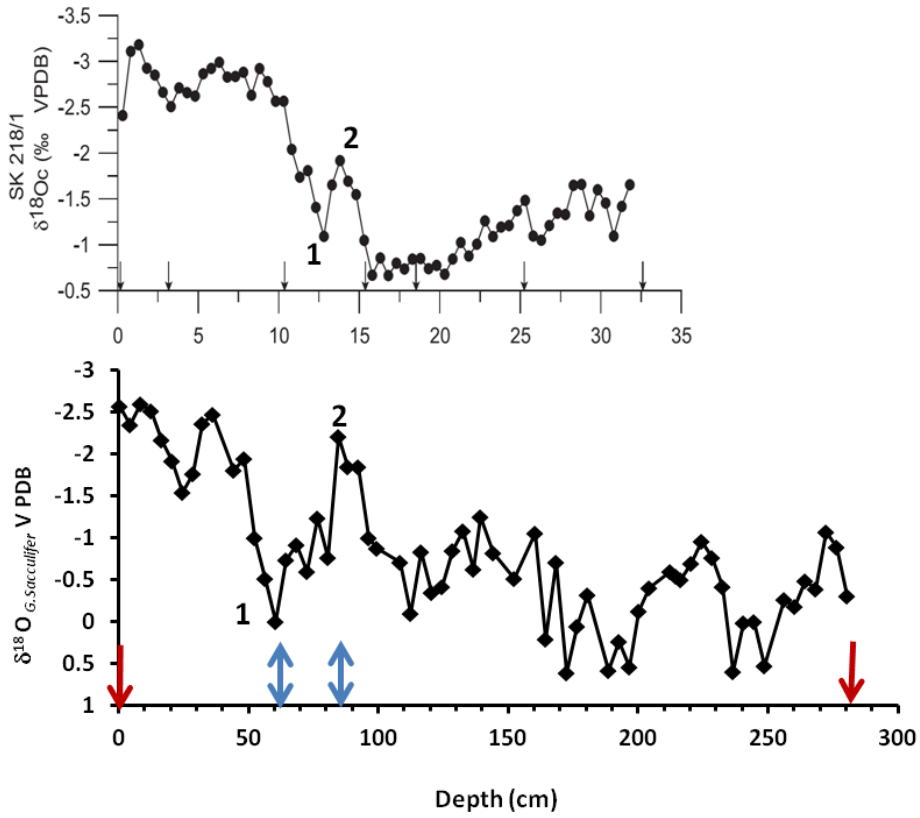

Figure 17. $\delta^{18}O_{G.sacculifer}$ depth-series of OMZ sediment core (bottom panel) and tuning this depth-series to two radiocarbon ages (red downward) arrow and to the structure of previously published record of a nearby sediment core (Govil and Naidu, 2011) which is based on seven radiocarbon dates (top panel). The double headed blue arrows show the two well pronounced climatic events (1-YD; 2- Bølling) utilized for time-scale tuning of the present sediment core.

The depth-series of both the sediment core were translated in to time-series utilizing radiocarbon dates, the prominent features in the $\delta^{18}O$, and tuning the depth-series of $\delta^{18}O$ with the time-series of previously published nearby sediment core (Govil and Naidu, 2011) (Figure 17). The $\delta^{18}O$ events and the radiocarbon dates together suggest that the OMZ sediment core covers the last 42.7 kyr climate record, while the Base-OMZ sediment core covers only part of the last deglaciation to Holocene climate (i.e., last 15.7 kyr) (see Figure 19).

In the OMZ sediment core, the enriched $\delta^{18}O_{G.sacculifer}$ (>0 %) are evident at 38-36 ka BP, 31-26 ka BP and ~12 ka BP, which apparently indicate the coldest climate similar to LGM. But, in almost all previous foraminifera $\delta^{18}O$ records, the LGM (MIS-2) has been assigned to 24 to 11 ka BP based on SPECMAP (Imbrie et al., 1973; Bassinot et al., 1994). However, this time-slab of LGM was modified following the stacking and modeling of all the available global radiocarbon, ^{10}Be and ^{3}He data (Clark et al., 2009). These authors have clearly demonstrated that the fully developed coldest LGM conditions were already in place by ~26 ka BP and the LGM conditions began to develop ~33 ka BP itself. It is also noteworthy that a

rapid increase in the benthic $\delta^{18}O$ occurred from 38 ka BP and terminated with highest $\delta^{18}O_{benthic}$ at ~29 ka BP to continue through 19 ka BP in the global benthic foraminifra $\delta^{18}O$ stack (popularly known as LR-04 benthic stack: Leisiki and Raymo, 2005). This trend of growth in $\delta^{18}O_{benthic}$ clearly suggested that the growth of coldest LGM in fact started nearly 38 ka BP and reached the coldest LGM condition at around 29 ka BP and terminated at ~19 ka BP. In other words, the previously marked LGM between 24 and 18 ka BP in SPECMAP is much shorter than the actual. The most enriched $\delta^{18}O_{G.sacculifer}$ in OMZ sediment core (between ~40 and 20 ka BP) probably indicates that the LGM cooling in BoB mixed layer began in accordance with the global climate cooling trend (Figure 18). However, the moderate depletions of $\delta^{18}O_{G.\ sacculifer}$ within the demarcated cold climate (i.e., ~33 and 22 ka BP) (Figure 18) may suggest an increased freshwater input to the BoB due to intermittently intensified monsoons or intermittent warming causing enhanced melt-water input. This interpretation however remains tentative until supported by other evidences. The third prominent $\delta^{18}O_{G.sacculifer}$ enrichment at ~12 ka BP (Figure 18) occurs in most of the previously published records from AS (Schulz et al., 1998; Kessarkar et al., 2013, and references therein) that has already been identified as Younger Dryas (YD).

The LGM identified and marked in the present $\delta^{18}O_{G.sacculifer}$ record is punctuated by warmer insterstadial-like events at ~35-30 ka BP and ~25-20 ka BP suggesting that the oxygen-isotopic response of the BoB surface to LGM climate is not monotonous but resembles the Greenland-type climate variability. This is further supported by the presence of warm Bølling-Ållerød (BA) interstadial and YD stadial like events in the deglacial section of the present OMZ sediment core (Figure 18).

The newly designated LGM (26 - 19 ka BP: Clark et al., 2009) in the present OMZ sediment core does not exhibit expected heaviest-$\delta^{18}O$ (Figure 18). The feasible causes for this discrepancy are, 1) enhanced freshwater input, i.e., dramatically increased Indian Summer Monsoon (ISM) compared to the Pre-LGM period, and/or 2) weakening of winter-spring coastal currents, which transfer low-salinity water from the bay into Eastern Arabian Sea (EAS) (Shetye et al., 1993). The former is unlikely because most of the palaeo-records suggest significantly reduced ISM during the LGM and YD (Banakar et al. 2010; Deplazes et al., 2013; Sinha et al., 2001 and references therein), hence there was decreased freshwater input to the BoB. When the low-salinity water out-flow from coastal BoB in to the EAS in the form of coastal currents is reduced or weakened, then the surface salinity in the coastal bay is expected to decrease. The low-salinity tongue in the EAS caused by the BoB low-salinity water inflow

during the LGM has been shown to have weakened significantly (Chodankar et al., 2005), suggesting restricted flow of the low-salinity water originating in the BoB flowing into the EAS. This reduced flow would automatically decrease the surface salinity in the east-coast BoB waters, in which the present OMZ sediment core is located. Therefore, a significantly weakened advection of the BoB low-salinity water appears to have reflected as decreased $\delta^{18}O_{G.sacculifer}$ during the LGM (Figure 18).

The commencement of LGM climate at ~38 ka BP as represented in the OMZ sediment core oxygen-isotope record is nearly consistent with Clark et al., (2009). The YD and BA are well-expressed in the $\delta^{18}O_{G.sacculifer}$ record and are comparable in timing with the NGRIP ice-core (NGRIP, 2004) and Tibetan Cave deposit (Dutt et al., 2015), although with certain timing offsets (Figure 18). This timing offset is expected as the present record is based on only two radiocarbon dates.

The ISM and the northern high-latitude (Greenland) climate connection is well-known (see Schulz et al., 1998; Kesserkar et al.,2014 and references therein), which suggest that the ISM was intensified during warm Bølling and DO interstadials, while the cold YD forcing has been invoked for explaining the weakening of the ISM. Therefore, the identified climate events in the present $\delta^{18}O_{G.sacculifer}$ record can be interpreted in terms of ISM intensity. Although the ISM intensity appears to have fluctuated throughout the last glacial period, as the overall variation of $\delta^{18}O_{G.sacculifer}$ is around ± 0.4 ‰ between ~42 and ~20 ka BP (Figure 18), a major shift in the ISM intensity occurs only at the commencement of deglaciation ~18 ka BP. From the beginning of the deglaciation, the $\delta^{18}O_{G.sacculifer}$ rapidly decreases from –0.2 ‰ at 18 ka BP to –2.2 ‰ at 14.5 ka BP, i.e., 2 ‰ decreases, which appears to represents the Bølling warming in Greenland. If the global $\delta^{18}O_{SEAWATER}$ decrease of 1 ‰ during the last deglaciation caused by decreased ice volume/warming (Shackleton, 2000) is subtracted from the observed decrease of 2 ‰ in the present record (Figure 18), the remainder of ~1 ‰ decrease must have been due to intensified freshwater input to the bay coinciding with Bølling warming in the northern hemisphere. In contrast, during the cold YD in Greenland the ISM appears to have significantly weakened as indicated by rapidly increased $\delta^{18}O_{G.sacculifer}$ by ~2.2 ‰ since the Bolling (Figure 18). The Greenland climate connection with the ISM interpreted from present OMZ sediment core record is consistent with previously observed intensification of ISM during the warm Bølling and weakening during the cold YD (Banakar et al. 2010; Deplazes et al., 2013; Dutt et al., 2015; Kessarkar et al., 2014; Schulz et al., 1998; Wang, 2001; Sinha et al., 2005).

Within the Holocene a minor but distinct depletion of $\delta^{18}O_{G.sacculifer}$ is evident ~8 ka BP followed by enrichment at ~6 ka BP (Figure 18), suggesting a strengthening of ISM followed by its weakening respectively. The strengthening of the ISM at ~8 ka BP observed in the present $\delta^{18}O$ record has also been reported by Overpeck et al (1996) from the AS sedimentary records. These Holocene ISM events have significance with respect to development and decline of Harappan Civilization. The 8 ka BP intense ISM might have not allowed the human settlements to be established in Indus Valley due to perennially flooded Indus and its tributaries until ~6 ka BP when the ISM weakened. At around this time the floodplains suitable for agriculture might have got exposed and stabilized favoring the establishment of human settlements. This ISM weakening at ~6 ka BP recorded in the present OMZ sediment core (Figure 18) appears to be similar to that observed ~5 ka BP in other BoB sedimentary records (Rashid et al., 2011), cave deposits (Dutt et al., 2015) and Tibetan Lake sediments (Nishimura et al., 2013), which has already been linked to the growth of Harappan Civilization on the Indian Subcontinent (Staubwasser et al., 2003; Ponton et al., 2012; Dixit et al., 2014).

The $\delta^{18}O_{G.sacculifer}$ during 26 to 18 ka BP (i.e., LGM) does not exhibit expected enrichment, instead, most enriched values are evident prior to 26 ka BP (Figure 18). The probable cause for this could be either an enhanced freshwater input (i.e., intensified ISM), or weakening of Eastern India Coastal Current (EICC). The EICC transfers low salinity water from the northern bay into AS via the east-coast of India (Shankar et al., 2002; Shetye et al., 1993). This current is largely responsible for balancing perennially high-salinity AS. Any restriction to the flow of EICC in to AS would cause the east coast waters to become fresher as the loss of low-salinity water from the bay to the AS is prevented or reduced. The intensification of ISM during the LGM is unlikely because most of the palaeo-records suggest significantly reduced ISM during the LGM and YD as expected under the then prevailed ITCZ-ISM coupled dynamics (Gadgil, 2003). On the other hand, the EICC has been shown to have restricted to the southernmost AS during the LGM that has adversely affected freshening of the eastern AS (Chodankar et al., 2005). Therefore, the moderate decrease in the $\delta^{18}O_{G.sacculifer}$ during the LGM (26 - 18 ka BP) as compared to the preceding period can be speculated to be a result of accumulation of low salinity northern bay water along the eastern margin of India due to reduced strength of EICC. Such restriction to the EICC out-flow occurs when the sea level gradient between the western-BoB and the Eastern AS is reduced probably as result of declined freshwater flux to the BoB. The reduced sea level gradient between these two basins apparently reduces this out-flow, which might have caused the observed depletion

of $\delta^{18}O_{G.sacculifer}$ during the LGM. This interpretation is consistent with reduction in the ISM during the coldest LGM, which is the main cause of lowering of sea level in the BoB that receives huge freshwater flux mostly from ISM. The modern ISM intensity influences the biogeochemistry of northern Indian Ocean (Dileepkumar, 2009), which in turn might have influenced the status of the OMZ in the BoB (Sarma et al., 2013). However, whether such ISM-OMZ coupling existed in the past-BoB is not known and can be understood with the help of geochemical tools.

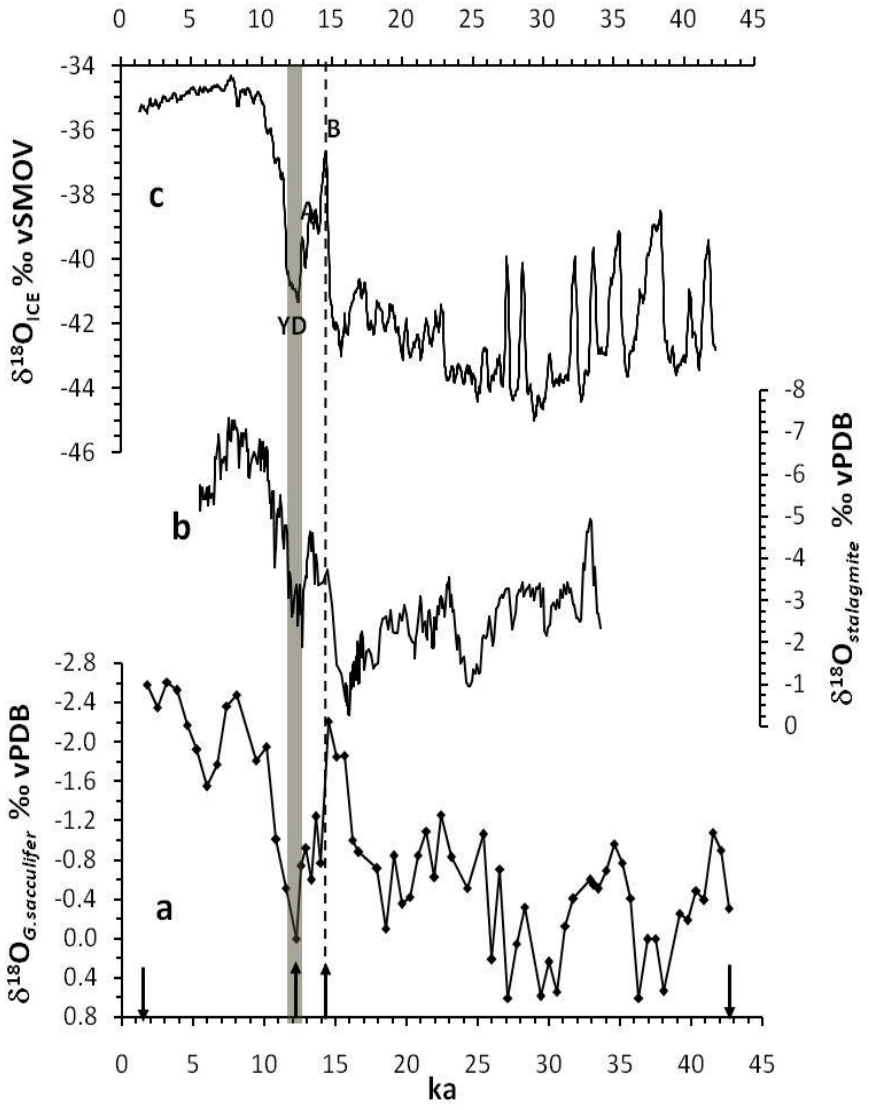

Figure 18. Time-series of $\delta^{18}O_{G.Sacculifer}$ from OMZ sediment core (GC14) is compared with NGRIP ice-core $\delta^{18}O$ (NGRIP Proj. Members, 2004) (10-point running mean) and $\delta^{18}O$ of Mawmluh Cave deposit of Meghalaya (Dutt et al., 2015). The downward arrows are the two measured radiocarbon ages, and upward arrows are the two tie-points (YD and Bølling) adopted from a nearby sediment core (Govil and Naidu, 2011). Note the consistency of deglacial and 8 ka BP events in all records.

The Base-OMZ sediment core (GC13: water depth = 1474 m), as mentioned in material section, is nearly devoid of planktic foraminifera. All the available tests of *Uvigerina perigrina* (benthic foraminifera) species were analyzed for $\delta^{18}O$. The chronology for this sediment core is based only on one radiocarbon date obtained for 200 cm depth (considered here as the bottom of the core), as there were no adequate numbers of benthic tests required for radiocarbon dating (equivalent to ~10 mg of carbonate) in the entire core-length. The radiocarbon age obtained for this bottom section is 15705 y BP and the top of the sediment core is assumed as 'Present' (refer to material and methods section for details).

The time-series of $\delta^{18}O_{U.\ perigirina}$ exhibits a clear trend of nearly constant values in the Holocene 12 ka BP – Present) and relative enrichment in preceding later part of the deglaciation (16 ka BP – 12 ka BP) (Figure 19). The timing of the end of the last deglaciation is consistent with well-established commencement timing of the Holocene in both SPECMAP (Imbrie et al., 1973) and also in the LR-04 Benthic Stack (Liesicki and Raymo, 2005).

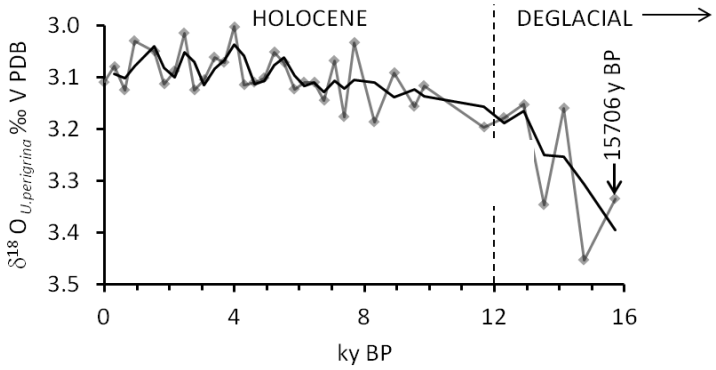

Figure 19. Time-series of $\delta^{18}O_{U.perigrina}$ of the OMZ-base sediment core (GC13). The vertical downward arrow is the measured radiocarbon age; horizontal arrow indicates that the deglacial section continues further down in the sediment column beyond the length of this sediment core; the dotted vertical line separates Holocene and Deglacial climate stages.

The $\delta^{18}O_{U.perigrina}$ varies in a narrow range (between 3.0 ‰ to 3.5 ‰: Figure 10 and Table 5) and exhibits a nearly uniform depleted values of ~3.5 ‰ after 12 ka BP as compared to 15.7 ka BP (Figure 19). The rapid and highly fluctuating decrease in $\delta^{18}O_{U.perigrina}$ from 15.7 ka BP to ~12 ka BP indicates that the later part of the last deglacial warming was not smooth but through rapid adjustments in deepwater properties. The identified Holocene, on the other hand, exhibits negligible variation in the $\delta^{18}O_{U.perigrina}$ (3.1 ± 0.1 ‰: Figure 19) suggesting nearly uniform climate forcing on deepwater in BoB. The ISM variability from this core cannot be assessed as the depth of habitat of *U. perigrina* in the present instance is 1474 m which is beyond the depth of influence of monsoon forcing.

5.3. Sediment sources to eastern margin – geochemical approach

The ISM intensity has a great influence on river-transported terrigenous matter input to the eastern continental margin of India, because several seasonal peninsular rivers drain into the western BoB. The combined terrigenous input by the eastward flowing Mahanadi-Kaveri-Krishna-Godavari system is next to the Ganga-Brahmaputra river sediment input. Hence, the changes in terrigenous input to western BoB along the Indian east-coast should reflect the changes in the strength of the peninsular rivers, in turn, the ISM intensity. The sediment flux to the bay and its chemical properties have demonstrated that climate has significant role in regulating the peninsular erosion (Goodbred, 2003; Tripathy et al., 2014).

The Holocene sedimentation rate of 5.7 and ~13 cm/ky are recorded respectively by the OMZ and Base-OMZ sediment cores (GC14: 325 m water depth and GC13: 1474 m water depth respectively). The LGM sedimentation rate of 6.9 cm/ky is recorded in the former sediment core. That is, an average sedimentation rate of ~6.8 cm/ky in the OMZ sediment core for the last ~42 kyr. Another well dated deep-water sediment core from the BoB (SK 218/1 – 3300 m water-depth Pavan and Govil, 2011; Pattan et al., 2013) records further higher average sedimentation rate of ~15 cm/ky for the last ~35 kyr. These data appear to indicate that the sedimentation rate in BoB increases with increasing depth of deposition, which is puzzling. This increased sedimentation rate with increasing depth in the bay may be due to enhanced influence of fan sediments on sedimentation rates with increasing water depth in the distal bay.

The OMZ sediment core location is in the vicinity of discharge points of Krishna-Godavari-Kaveri (KGK) river system draining the peninsular India. Therefore, it receives pristine silicate detritus derived from the peninsular India, which is directly under the influence of ISM. The erosion strength of this river system is directly related to the strength of the ISM. Further, it is necessary to know the average composition of KGK derived sediment to assess the provenance of terrigenous material variation in this sediment core.

The Table 16 provides details of composition of sediments of KGK river system. Although the location of the present OMZ sediment core is in the vicinity of KGK discharge points (Figure 8), the presence of Ganges-Brahmaputra derived sediment cannot be ruled-out, because seasonally reversing EICC is expected to disperse sediment all along the east-coast of India (Selvaraj et al., 2004). The Nd - Sr isotopic compositions of east coast sediments are significantly different from those of proper Bengal Fan sediment, but closely follow the Deccan basalts and peninsular granites. On the other hand, the fan sediment falls between the mixing line of Himalayan granites and Deccan basalts (Galy et al., 2010). The KGK rivers originate in the peninsular south India and share a common tectonic history (Sastri et al.,

1973). Hence, these three rivers must have acted as a major sediment transport agents to the BoB. This observation clearly indicates that the peninsular rivers are the main source for the terrigenous component in the sediment of the eastern coastal region of India. Thus, the OMZ sediment core is expected to receive most of the terrigenous silicates from KGK river system than the Himalyan Rivers. It is noteworthy that over 34 % of the terrigenous component in sediment of the deep western BoB has been accounted for peninsular rivers (Goodbred, 2003), hence, changes in terrigenous element composition of the OMZ sediment core (GC14) is expected to respond to monsoon variation. The sediment flux to the bay and its chemical properties have demonstrated that climate has significant role in regulating the peninsular erosion (Goodbred, 2003; Tripathy et al., 2014). Therefore, sediment composition in the study area should exhibit comparable behavior with the average KGK sediment. For this, I have considered the available element composition of KGK sediment (Table16: Subramanian et al., 1985) to calculate the average composition of the source sediment to the depositional site of the present sediment cores.

Table 16. Comparison of major element composition of bulk sediment of the present sediment core with potential terrigenous sediment Source Rivers (all values in wt. % and data from Subramanian et al., 1985)

	OMZ sediment. Core (GC14) (Average of 64 samples)	Krishna River sediment	Kaveri River sediment	Godavari River sediment	Average River sediment
Al	6.1	3.4	4.8	4.3	4.3
Fe	4.8	4.2	1.8	5.7	3.4
Ti	0.4	0.6	0.3	0.9	0.5
Mg	1.4	1.3	1.1	1.4	1.3
Mn	0.02	0.10	0.03	0.10	0.07
Ca	9.0	5.3	1.1	4.5	3.3

5.4. Depositional environments in the OMZ depths vis-à-vis monsoon variability

The Al, Fe, Mg, Ti and Mn concentration in the bulk sediment of both sediment cores exhibit a remarkable similarity to the KGK sediment composition. In particular, the OMZ sediment core composition is closest to the KGK sediment (Table 16). Thus, the main source of terrigenous matter to the present core locations appears to be the erosion products of the Peninsular India. However, there are subtle differences with respect to individual elements in the sediment core and the source-river sediment. The marginal enrichment of Al – a primary

indicator of silicate detritus, than the average KGK sediment may be due to hydrodynamic sorting of material in the river system before reaching the open-ocean (Garzanti et al., 2010). The Mn shows a significant depletion in the OMZ sediment core compared to KGK sediment (Table 16) and average continental crust (Rudnick and Gao, 2003). This may be due to the extreme suboxic conditions at the seafloor (325 m water-depth) as it is under the influence of the modern most intense OMZ waters. Due to lowest DO at this depth, the sedimentary Mn at the sediment-water interface reduces and migrates out of the sedimentary system. The Ca shows three times enrichment in this sediment core compared to KGK sediment average suggesting that this excess-Ca must be of biogenic origin that can be supported by presence of foraminifera skeletons in the coarse fraction.

The depth-series of elements in bulk composition of the OMZ sediment shows significant depletion of all elements (Al, Fe, Mg, Ti, and Mn) except Ca at around 60 cm and moderate depletion at around 240 cm. The remaining sections of the core show only minor fluctuations (Figure15 and Table 14). In contrast, the Ca shows enrichment in the sections where other elements are depleted. This down-core opposite variation trends of Al, Fe, Mg, Mn and Ti as compared to Ca warrants an explanation. The Ca-enrichment could be either due to significant increase of Ca-rich minerals such as calcite and calcic-feldspars derived from peninsular rocks, or due to increased abundance of skeletons of calcite secreting organisms such as foraminifera and coccoliths. The calcic-feldspar enrichment can be ruled out because it results in corresponding enrichment of Al. The increased supply of terrestrial calcite derived from limestones also can be ruled out because the drainage basins of KGK river system is devoid of limestone or dolomite formations as evident from very low Ca content in KGK sediment (Subramanian et al., 1985: Table 16). Therefore, the likely candidate for the observed contrasting down core behavior of Ca with respect to other elements could only be due to presence of biogenic calcite skeletons. To confirm this, the coarse fractions of the sediment sections were carefully examined under the microscope. The sections enriched with Ca are found to be enriched with foraminifera tests.

Thus, the sections showing depleted terrigenous elements (Al, Fe, Mg, Ti and Mn) are not the result of decreased supply of the terrigenous matter by the KGK system, but because of dilution by biogenic calcite. The organic matter (OM) and authigenically precipitated oxides form minor components in the sediment cores. Therefore, it is necessary to unscramble different phases of element carriers in the bulk sediment. The inter-elemental correlation analysis is used to identify different group of elements in the bulk sediment (see Table 17). The element Al is considered as a proxy for detrital (terrigenous) silicate material and Ca is

considered as the proxy for biogenic calcite.

Table 17. Inter-elemental correlation matrix obtained for the composition of bulk sediment

	Al	Ti	Fe	Mn	Mg	Ca	Co	Zn	Cr	V
Al	1.00									
Ti	**0.89**	1.00								
Fe	**0.68**	**0.67**	1.00							
Mn	**0.78**	**0.93**	**0.73**	1.00						
Mg	**0.81**	**0.90**	**0.81**	**0.88**	1.00					
Ca	**-0.76**	**-0.68**	-0.42	**-0.61**	-0.47	1.00				
Co	0.43	0.56	-0.02	0.47	0.18	-0.59	1.00			
Zn	**0.88**	**0.76**	**0.63**	**0.66**	**0.68**	**-0.66**	0.41	1.00		
Cr	**0.81**	**0.72**	0.56	0.62	**0.68**	-0.51	0.33	**0.87**	1.00	
V	**0.95**	**0.91**	**0.75**	**0.85**	**0.86**	**-0.77**	0.43	**0.85**	**0.79**	1.00

n = 64; r = 0.65 is significant at 99% confidence level shown with bold fonts

A strong mutually sympathetic association of Al, Ti, Mg, Mn, Zn, Cr and V ($r > 0.8$; $n = 64$) and their strong inverse association ($r > -0.5$) with Ca (Table 17) confirms that the sediment core contains two primary components, *viz.*, terrigenous silicate and biogenic carbonate. Further, it can be seen in the last 32 kyr time-series of C_{org} and Ca that, both these biogenic components (OM and calcite) exhibit as expected a comparable variation through time (Figure 22). These together confirm that most of the Ca is bound to biogenic carbonate. The minor elements V, Co, Cr, and Zn are associated with terrigenous silicate detritus phase as evident from their strong sympathetic association with silicate phase elements and inverse association with biogenic-Ca (Table 17).

If the terrigenous matter input by KGK to the sediment core location vis-à-vis the monsoon variability to be understood, then it is necessary to remove the biogenic carbonate dilution effect on the bulk composition of sediment. The lowest Ca-content in the present sediment core of 2.2 % and is considered to be the silicate-supported Ca. This silicate-Ca is subtracted from the total Ca-content of every section of the sediment core to obtain excess-Ca or biogenic–Ca. Then all other elements were normalized with the estimated excess-Ca (biogenic-Ca) content of respective sub-sections. The normalized elements essentially are the elements exclusively associated with terrigenous silicates.

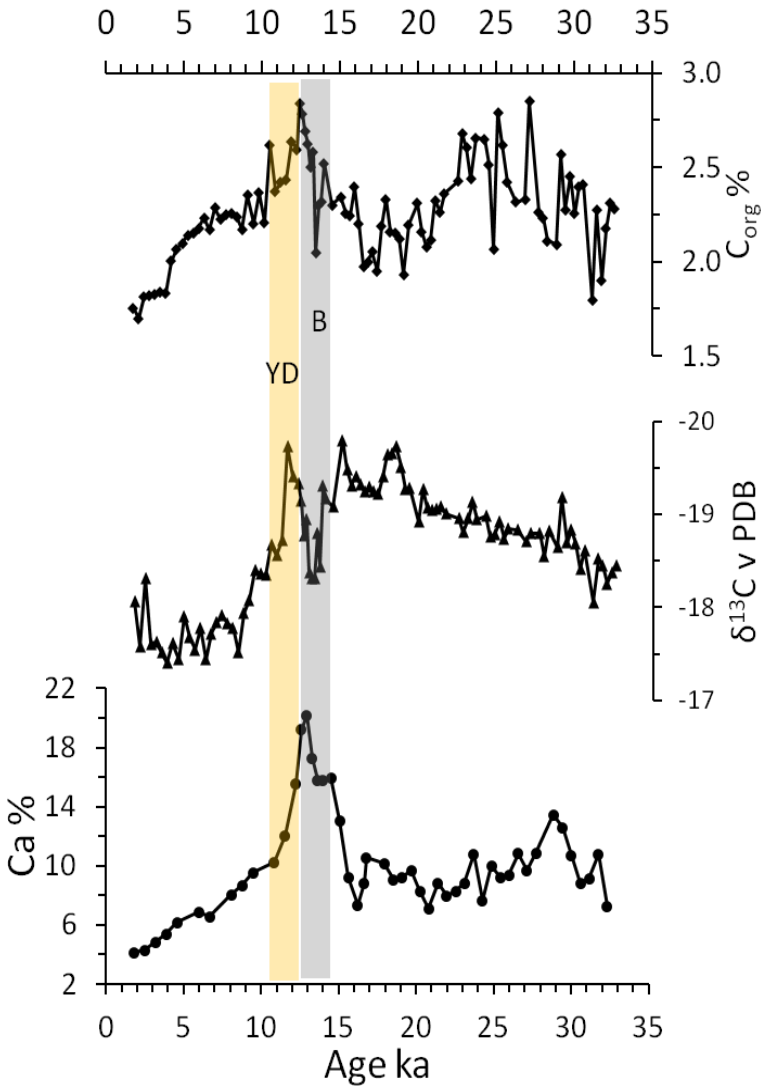

Figure 20. Last 32 ky time-series of productivity indicators in OMZ sediments core.

Table 18. Inter-elemental correlations for biogenic-Ca normalized composition of the OMZ-sediment core

	Fe	Mn	Ti	Al	Mg	Co	Cr	Zn	V
Fe	1.0								
Mn	0.9	1.0							
Ti	1.0	1.0	1.0						
Al	1.0	0.9	1.0	1.0					
Mg	1.0	1.0	1.0	1.0	1.0				
Co	0.8	0.9	0.9	0.9	0.9	1.0			
Cr	1.0	0.9	1.0	1.0	1.0	0.8	1.0		
Zn	1.0	0.9	1.0	1.0	1.0	0.8	1.0	1.0	
V	1.0	0.9	1.0	1.0	1.0	0.9	1.0	1.0	1.0

n = 63; r = 0.9 is significant at 99.9 % confidence level

The correlation matrix obtained for excess-Ca normalized terrigenous-silicate elements show significantly improved mutual positive association (r > 0.9: Table 18). This clearly suggests that the Ca in the present sediment core higher than the KGK sediment Ca is associated with biogenic fraction, which is a proxy of productivity, and all other elements are associated with the KGK derived terrigenous sediment. The estimated biogenic Ca (Table 14), therefore can be utilized as a proxy for understanding the past productivity changes in response to ISM variation. The biogenic-Ca normalized elemental concentrations are considered as reliable proxies to reconstruct the past changes in terrigenous matter supply to the location of the OMZ sediment core, which in turn should indicate the changes in the past-ISM.

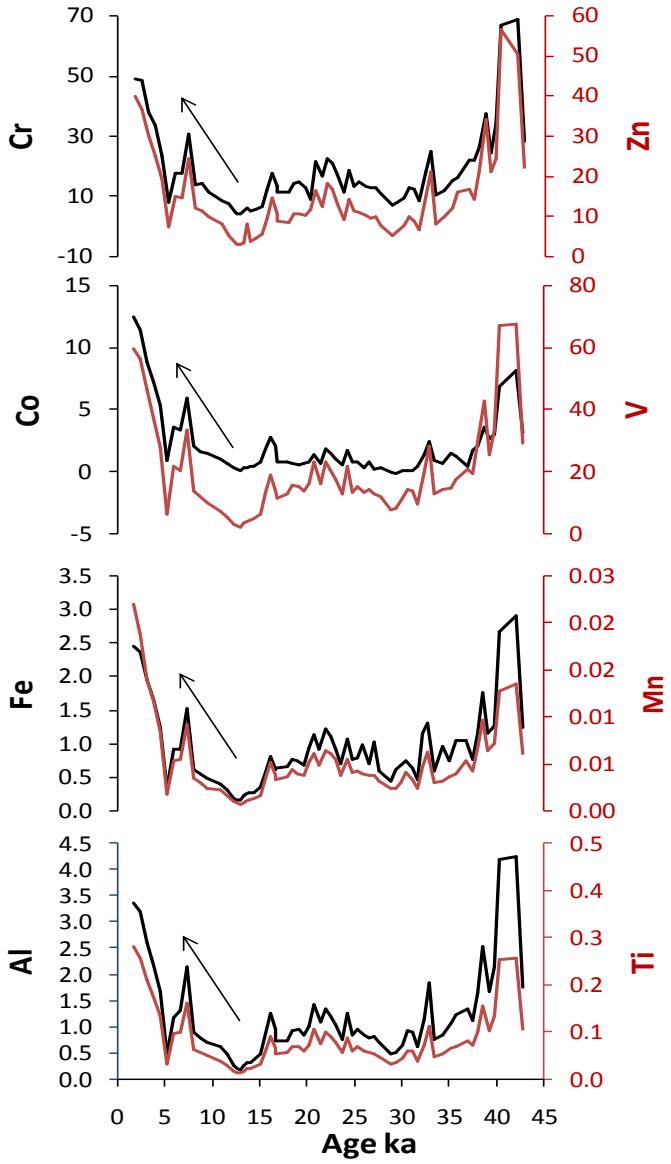

Figure 21. Time-series of biogenic-Ca normalized element composition reflecting the changes in terrigenous matter input to the OMZ sediment core location.

The time-series of terrigenous elements exhibit distinct depletion between 35 and 15 ka BP bound by pre-LGM and Holocene enrichment (Figure 21), suggesting that the river discharge in to the East Coast of India was significantly lowered during the LGM from its preceding period and significantly increased through the Holocene. This pattern of river discharge is consistent with several past monsoon records derived from sediments of the northern Indian Ocean, which have indicated significant weakening of ISM during the LGM, and intensification during Holocene (Schulz et al., 1998; Kessarkar et al., 2013; Banakar et al., 2017; Sinha et al., 2005). The rapid weakening of summer monsoon precipitation causing severe drought conditions within the Holocene at ~5 - 4 ky (Nishimura et al., 2014; Staubwasser et al., 2003) is also well-reflected in the terrigenous element time-series by decreased contents (Figure 21) indicating weakened river discharge. The timings of intensified ISM during the interstadials of last glacial period (~22, ~32 and ~42 ka BP) and ~8 ka BP during the Holocene as reflected in the $\delta^{18}O_{G.sacculifer}$ are also evident by moderate increases in terrigenous element contents at those timings (Figure 21). In addition, the mid-Holocene (~6 ka BP) weakening of the ISM is also reflected by the decreased terrigenous elements around that time (Figure 21). A noteworthy feature of the present $\delta^{18}O_{G.sacculifer}$ and terrigenous element records is that the ISM evolution during the deglaciation (~20-10 ka BP) appears to have evolved through rapid fluctuations as previously reported by several researchers from the AS sedimentary records.

The inter elemental correlation matrix for the OMZ-base sediment core (GC13) (Table 19) that covers last 15.7 kyr suggests the following dominant mineral phases in the sediment core which is different from the core of OMZ:

1. A very strong positive mutual association ($r > 0.8$) between Mn-Fe-Ti-Co-Ni-Zn-V, indicates presence of Fe-Mn oxide phase precipitated at the benthic boundary or sediment-water interface. The strong Ti association with Mn and Fe in fact has been observed previously in deep-water sediment of world oceans characterized by high DO content. This particular association of otherwise typically detrital (silicate detritus) associated Ti suggests its strong coupling with the Fe-Ti hydrate in the authigenically precipitated oxides (Koschinsky et al., 1994).
2. The mutual relationship among typical terrigenous elements Al and Mg is very strong ($r > +0.8$), but weak with Mn and Ti. The Fe also exhibits strong positive association with terrigenous characteristic elements Al and Mg ($r = 0.8$) suggesting that this element is partitioned almost equally between authigenic oxide and terrigenous silicate

phases. The moderately positive association of Mn and Ti with Al may be because of presence of minor amount of these two elements in the terrigenous silicate minerals.

3. The only element that exhibits negative association with all other analyzed elements is the Sr. This behavior of Sr apparently suggests that it is associated exclusively with such a mineral phase that acts as dilutant of the oxides as well as terrigenous silicate mineral phases. It is already observed in the OMZ sediment core (Table 17) that the Ca is anti-correlated with silicate and oxide elements. Since the Ca data is not available for this sediment core, only bulk composition is emphasized without normalizing for carbonate dilution.

Table 19. Inter-elemental correlation matrix for bulk-sediment composition of Base-OMZ sediment core (GC13)

	Al	Fe	Mg	Ti	Mn	Sr	Co	Ni	Zn	V
Al	1.0									
Fe	**0.8**	1.0								
Mg	**0.8**	**1.0**	1.0							
Ti	0.6	**0.9**	**0.9**	1.0						
Mn	0.5	**0.9**	**0.8**	**0.8**	1.0					
Sr	-0.7	-0.7	-0.7	-0.7	-0.4	1.0				
Co	0.6	**1.0**	**0.9**	**0.9**	**1.0**	-0.6	1.0			
Ni	0.7	**0.9**	**0.9**	**0.8**	**0.8**	-0.7	**0.9**	1.0		
Zn	**0.8**	**0.8**	**0.8**	0.7	0.5	-0.6	0.7	**0.8**	1.0	
V	0.7	**1.0**	**1.0**	**0.9**	**0.9**	-0.6	1.0	**0.9**	0.7	1.0

The time-series of elements analyzed in the Base-OMZ sediment core (GC13) is controlled by combination of surface productivity, oxide precipitation and terrigenous-silicate supply. All the analyzed elements show nearly similar temporal variation in sediment at the base of the OMZ (Figure 22). This is expected because except Sr all other elements are mutually highly coherent as evident in (Table 19). This mutual coherency is mainly because of their dominant association with terrigenous silicate matter is the sediment. This restricts the utility of these elements only to interpret changes in terrigenous silicate supply, in turn, ISM variability. There are three distinct trends in their temporal variability (see Figure 22).

a) A gradual increase although with intermittent fluctuations between ~16 and 12ka BP.

b) Attained more stable distribution between ~12 and 6 ka BP, as evident from minor fluctuation around constant concentrations.

c) Further increase from ~6 ka BP to assumed Present with moderate decrease ~ 4 ka BP.

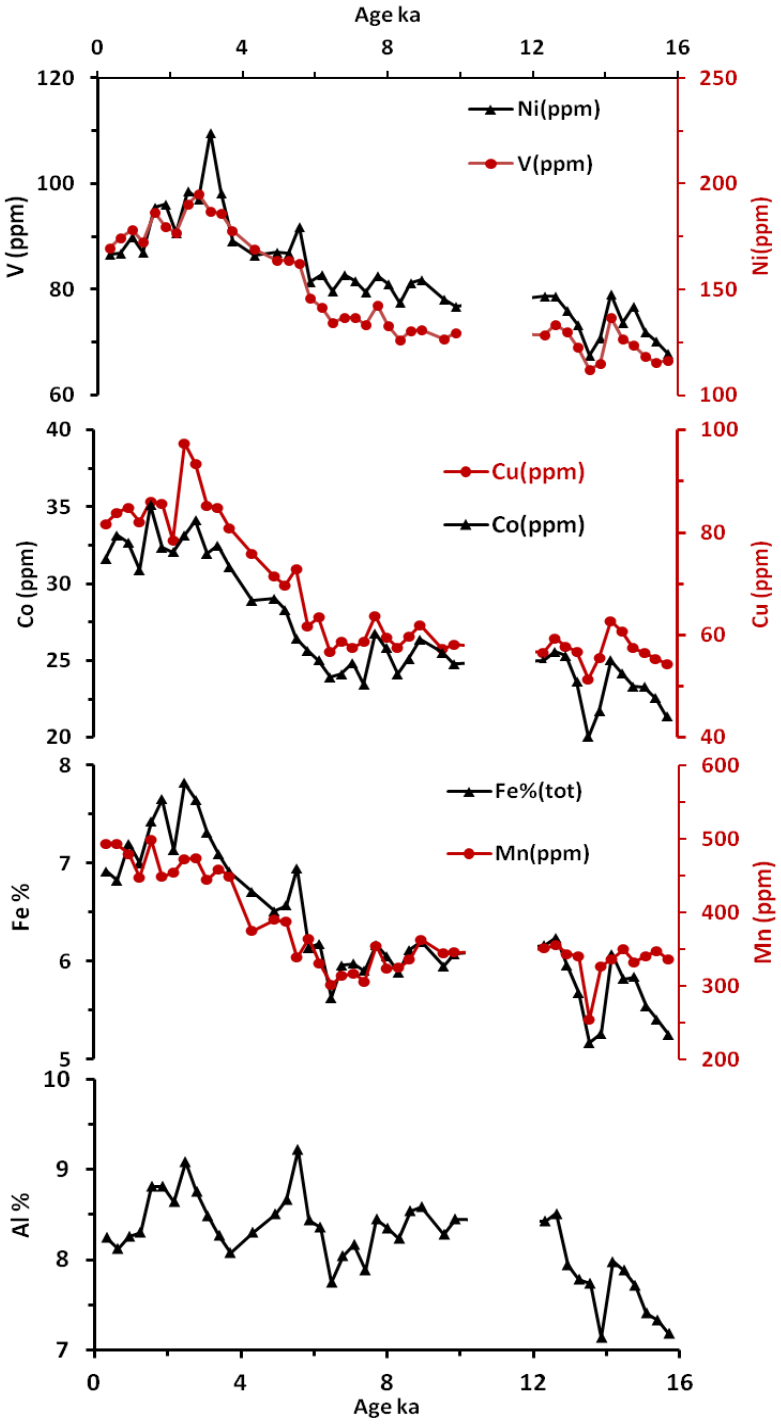

Figure 22. Time-series of bulk-sediment elemental concentrations at the base of OMZ (GC13)

The above trends suggest that the terrigenous silicate supply to the seafloor at the base of OMZ increased through the deglaciation and remained mostly constant during the early Holocene. A major shift towards rapid increase in terrigenous input occurred during the mid-Holocene until the Present in two pulses. These observations can be translated in to ISM variability. The ISM intensity began to increase during the deglaciation from its weakest mode of the LGM (as evident in OMZ sediment core – GC14 and also in several previous studies). The ISM intensity stabilized at moderately intensified level during early part of the Holocene, with a short-term decline between ~8 and 6 ka BP. After 6 ka BP the further intensification of the ISM is evident. The 8 – 6 ka BP ISM weakening event appears to be similar to that observed around 6 ka BP in the OMZ sediment core. The timing discrepancies in the terrigenous supply records of the two sediment cores may be due to very poor control on the chronology of this Base-OMZ sediment core. Otherwise, the changes in terrigenous supply to both locations for common time-slice (16 ka BP to Present) remain nearly similar. Therefore, the terrigenous material derived from the KGK appears to have reached the lower slope (1375 m water depth) via the shelf without much adulteration through the last ~16 kyr. The above interpretations shall remain highly speculative for this sediment core due to age constraints and require further confirmations. Until then, only the changes recorded in OMZ sediment core are emphasized in this thesis.

5.5. Paleoproductivity changes

A significant variation in the concentration of C_{org} (1.7 % to 2.7 %) through time is evident in the OMZ sediment core (GC14) (Table 8 and see Figure 20) suggesting remarkable change in the C_{org} burial in the eastern continental margin of India. The C_{org} to the core location can be of both terrestrial and marine origin. Hence, the observed changes in the time-series of C_{org} include relative changes in contribution of terrigenous carbon (soil-carbon) and marine productivity. The C_{org} variation in marine sediment can also be due to in changes in its post burial preservation. The problems associated with preservation of OM (C_{org}) in marine sediment is well-known (see Meyers, 1994), which has potential to reduce its utility as a reliable proxy of marine production. However, the preservation problem with OM normally encountered only when it is depositing in oxic environments where its remineralization or oxidation obliterate the actual productivity signals. But, the present sediment core is retrieved from the most intense depth of the OMZ where the water has remained oxygen depleted that prevents any loss of OM through remineralization. Therefore, the recorded temporal variation in the present OMZ sediment core can be considered as a faithful proxy for the productivity.

The δ^{13} C_{org} in the present OMZ sediment core (GC14) vary between within −17.3 ‰ and −19.8 ‰ (Table 8 and Figure 20) suggesting that marine OM may have mixed with terrestrial OM, as the pristine marine OM has δ^{13} C_{org} of ~ −23 ‰ and the terrestrial pristine OM of C3 plants has ~ −27 ‰ and of C4 plants has ~ −15 ‰ (Meyers, 1994). However, it is most likely that the soil OM can show significant enrichment of δ^{13} C_{org} over the original or pristine terrestrial OM as a result of preferential loss of ^{12}C over the time due to oxidation within the well aerated soil as a result of its exposure to atmospheric oxygen (Natelhoffer and Fry, 1988) through aging. Therefore, nearly 3 ‰ to 5 ‰ enriched δ^{13} C_{org} in the present OMZ sediment core may be due to some mixing of soil-carbon with marine-carbon, wherein, increasing δ^{13} C_{org} above marine OM value indicates increasing contribution of soil-carbon.

The enhanced terrigenous matter input is expected to enrich the coastal waters with nutrients and hence increased productivity (Sarma et al., 2013). To test this we assessed the C_{org} and biogenic-Ca variation in the last 32 kyr. The C_{org} shows distinct increase during deglacial period (16-12 ka) from ~2 % to 2.7 % and a monotonous decrease from ~2.7 % to ~1.7 % through the Holocene, with comparable trend in biogenic-Ca variation (Figure 20), which is in contrast to the recorded variation in the terrigenous sediment input (see Figure 15). At the outset, the coherent increase (decrease) of C_{org} and biogenic-Ca during deglacial transition (Holocene) suggest increased (decreased) marine production. If this variation in biogenic components reflect the marine productivity alone then the $\delta^{13}C$ of the OM should have been ~ −23 ‰ (Meyer, 1994), which is not the case. Hence, requires an explanation. The additional source of enriched δ^{13} C_{org} is necessary to account for 3 – 5 ‰ enrichment. The addition of KGK soil containing aged terrestrial-OM is only the possible additional source.

Although, it is not feasible to unscramble exact proportion of the soil-carbon from the total C_{org} in the sediment core, it is possible to estimate its approximate proportion considering the soil-carbon end-member δ^{13} C_{org} as −15 ‰ and marine-carbon end-member as −23 ‰. That is, for every 10 % of soil-OM in the total OM, the δ^{13} C_{org} of the total-OM would show an increase of $\delta^{13}C$ C_{org} by ~1.5 ‰ over the marine end-member value of −23 ‰. Thus, the Holocene average of −17.5 ‰ would suggest a presence of ~ 40 % of soil-OM in the sediment, which eventually works out as ~60 % of marine-OM; similarly, the deglacial average of −19.5 ‰ would suggest approximately 25 % of soil-OM (i.e. 75 % of marine OM); and the LGM average of −18.5 ‰ accounts to ~ 30 % of soil-OM (i.e. 70 % of marine OM).

The δ^{13} C_{org} average of ~ −19.5 ‰ during the deglacial transition is followed by an increase of ~2 ‰ through the Holocene (Figure 20), which suggests that around 15 %

enhanced input of soil-OM during the Holocene as compared to the deglacial average and around 10 % increase compared to the LGM. This observation is nearly consistent with terrigenous element increases in the present sediment core during the Holocene (Figure 21). Therefore, it is apparent from the significantly decreased biogenic Ca and C_{org} that during the Holocene the KGK river system might have debouched more soil-OM in the eastern continental margin. Increased terrigenous matter loading in coastal waters (enriching the nutrient load) during intensified ISM years in coastal BoB waters (Sarma et al., 2013) is expected to enhance the marine production instead of observed reduction in C_{org}. This anomaly is speculated to be a result of increased turbidity in coastal waters limiting the light availability for photosynthesis in-spite of enhanced nutrient availability, i.e., reduced nutrient utilization.

From Figure 20, it is also evident that during the Bølling warm period the productivity increased as evident from peak production of biogenic carbonate and increased C_{org}, but also the soil-carbon input shows an increase as evident from increasing δ^{13} C_{org}. The following cold YD climate appears to have witnessed reduced soil-OM input as evident in decreased δ^{13} C_{org}. This behavior of productivity proxies is on expected lines, because, it has been shown by previous studies that the ISM intensity significantly strengthened during the Bølling and weakened during the YD (see Kessarkar et al., 2013 and references therein) leading to strengthening and weakening of KGK river system responsible for delivering soil-carbon to the sediment core location.

The C_{org} in Base-OMZ sediment core (GC13) (Figure 23) is higher (~2.5 %) with a marginal change of < 0.2 % during most of the deglacial time (16 ka BP to 8 ka BP), and begins to decrease to a minimum of ~1.6 % through the Holocene (Figure 23). Interestingly, the δ^{13} C_{org} increases marginally from ~ –20.5 ‰ during deglacial time to ~ –19 ‰ through the Holocene suggesting that the soil-OM reaching the seafloor underlying the base of OMZ is considerably less than that reaching the seafloor underlying the OMZ. The last 16 kyr time-series of C_{org} in this sediment core as well as in the OMZ sediment core (GC14: Figure 24) exhibit comparable trends. This similarity in C_{org} distribution in the present sediment cores indicates that the C_{org} records are faithful representatives of the surface productivity in the present case.

As the $\delta^{13}C_{org}$ change is <1 ‰ throughout the last 16 kyr time covered by this sediment core, the relative changes in the proportion of soil OM and the marine OM appear to be insignificant. These observations apparently indicate that, a) the KGK derived sediment is

mostly locked in the shelf region and b) the productivity through the Holocene decreased significantly as compared to the preceding deglacial time. The decreased productivity during the Holocene recorded by both the sediment cores is consistent with the previous studies based on OM and lipid biomarker proxies in sediments of NIO (Banakar et al., 2005; Punyu et al., 2014; Tamburini et al., 2003). This observation on decreased/increased productivity during Holocene/LGM in BoB along with similar previous observations from AS is of significance because the entire Northern Indian Ocean might have contributed to the global cooling during the LGM through enhanced burial of OM.

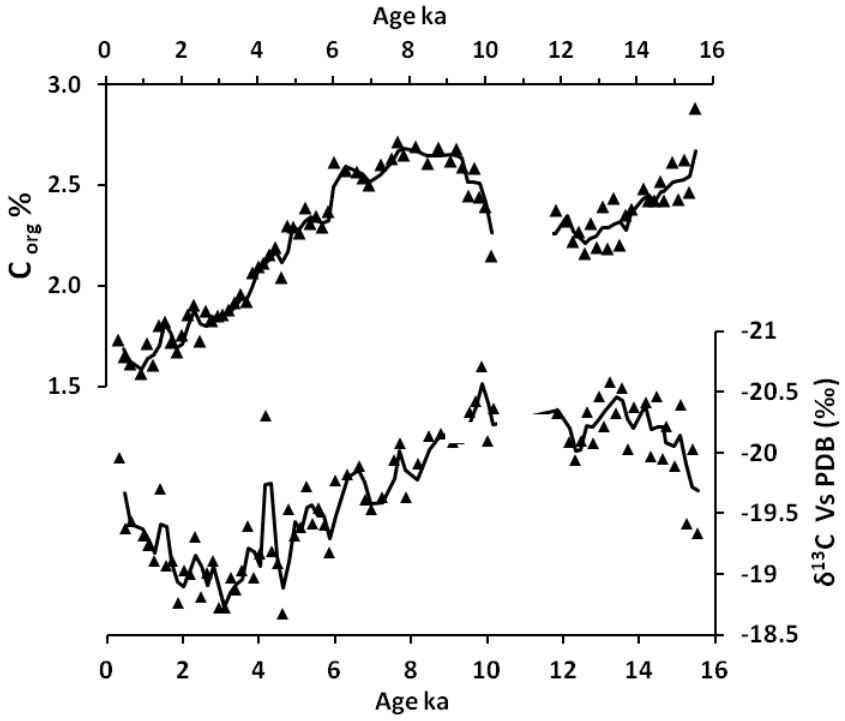

Figure 23. Time-series (2-point running mean) of C_{org} and $\delta^{13}C$ C_{org} in OMZ-base sediment core (GC13)

5.6. Inter elemental association in the Mn-oxide

The correlation analysis of the elements in leachable (oxide) fraction in the OMZ sediment core (GC14) (Table 20) is examined to understand the behavior of set of elements under suboxic environment. The formation process of open ocean Fe-Mn crusts and the particulate-oxides in sediment are similar as both these are formed by the accumulation of colloidal particles precipitated from the seawater and mainly composed of Mn and Fe enriched amorphous (cryptocrystalline) material, which act as carrier for other minor elements (Koschinsky and Halbach, 1995). Two minerals have already been identified previously in the authigenically precipitated oxides viz. Mn-oxide (δMnO_2) and goethite (FeOOH) precipitating independently as evident from very poor correlation between them in the hydrogenetic Fe-Mn

crusts of the Indian Ocean (Banakar and Borole, 1991; Banakar et al., 1997) and from other oceans (see Koschinsky and Halbach, 1995).

Table 20. Inter-element correlation matrix in authigenic fraction of OMZ sediment core.

	Fe	Mn	Co	Cr	V	Mo	U	Re	Ti
Fe	1.0								
Mn	0.0	1.0							
Co	0.3	**0.8**	1.0						
Cr	0.3	0.5	0.5	1.0					
V	0.4	0.1	0.0	0.5	1.0				
Mo	0.2	0.0	-0.1	0.5	0.4	1.0			
U	-0.1	0.6	0.5	0.4	-0.3	0.2	1.0		
Re	0.2	0.4	0.5	0.4	0.0	0.1	0.4	1.0	
Ti	-0.2	0.5	0.5	0.3	-0.4	0.0	**0.9**	0.4	1.0

r = 0.8 is significant at 99.9 % confidence level

The strong positive association of Co with Mn evident in the present sediment core Mn-oxide fraction (r = 0.8: Table 20) has also been observed in Fe-Mn crusts forming in oxygen deficient mid-depth open oceans (Banakar et al., 1997; Koschinsky and Halbach 1995). The closely comparable inter-elemental relationships of primary elements in oxide fraction of the OMZ sediment core and the hydrogenous Fe-Mn crust suggest that the inter-elemental associations exhibited by the leached oxide fraction from present sediment cores (Table 20) are expected relationships in marine environment.

The strong positive relationship of U with Ti (r = 9) and their moderately positive relationship with Mn (r ~ 0.5) and no relationship with Fe (Table 20) suggest that the Mn-phase in the oxide fraction of the sediment is main carrier of Ti and U. The moderately positive association of U, Re and Cr with Mn (r = 0.5) and strong positive association of Co with Mn (r = 0.8) and their no association with Fe (Table 20) indicate that Mn is the carrier of all these minor elements in the leached fraction. But, with increasing suboxic conditions (decreasing DO below 2 ml/l: see Figure 24) the Mn reduction intensifies, while Re precipitation enhances. The non-association of U with Mo (r = 0.2) which are co-precipitating elements with increasing anoxia is also puzzling. These non-coherent associations appear to suggest that with the dissolution of oxides at the sediment-water interface under OMZ conditions the removal of one set of elements from sediment and precipitation of another set

of elements at the sediment-water interface the expected relationships are broken-down. However, the non-association of Mo with Mn or Fe ($r < 0.2$: Table 20) is on the expected line, because, the Mo precipitation is associated with the degree of sulphate reduction (intensity of anoxia), while Mn or Fe precipitation is associated with the degree of oxygenation.

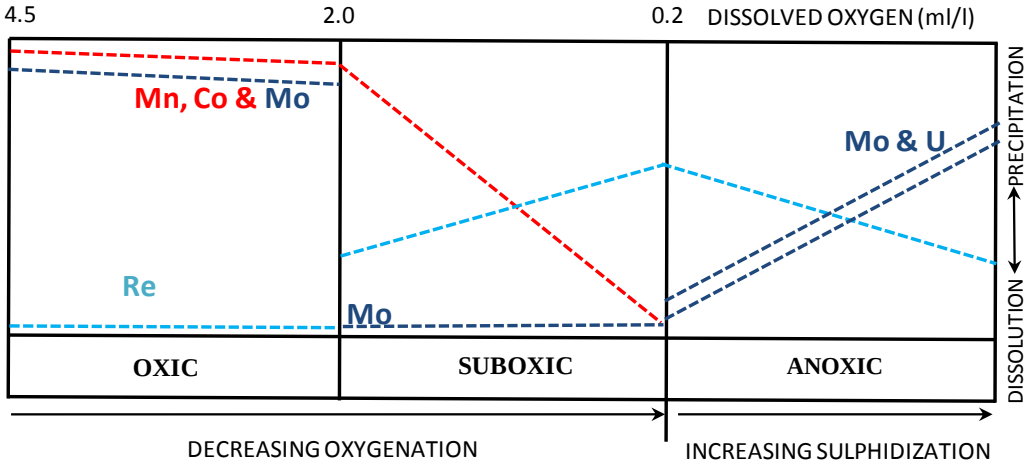

Figure 24. Schematic diagram showing behavior of redox-sensitive elements in oxic, suboxic and anoxic environments. The disappearance of solid-phase Mn (Mn-oxide) at the suboxic/ anoxic boundary associates with the beginning of the precipitation of Mo and U as sulphides via the sulphate reduction. On the other hand, when the solid-phase Mn is rapidly reducing with increasing suboxic conditions the Re begins to precipitate and enrich in the sediment. The redox-behavior of these elements is elaborately discussed by Crusius et al. (1996), Crusius and Thomson (2000), Tribovillard et al. (2006). This well-tested behavior of redox sensitive elements in the sediments is used as basis for discussing their time-series. However, there have been isolated studies arguing that the Re, Mo and U behavior in the oceans is controlled by the salinity and OM rain (Goswami et al., 2012) rather than their responses to oxygenation conditions at the sediment-water interface. In spite of these contradictions, the thermodynamics of these elements in the oxygen depleted conditions suggests that the degree of depletion of DO at sediment-water interface has a definite control on the distribution of these elements in the sediment.

At the base of OMZ also the Mn and Fe appear to have independent precipitation as evident from their poor mutual relationship ($r = -2$) (Table 21). The strong positive association of Co with Mn further strengthens similar association observed in OMZ sediment core ($r = 0.9$: Tables 21). The U, Re and Cr show negative association with Mn ($r = -0.6$) unlike positive association found in OMZ sediment core (Table 20). These observations clearly suggest that the contents of U, Re, and Cr in sediment swept by extremely suboxic core of the OMZ and weakly suboxic base of the OMZ are governed by two different processes. As the sediment-water interface at the location of this sediment core experiences oxic/suboxic boundary condition, the Mn^{2+} is expected to oxidize and precipitate and the Mo, Re and U are unlikely to precipitate as oxygenation conditions need to be below the suboxic levels to initiate their precipitation. Hence, the observed negative relationship of these three elements with Mn

and Co is expected under the weak suboxic conditions at the base of OMZ. In other words, the oxygenation at the sediment-water interface presently swept by the base of OMZ appears to have remained nearly under same conditions since the last 16 kyr.

Table 21. Correlation matrix for leached oxide fraction from the sediment at the base of OMZ

	Mn	Fe	Ti	U	Re	Mo	Co	V	Cr
Mn	1.0								
Fe	-0.2	1.0							
Ti	0.2	-0.1	1.0						
U	-0.6	0.4	0.1	1.0					
Re	-0.6	0.1	0.1	0.6	1.0				
Mo	-0.5	-0.4	0.3	0.5	0.5	1.0			
Co	**0.9**	0.2	0.1	-0.6	-0.6	**-0.8**	1.0		
V	0.1	**0.9**	0.0	0.2	0.0	-0.5	0.4	1.0	
Cr	-0.6	0.6	0.1	**0.9**	0.6	0.4	-0.5	0.4	1.0

r = 0.8 significant at 99.9 % confidence level; n = 40

5.7. Tracking past-OMZ in Bay of Bengal

As already mentioned in Introduction Section, the world ocean OMZs are formed by the combination of productivity and sluggish intermediate water ventilation (Olson et al., 1993; Helly and Leven 1990; Sarma, 2002). The DO in subsurface waters is controlled by, a) advection of oxygenated waters (ventilation) from the areas where it directly interacts with the atmosphere and sinks to intermediate depths and spreads, and b) the consumption of DO by the settling OM through respiration or remineralization of the dead settling OM. Hence, the rate of oxygenated water advection and the amount of OM produced in the photic layer (primary productivity) determines the DO levels of the intermediate (OMZ) waters. The deep and bottom waters have very high DO concentration (>4 ml/l) as compared to the OMZ waters primarily due to their origin at high-latitude (cold) oceanic surfaces.

A high E-P in the AS leads to the formation of high-salinity mixed layer below which three distinct water masses feed the OMZ depths. In the increasing order of depth they are Arabian Sea High salinity water mass (ASHSW) in mixed layer, the Persian Gulf Water (PGW) and Red Sea Water (RSW) (Ivanov-Frantskevich, 1961; Shenoi et al., 1993; Shetye et al., 1994). The intermediate depth in which the OMZ occurs is also ventilated by the Subantarctic Mode Water (SMAW) of the Indian Ocean sector (You and Tomczak, 1993) and

minor contribution from Indonesian Through flow Water (ITF) and Antarctic Intermediate Waters (AIW) (You and Tomczak, 1993). In the intermediate depth of the NIO all these water masses mix and result in Indian Central Water (ICW). The PGW and RSW originate in the very high salinity evaporative marginal seas located in the west of the AS. The PGW occurs between 150 and 400 m and RSW occupy a depth range of 600 m - 800 m (Wyrkti, 1971). The high salinity-warm (36.8 psu and 18°C) PGW (Shenoi et al., 1993) that enters into the northern end of AS from the Gulf of Oman at a depth of around 70 m which is the sill-depth separating both these basins, sinks to around 200 m with a inherently low DO of 3.5 ml/l (Olson et al., 1993). It spreads below the ASHSW across the AS and enters in to the BoB (Shankar et al., 2005). The second source of DO to the AS and BoB intermediate depths are RSW that spread in a depth range of 300-600 m with very low DO (2.5 ml/l: Grasshouf, 1969).

As the PGW and RSW are characterized by inherently low DO contents, their presence in intermediate depths of both AS and BoB (Jain et al., 2016) itself provides the first necessary basis for the development of OMZ. The SMW, although originally has very high DO, but due to very long transit distance before entering the NIO loses significant amount of oxygen and ultimately becomes oxygen depleted in AS and BoB similar to RSW (Olson et al., 1993). Thus, the water masses feeding the intermediate depths in the NIO are fundamentally oxygen depleted (DO < 3 ml/L). Based on the incoming and out-going waters in a box model, Sarma (2002) computed residence time of 6.5 years for the OMZ waters in the AS which indicates a sluggish renewal of water at the intermediate depths that provides another favorable condition for sustained OMZ. The OMZ in the AS is known for its intense de-nitrification throughout the year (deSouza et al., 1996; Morrizon et al., 1998).

All the above described water masses enter in to BoB maintaining their depth during their horizontal advection. The surface layer stratification in BoB is very strong due to the formation of a freshwater plug caused by huge river discharges and very high overhead precipitation (Ostlund et al., 1980). The ASHSW slips just below this very low-salinity stratified surface water of the bay. The PGW and RSW spreads in the BoB after travelling across the intermediate depth of AS. However, the DO of these waters is reduced to around 1 ml/l at their entry point in to BOB in the southern-tip of India, from their original 2 – 3 ml/l (Jain et al., 2016). The presence of these water masses at intermediate depths of the BoB has been confirmed at depth ranges of 200-450 m and 500-600 m respectively, but the RSW gradually loses its identity through mixing with ICW and PGW (Jain et al., 2016). Although

the intermediate water replenishing the OMZ in BoB has significantly lower DO compared to that spreads in the AS and both basins experiencing high primary productivity, a relatively weaker OMZ of the bay not warranting denitrification is puzzling.

A recent modeling (Azhar et al., 2017) and particle flux studies in the deep bay (Ittekkot et al., 1991; Lutz et al., 2002) indicated that huge potential for the formation of mineral aggregate with settling OM enhances the settling rate of OM, hence reduces remineralization of the OM in the water column of the bay (Sarma, 2002). This is a strong reason for observed deeper depth of remineralization of OM in the bay (over 1000 m) than that found in the AS (around 500 m) (Sarma, 2002; McCreary et al., 2012; Azhar et al., 2017). Therefore, the burial rate of OM in the bay is significantly higher than in the AS. This dynamics of the export production in the bay plays vital role for maintaining the OMZ in the above the de-nitrification level (Azhar et al., 2017; Sarma, 2002). Further, there is no major difference in the residence time of the intermediate waters ventilating the OMZ depths in the AS and BoB, where it is around 6-8 years in the former and ~10 years in the latter (Sarma, 2002). Despite the large spatial and seasonal variability in productivity and circulation, oxygen levels in the BoB OMZ are more or less constant which is regulated and sustained by both physical and biological pumps (Sarma, 2002).

The strong surface stratification in BoB restricts the entrainment of nutrients injected from the thermocline. Because of this the BoB has a relatively low net primary productivity as compared to the AS, which reduces the oxygen demand via respiration. The two major factors which differentiate BoB-OMZ from the AS-OMZ are the organic matter remineralization depth and the mesoscale eddies in ventilating the BoB-OMZ. The upper OMZ in the BoB is ventilated by the mesoscale anticyclonic eddies which also spread nutrients both vertically and horizontally (Resplandy et al., 2011; Kim et al., 2001) in addition to oxygenating the upper water column, which extend even to the sub-thermocline depths (Davis et al., 2005; Bower et al., 2005; Sarma and Udaya Bhaskar, 2018).

As already mentioned in material section, the shallow water sediment core (OMZ sediment core: GC14) is from the seafloor that is presently swept by most intense zone (suboxic) of the OMZ (Figure 8). Therefore, this sediment core is expected to preserve the past record of changes in the intensity of OMZ in the form of geochemical signals. The redox-sensitive elements which are associated with authigenically precipitated oxide particulate fraction of the sediment can be considered as potential tools for this purpose. As per the working hypothesis, the increased oxide-bound elements (Mn, Fe, and Co) in sediment from OMZ environment would indicate decreasing intensity of the OMZ and vice-versa. The other

equally important redox-sensitive trace elements Re and Mo in authigenic fraction of the sediment would tell more refined story about the past OMZ. At sediment-water interface the Re and Mo enter the sediment from seawater and under suboxic (Mn-reduction) and anoxic conditions (sulfate reduction) respectively (Crusius et al., 1999; Nemeroff et al., 2000). In such set-up it is expected that the Re and Mo to exhibit anticorrelation with oxide-bound elements (Mn and Co). But, this expected relationship is not observed in the present sediment core, wherein, Re and Mo show weak positive or no relationship with oxide-bound elements (Table 20). If the sediment is depositing under oxic conditions the Mn is enriched because of the precipitation of MnO_2. Wherein, Mo also is enriched because of scavenging by particulate Mn-oxides, but the Re is not scavenged by the oxide particulates under oxidizing conditions. When the depositional environment reaches suboxic conditions MnO_2 is reduced releasing out the adsorbed Mo into seawater at sediment-water interface and Re is enriched in sediment through authigenic precipitation at the sediment-water interface (Crusius et al., 1999; Nemeroff et al., 2000; Boning et al., 2004). In other words, the Mo depends on oxide particulates, while, Re is independent. In such circumstance these two elements exhibiting no relationship with Mn or Fe is expected. Under the suboxic conditions the Mo diffuses deeper in to the sediments and precipitate as solid phase Mo as and when anoxic conditions are encountered within the sediment.

The Mn content in bulk sediment is lower than the average KGK sediment (Table 16) clearly suggests that the sediment core location has remained under Mn-reducing conditions (below oxic/suboxic boundary) throughout the last 40 kyr, because, under suboxic environment the oxide-bound Mn reduces and redirected to the surrounding water column (Dickens and Owen, 1994). Assuming that the crustal contribution of Mo is negligible (1.5 ppm: Taylor and McLennan, 1985), its significantly lower concentration in the extracted oxide fraction (~10 ppb: Table 11) and nearly similar concentration as compared to seawater composition (10 ppb: Turekian, 1968) also indicate that the core location (or the core of the OMZ) never experienced anoxic (or sulfidic environment) in the last 40 kyr. Thus, the OMZ in the core location appears to have fluctuated mostly within the suboxic limits. Therefore, the time-series of Mn, Co, and Re essentially record the past variation of DO within the level of suboxic range in the study region.

The higher Mn and transition metal contents in KGK sediment than the average crust have been attributed to the presence of authigenic oxides in river environment (Sastri et al., 1973). Considering that the average terrigenous sediment supplied to the core-location had around ~700 ppm of Mn (see Table 16), then, a range of 200 – 400 ppm Mn in the entire

sediment core must be due its loss from the sediment, which is possible only when the depositional environment is suboxic or anoxic. As the Mn readily dissolves/precipitates at suboxic/oxic boundary (Pederson and Calvert, 1993; Dickens and Owen 1994), its concentration is linked to slight changes in DO concentration at sediment-water interface, which is presently suboxic. Therefore, it is possible that certain amount of Mn in the sediment core might be associated with the residual oxide-phase remained in the sediment after interacting with OMZ waters during its burial. Hence, its changes through time can provide information about past variation in the relative intensity of the OMZ (Reichart et al., 1998; Schenau et al., 2002).

5.8. Temporal changes in the OMZ

The water depth (325 m) from which the sediment core GC14 (OMZ Sediment Core) was retrieved, is presently swept by most intense OMZ waters (core of the OMZ) (Figure 8). From the bulk-sediment Mn distribution (Table 13 and Figure 15), it is evident that this element is invariably lower than the average crustal composition and also the average KGK (Table 16) sediment throughout the sediment core. The concentrations of Mn and Co in leachable fraction of the sediment core vary in a narrow range of 20 - 35 ppm. A significantly low leachable Mn compared to its content in the bulk sediment (Av Mn = 250 ppm) confirms that the core location has remained within the oxygen depleted environment throughout the last 42 Ka BP. These observations led Sarathchandraprasad and Banakar (2018) to suggest that the intense suboxic OMZ similar to modern has been in existent in the study region for the last 42 kyr. However, there have been subtle variations in the distribution of OMZ proxies Mn and Co. To eliminate the random variations in the time-series of all elements analyzed in the leachable fraction, i.e., Mn-oxide particles, the temporal variations based on a 3-point running mean through of the data are presented (Figure 25). Therefore, the responses of these elements to changes in contrasting monsoon intensity during the warm Bølling and cold YD are smoothed-out.

The time-series of Mn and Co (Figure 25) exhibit distinct changes through time indicating variations in the suboxic levels. At the outset the “M” shape variation is observed, wherein, the high content peaks are centered on 10 and 35 ka BP and low content trough in between at 20 ka BP (Figure 25). Through the Holocene the contents decrease monotonously to minimum at ~5 ka BP forming left side limb of the ‘M’. The right side limb is formed by moderate depletion of these elements at 42 ka BP. Interestingly, the time-interval between two adjacent minima or maxima are spaced at around 20 kyr, which is a Precession Cycle in the

astronomical scheme of climate change (Milankovitch, 1942). The cyclicity found in the past ISM variability has been dominated by the Precession component (Clemens et al., 1991; Reichart et al., 1998). Therefore, the OMZ sensitive Mn and Co showing similar characteristics suggest that the ISM appears to have played a role in the past changes of the BoB-OMZ. As the decreasing intensity of suboxia leads to decreased removal of Mn and Co from sediment or vice versa (see Figure 24), the increasing Mn and Co in the leachable oxide of the OMZ- sediment core suggests weakening in the intensity at the core of OMZ. Therefore, the timings of increased Mn and Co at around 35 and 10 ka BP (Figure 25) might have been the result of increased DO in the core of OMZ. In contrast, the OMZ appears to have intensified at around 40, 20 and 5 ka BP. These timings however do not strictly follow the global climate pattern.

The increasing trends of Mn and Co, along with the increasing Mo, U, and Re (Blue shaded bars in Figure 25) together suggest intensification of the suboxia in the core of the BoB OMZ during pre-LGM and last deglacial climate. In other time-slices there is no coherency in the variation between these elements probably because of differential forcing on the OMZ by different parameters governing the overall OMZ fluctuations in the BoB, such as, productivity, ventilation, and remineralization depth. To some extent, such observed behavior can be unscrambled by considering the behavior of each of these elements under variable suboxia in OMZ as schematically presented in Figure 25. Between 30 and 20 ka BP all these elements exhibit decreasing trend suggesting intensification of suboxia within the OMZ (Figure 25). A decoupling of U from Mo at ~10 ka BP is noticed, where U begins to increase in spite of Mo showing decrease. As per Figure 24, the U is expected to behave coherently with Mo under both suboxic and anoxic conditions.

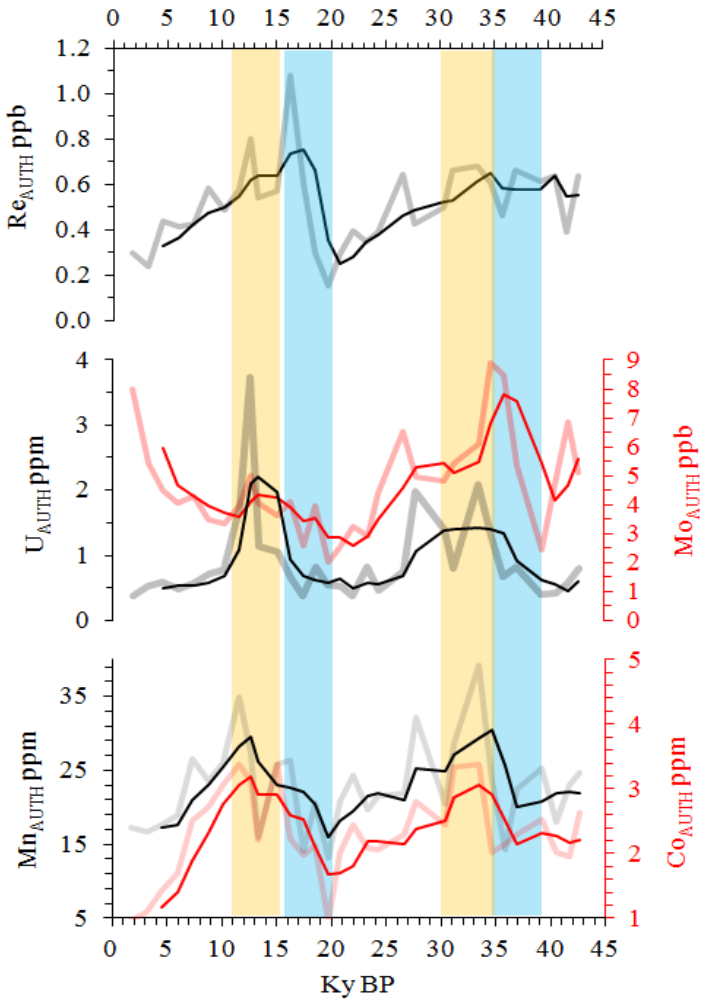

Figure 25. Smoothed time series of redox sensitive elements Mn, Co, U, Mo and Re in the authigenic fraction from the sediments at the core of modern OMZ (GC14). The shadow lines are the data series and the thick lines are the 3 point moving average of each element.

After having identified major changes in suboxia within the core of the OMZ, I have attempted to explain past suboxic levels by comparing the observed changes (Figure 26A) with changes in productivity (Figure 26 C), ventilation (Figure 26D) and the remineralization depth (Figure 26B). The C_{org} representing the productivity, the Al content in bulk sediment representing mineral ballast and the sea-level changes representing the ventilation are compared with the variation in the suboxia represented by Mn and Co in the leachable authigenic oxide fraction. The ventilation of intermediate depth in the study location is largely contributed by PGW and RSW (Jain et al., 2016). These two water masses originating respectively in the Red Sea and Persian Gulf are controlled by their sill depths (~300 m and ~70 m respectively, Olson et al., 1993). When the sea-level was lowered by ~120 m during the LGM, the PGW would have been totally cut-off along with significant reduction in the entire NIO. Such situation is expected to intensify the suboxia in the core of the BoB-OMZ.

Several major rivers systems debouch large amount of land-derived silicate detritus (terrigenous or mineral load) in to the BoB 1350 million tons of sediments per year (Milliman, 1992; 2001), which act as ballast for settling organic matter unlike in AS. Observation of the vertical fluxes of the particulate OM show that although the productivity of the BoB is lesser than AS, higher particulate fluxes have been reported in deep-BoB compared to the AS (Ittekkote, 1991). This anomaly is due to the formation of OM-aggregates with abundantly available mineral particles in the BoB. The mineral and OM aggregate slows down decomposition of OM in addition to increasing its settling speed (Rao et al., 1994; Howell et al., 1997) resulting in substantially increased remineralization depths all across the BoB (Azhar et al., 2017). Therefore, the oxygen demand at intermediate depths of BoB is lesser than in the AS. These remarkable previous observations essentially suggest that the terrigenous input plays vital role in the BoB-OMZ dynamics in contrast to AS-OMZ. This further leads to suggest that the BoB-OMZ is description is not as straightforward as that of AS. Therefore, intensified monsoons can intensify the BoB-OMZ by increasing the productivity, but also can weaken the OMZ by increased input of terrigenous detritus. Hence, the past variation in geochemical proxies of BoB sediment requires careful evaluation in light of terrigenous input (monsoon intensity), productivity and mid-depth ventilation by sea-level dependant PGW and RSW.

All the three time-series of proxies representing three primary parameters (productivity, ventilation and OM reminerilization depth) responsible collectively or individually for sustaining the BoB-OMZ (Olson et al., 1993; Rao et al., 1994; Sarma, 2002; McCreary et al., 2012; Helly and Leven, 2009; Azhar et al., 2017) are presented in Figure 26. First, productivity (C_{org}) variation is compared vis-à-vis suboxic level in the core of the OMZ as represented by leachable Mn and associated Co. As expected, the increased productivity during the initial LGM conditions (around 32 – 25 ka BP) (Figure 26C) has caused intensification of suboxic conditions as evident by decreasing authigenic Mn oxide particulates in the sediment core (Figure 26A). In contrast, a similar increase in the productivity during deglacial transition (around 18 – 12 ka BP) is not associated with similar intensification of suboxia and decreased productivity during the Holocene is not associated with expected weakening of suboxia (Figure 26A and C). Under such circumstances, this mismatch between suboxic status and the productivity need to be examined in light of other two forcing parameters (ventilation and OM-remineralization). The remineralization depth of the OM appears to have remained constant throughout the deglacial time as evident by nearly unchanged Al content (Figure 26B), hence not contributed to the above described mismatch.

The deglacial period has witnessed rapid increase in the global sea level (Figure 26D). This rise is expected to increase the inflow of oxygenated PGW and RSW in to the core of BoB-OMZ. The increased inflow of these two waters therefore appear to have enhanced the replenishment of oxygen level in the then existing intense suboxic OMZ of the LGM, resulting in weakening of suboxia in spite of increased productivity.

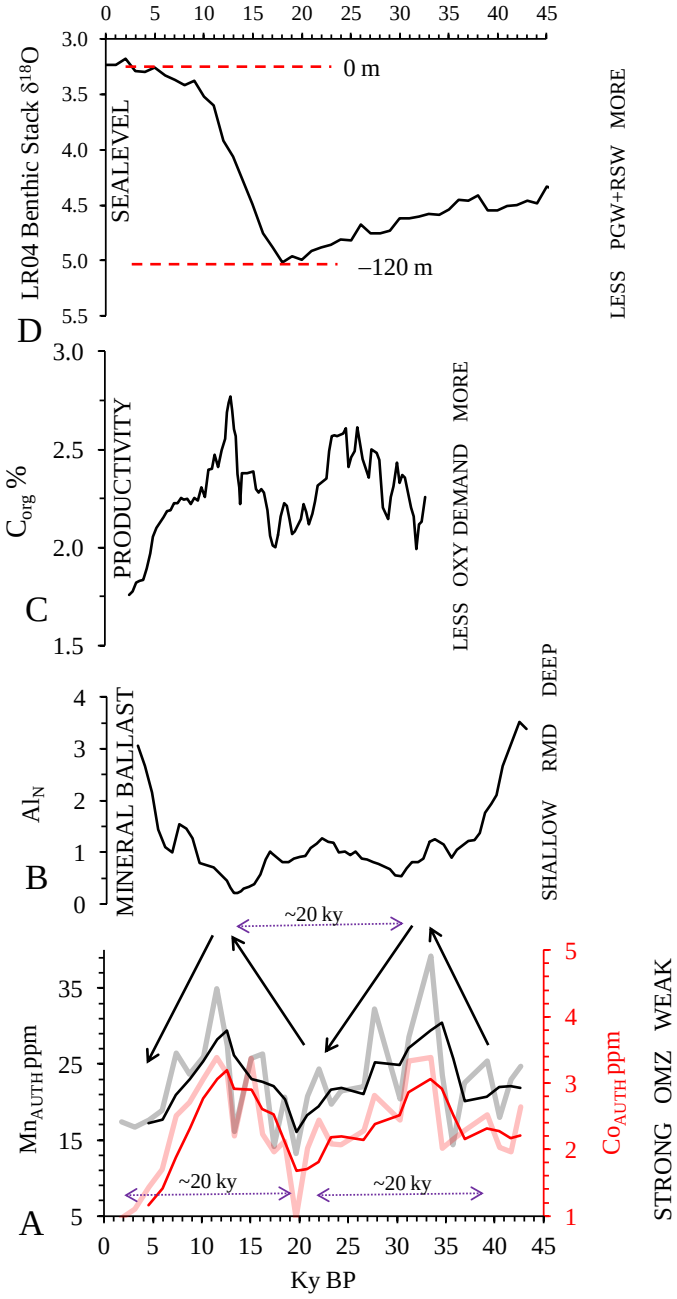

Figure 26. The time series composite of A) OMZ variability indicated by Mn Authigenic, B) variation in remineralization depth indicated by Al content, C) Oxygen demand indicated by organic matter content D) changes in the ventilation suggested by the global sea level pattern changes (LR04). The identified intensification and weakening of BoB OMZ are indicated by the hard line arrows. The identified 20 ky OMZ cyclicity is indicated by the dotted arrows in the bottom panel of the figure.

The Holocene intensification of suboxia, however, cannot be explained by invoking productivity and ventilation together or individually as dominant forcing on the OMZ, because, the ventilation remained unchanged due to nearly constant sea-level (Figure 26D) and productivity actually decreased (Figure 26C). The third potential forcing parameter, the OM remineralization-depth, must have increased through the Holocene as a result of increased terrigenous silicate input as depicted by Al variation (Figure 26B) due intensified ISM. The increased mineral-ballast (terrigenous-silicates and decreased productivity under nearly constant ventilation of intermediate waters (thermocline) in the BoB are expected to result in weakening of the OMZ instead of observed intensification. Therefore, it may be speculated that, the suboxic conditions in the core of the Holocene OMZ appear to have controlled by a complex interplay of several forcing parameters, which are not yet understood completely. Alternatively, a significant decrease in the DO of PGW and RSW may have occurred before they exit the AS to enter in to BoB as a result of increased respiration within the AS during the Holocene. This interpretation is based on the fact that, the AS-OMZ stabilized to most intensified present level nearly 7 ka BP (von Rad et al., 1999). It means, the PGW+RSW entering in to the BoB via AS were significantly depleted in DO since the Holocene. Thus, in spite of decreased productivity and increased mineral ballast in the BoB during Holocene the OMZ intensified instead of weakening. In light of this interpretation, it appears that the PGW and RSW in BoB have played a vital role in dictating the OMZ of the bay through the last 42 ka BP.

5.9. Effect of climatic events in BoB OMZ dynamics

The effect and consequences of North Atlantic climatic events such as YD (Carlson, 2013), Bølling, and Hienrich events (H1, H2, H3 and H4: Bond et al., 1992; Hemming et al., 2004)) on hydrography and circulation of NIO have been well studied (vonRad 1999; Pattan et al., 2013; 2017). These climatic events have shown to have role in the fluctuations of OMZ in the AS (Schulte et al., 1998; von Rad et al., 1999; Reichart et al., 1998; 2002), which also have influenced OMZ variability in different regions of the world ocean (Shibahara et al., 2007; McKay et al., 2005). In this section the effect of global rapid climatic events on the BoB OMZ fluctuations are presented.

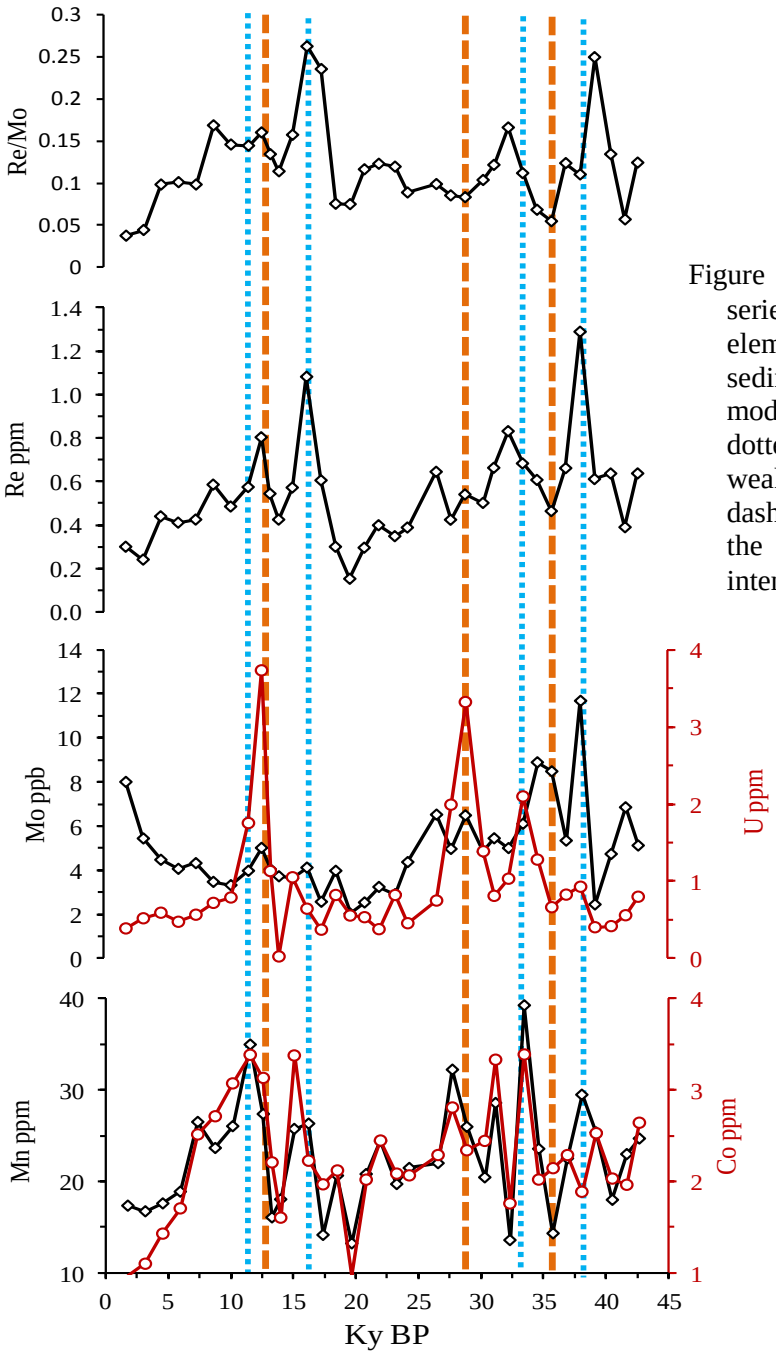

Figure 27: Unsmoothed time series of redox sensitive elemental concentration in sediments from the core of modern OMZ (GC14). The dotted blue lines the weakening periods and dashed orange lines indicate the periods of OMZ intensification.

At the outset, the unsmoothed time-series of few redox sensitive elements appear to show approximate relationship with rapid climatic events recorded in high-latitude North Atlantic region (Figure 27). The weakened OMZ during ~37-40, ~32, ~22, ~16 and ~12 Ka BP as depicted by increased Mn, Co, and Re in oxide-fraction are tentatively correlated with Heinrich events and YD, i.e., cold stadials. As the increasing Re/Mo indicates decreasing suboxic conditions (Crusius et al., 1999), the elevated Re/Mo in the time-series (Figure 27) further confirms the weakening of OMZ during the periods when the global climate transited in to extreme cold conditions intermittently. During ~36-35, 27-26 ~ and ~12-11.5 Ka BP the

Mn and Re/Mo depleted and U and Mo are enriched (Figure 27) indicating intensification of OMZ. These periods roughly correlate with the interstadial warm events including Bolling of the deglaciation during which the ISM was intensified. These correlations are comparable to those already observed in the AS (Rad et al., 1999; Schulte et al., 1999) and apparently suggests that the rapid cooling in the northern hemisphere high-latitudes had a bearing on the OMZ status of the entire NIO. The changes in the deep thermohaline circulation (THC) during the YD and H events may have caused the BoB OMZ to weaken. It has been argued that during the YD the reduction in NADW formation gave way for increased contribution of the southern sourced water (Antarctic Intermediate Water and SAMW) to the NIO (Carlson, 2013) resulting in improved supply of DO at intermediate depths. From these observations it is speculated that that the past OMZ variations in BoB might have been to some extent modulated by changes in global intermediate circulation causing changes in the ventilation and affecting the ISM intensity.

5.10. Last 16 ky variation at the base of OMZ

The authigenic Mn and Co pair shows a depleted concentration during ~16 to 8 ka BP (deglaciation to early Holocene) and a gradual increase in concentration from 8 ka BP onwards to the present (Figure 28). This indicates that at the base of OMZ the availability of oxidizable-Mn increased through the Holocene. Such condition at the base of OMZ is possible when Core of the OMZ is intensified resulting in enhanced reduction of sedimentary Mn-oxide. Thus reduced Mn^{2+} exits the sedimentary reservoir and enriches the OMZ waters with dissolved Mn (Koschinsky and Halbach, 1995). The DO at the base of OMZ is higher (moderately suboxic) and provides ample opportunity to the dissolved Mn-pool to precipitate in to Mn-oxide particulates, in a way similar to the formation of seamount hydrogenous Fe-Mn crusts (Koschinsky and Halbach, 1995; Banakar et al., 1994).

The trends of Mo, U and Re which are opposite to Mn variation through the last ~16 kyr covered by this sediment core supports existence of suboxic conditions at the Base of OMZ through the Holocene. The location of this sediment core is well beyond the PGW spreading depths. Hence, the source of oxygen required for changes in the suboxia at the base of the OMZ may have been associated with Antarctic Intermediate Water (AAIW) and Indonesian Intermediate Water (IIW). Although, these water masses do not enter directly in to the BoB they do retain their characters in spite of long transit along the south of equator before entering the BoB (You, 1998). You (1998) demonstrated that the IIW contribution to BoB-intermediate depth below ~800 m is dominated by (>50%) with minor contribution from

AAIW and RSW. Therefore, the alternate reason for increased concentration of Mn in sediment through the Holocene might be due to weakening of suboxia as a result of increased flow of IIW and AAIW in the BoB that gradually reduced the removal of Mn from the sediment through the Holocene.

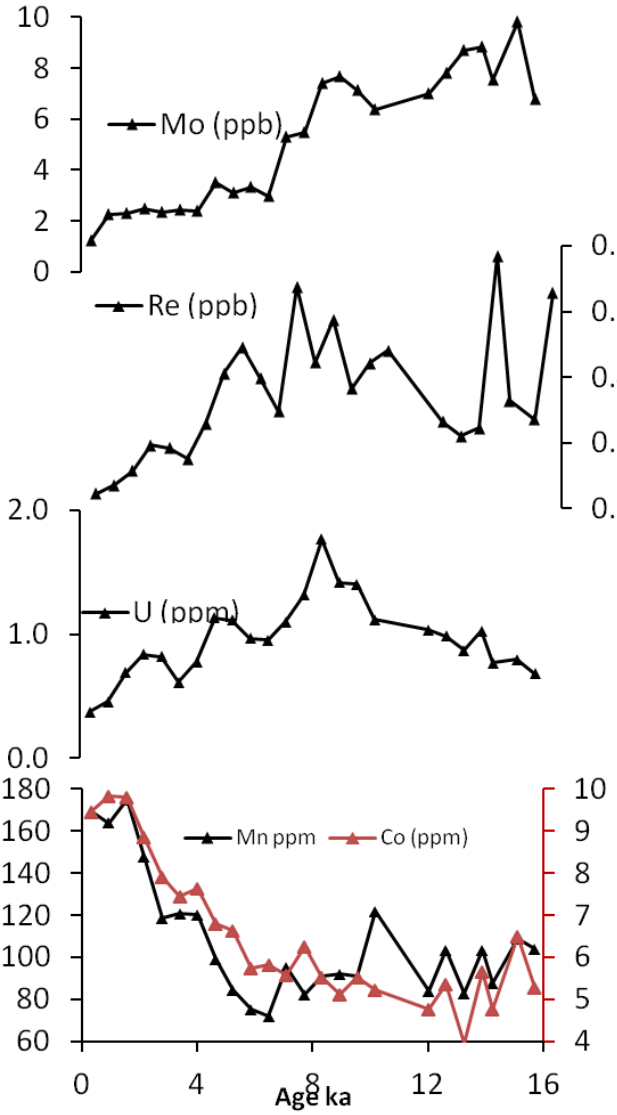

Figure 28. Time-series of redox-elements in OMZ-base sediment core.

The other possibility of changes in the Mn inventory of the Base-OMZ sediment core could be due to changes in the vertical extension of OMZ due to changes in its intensification. To understand this it is necessary to compare the respective geochemical data for a common time-period. This comparison is provided as Figure 29.

Before going in to the details of suggested vertical expansion/contraction of the OMZ, it is re-emphasized in light of the working hypothesis (Figure 7) that the vertical expansion of the OMZ at a given time-slice should produce covariation of redox-elements in both the

sediment cores, i.e., both in the core of OMZ and at the base of OMZ. In case, the OMZ is vertically contracted, then the base of the OMZ comes improved oxygenation resulting in reduced suboxic conditions, while the core of the OMZ still remaining in the intense suboxic conditions. This situation would result in opposing trends of the redox elements in a given time-slice. It should be further noted that the Mn content in both the sediment cores is lower than the KGK average sediment or crustal composition (Table 16) indicating that the Mn-oxide has been reducing throughout the time spans covered by both the sediment cores.

5.11. Deglacial to late Holocene OMZ dynamics

In this section the changes in the redox-elements composition in oxide-fractions from both the sediment cores are compared for the common time-period covered (16 Ka BP to 1.7 Ka BP) (Figure 29). The concentration of Mn in OMZ sediment core is always lower (15 - 35 ppm) than in the Base-OMZ sediment core (65 - 165 ppm) (Figure 29), as expected, because, the former sediment core location is swept by extremely suboxic waters (~0.5 ml/l) and the latter sediment core location by moderately suboxic waters (~ 2 ml/l) (Figure 4). The ventilation during this time period is assumed to be constant due negligible changes in the Holocene sea level. The C_{org} variation is nearly coherent at both core locations. The Mn content decreases in the OMZ sediment core through the Holocene while it rapidly increases through the mid-Holocene in the Base-OMZ sediment core. These trends indicate that at the core of the OMZ the DO depleted and at the base of the OMZ the DO increased. The increasing Mo through the Holocene in the OMZ sediment core and decreasing in Base-OMZ core (Figure 29) confirm the above observation. As the C_{org} in both the sediment core exhibits a decreasing trend through the Holocene, the observed changes in the status of OMZ cannot be explained by the productivity changes. Alternatively, the changes in the DO of ventilating water might have been the primary cause of observed trends in oxide-elements. It has been shown that for the last 7 kyr the OMZ of the AS has been stable (VonRad et al., 1999). This means that the AS OMZ has been extremely intense since then. Therefore, the PGW and RSW that enters the BoB-OMZ via the AS-OMZ must have been extremely oxygen deficient since the last 7 kyr. This might have intensified the BoB-OMZ resulting in depleting Mn in the OMZ sediment core. On the other hand, at the base of OMZ the improved DO within the suboxic (Mn-leachable) limit might have reduced the removal sedimentary Mn.

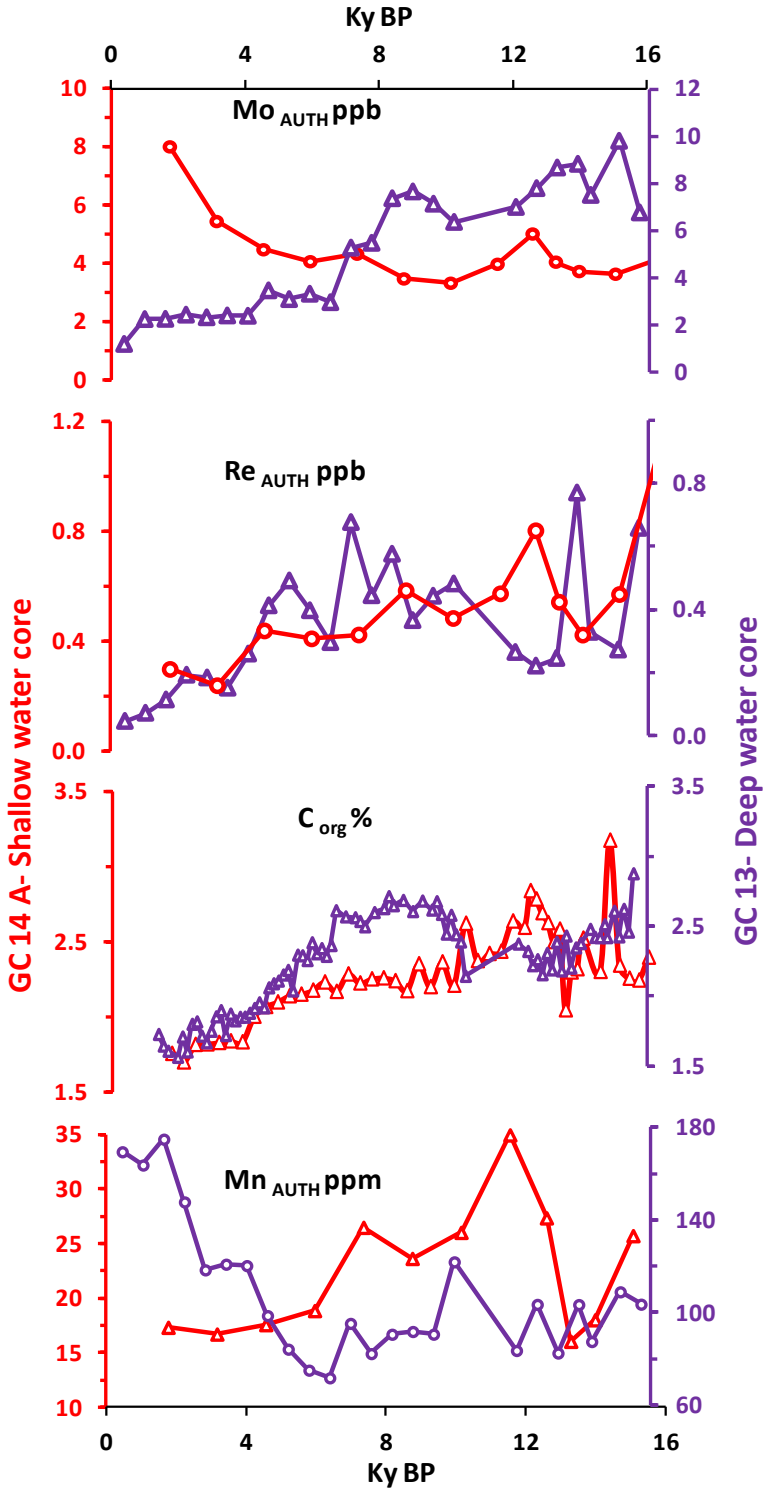

Figure 29. Last 16 ky time-series of Mn, C_{org} and Re and Mo in the oxide-fractions cores

6. CONCLUSIONS

A. The geochemical characteristics of few index elements and oxygen isotope time-series from two sediment cores of the eastern continental margin of India (western Bay of Bengal) record the past changes in summer monsoon related biogeochemical changes and OMZ variability.

B. The Mn concentration in sediment cores from present day Core of the OMZ and from the base of the OMZ are consistently lower than the average crustal composition and also composition of terrigenous sediment supplied to the core locations suggest that the OMZ in the eastern margin of India has been under sub-oxic conditions since the last 42 kyrs.

C. The weakening and strengthening of perennially suboxic OMZ in the study region appears to be (speculated) rhythmic with around 20 ky cyclicity. In that, the suboxia weakened during the pre-LGM, strengthened through the LGM, again weakened through the deglacial transition and strengthened through the Holocene.

D. The absence of denitrification in modern Bay of Bengal as revealed by previous studies when coupled with above observations may indicate that the OMZ in the study region never reached suboxic-anoxic boundary conditions.

E. The past changes in the OMZ of the eastern margin of India are complex and appear to have governed independently by changes in productivity, changes in ventilation and changes in terrigenous silicate supply at different times.

F. The $\delta^{18}O_{G.sacculifer}$ time-series contains well-defined climatic events of the last 42 kyr, such as LGM, Deglacial Bolling warm period and YD cold period and the Holocene.

G. The observed Greenland climate connection with the Indian summer monsoon variation recorded by the present sediment cores is consistent with previous studies based on Arabian Sea sediment cores.

H. The bulk sediment composition revealed that the terrigenous matter supply to the eastern continental margin of India was high during the pre-LGM, minimum during the LGM and increased through the Holocene in accordance with the established glacial-interglacial summer monsoon variability.

I. The C_{org} and δ^{13} C_{org} time-series suggest that the organic matter in the sediment is a mixture of marine productivity derived carbon and the soil carbon delivered by east flowing rivers draining the peninsular India.

J. The decreased (increased) productivity during Holocene (LGM) in Bay of Bengal along with similar previous observations from Arabian Sea is of significance because the entire Northern Indian Ocean might have contributed to the global cooling during the LGM through enhanced burial of the organic matter.

BIBLIOGRAPHY

Akhil, V.P, Fabien Durand, Matthieu Lengaigne, Jerome Vialard, M.G Keerthi, V. V. Gopalakrishna, Charles Deltel, Fabrice Papa, and Clement Montegue. (2014). Journal of Geophysical Research : Oceans. 119: 3926–47. https://doi.org/10.1002/ 2013JC009632

Algeo, Thomas J., Jennifer Morford, and Anna Cruse, 2012. New Applications of Trace Metals as Proxies in Marine Paleoenvironments. Chemical Geology, 324–325: 1–5. https://doi.org/10.1016/j.chemgeo.2012.07.012

Alley, Richard B., and Anna Maria Agustsdottir, 2005. The 8k Event: Cause and Consequences of a Major Holocene Abrupt Climate Change. Quaternary Science Reviews, 24: (10–11): 1123–49. https://doi.org/10.1016/j.quascirev.2004.12.004

Aoki, S., Kohyama, N., and Ishizuka, T, (1991). Sedimentary history and chemical characteristics of clay minerals in cores from the distal part of the Bengal Fan (ODP 116). Marine Geology, 99(1–2), 175–185. https://doi.org/10.1016/0025-3227(91)90090-Q

Azhar , Muchamad Al, Zouhair Lachkar, Marina Lévy, and Shafer Smith. 2017. Oxygen Minimum Zone Contrasts between the Arabian Sea and the Bay of Bengal Implied by Differences in Remineralization Depth. Geophysical Research Letters. https://doi.org/10.1002/2017GL075157.

Babu, C. P., Pattan, J. N., Dutta, K., Basavaiah, N., Prasad, G. V. R., Ray, D. K., and Govil, P, (2010). Shift in detrital sedimentation in the eastern bay of Bengal during the late quaternary. Journal of Earth System Science, 119(3), 285–295. https://doi.org/10.1007/s12040-010-0022-9

Banakar, V. K., B. S. Mahesh, G. Burr, and A. R. Chodankar. (2010). Climatology of the Eastern Arabian Sea during the Last Glacial Cycle Reconstructed from Paired Measurement of Foraminiferal $\delta^{18}O$ and Mg/Ca. Quaternary Research 73 (3). https://doi.org/10.1016/j.yqres.2010.02.002

Banakar, V. K., T. Oba, A. R. Chodankar, T. Kuramoto, M. Yamamoto, and M. Minagawa. 2005. Monsoon Related Changes in Sea Surface Productivity and Water Column Denitrification in the Eastern Arabian Sea during the Last Glacial Cycle." Marine Geology 219 (2–3): 99–108. https://doi.org/10.1016/j.margeo.2005.05.004.

Banakar, V.K., Baidya, S., Piotrowski, A.M. D.Shankar, (2017). J. Earth Syst. Sci. 126: 87. https://doi.org/10.1007/s12040-017-0864-5.

Bassinot, Franck C, Laurent D Labeyrie, Edith Vincent, Xavier Quidelleur, Nicholas J Shackleton, and Yves Lancelot. (1994). "Of the Brunhes-Matuyama Magnetic Reversal" 126: 91–108.

Bayon, G., C.R. German, R.M. Boella, J.a. Milton, R.N. Taylor, and R.W. Nesbitt. (2002). An Improved Method for Extracting Marine Sediment Fractions and Its Application to Sr and Nd Isotopic Analysis.Chemical Geology 187 (3–4): 179–99. https://doi.org/10.1016/S0009-2541(01)00416-8

Bertine, K. K,(1972). The Deposition of Molybdenum in Anoxic Waters. Marine Chemistry 1 (1): 43–53. https://doi.org/10.1016/0304-4203(72)90005-9.

Bond, Gerard, Hartmut Heinrich, Wallace Broecker, Laurent Labeyrie, Jerry McManus, John Andrews, Sylvain Huon, (1992). Evidence for Massive Discharges of Icebergs into the North

Atlantic Ocean during the Last Glacial Period. Nature 360. http://dx.doi.org/10.1038/360245a0.

Bond, Gerard, William Showers, Maziet Cheseby, Rusty Lotti, Peter Almasi, Paul Priore, Heidi Cullen, Irka Hajdas, and Georges Bonani, (1997). A Pervasive Millennial-Scale Cycle in North Atlantic Holocene and Glacial Climates. Science 278, 1257-1266.

Bradley, R.S. and Eddy, J.A., 1991. Records of past global changes. In: Global Changes of the Past (R.S. Bradley, ed.). Boulder: University Corporation for Atmospheric Research, p.5-9.

Breit, George N., and Richard B. Wanty, (1991). Vanadium Accumulation in Carbonaceous Rocks: A Review of Geochemical Controls during Deposition and Diagenesis. Chemical Geology 91 (2): 83–97. https://doi.org/10.1016/0009-2541(91)90083-4.

Broecker, Wallace S, (1997). Thermohaline Circulation, the Achilles Heel of Our Climate System: Will Man-Made CO_2 upset the Current Balance?. Science 278 (5343): 1582 -1588. http://science.sciencemag.org/content/278/5343/1582.abstract.

Bruland, K. W, (1980). Oceanographic Distribution of Cadmium, Zinc, Nickel, and Copper in the North Pacific. Earth and Planetary Science Letters 47: 176–98.

Cabre, A., I. Marinov, R. Bernardello, and D. Bianchi, (2015). Oxygen Minimum Zones in the Tropical Pacific across CMIP5 Models: Mean State Differences and Climate Change Trends. Biogeosciences 12 (18): 5429–54. https://doi.org/10.5194/bg-12-5429-2015

Calvert, S. E., and T. F. Pedersen. (1993). Geochemistry of Recent Oxic and Anoxic Marine Sediments: Implications for the Geological Record. Marine Geology, 113 (1–2): 67–88. https://doi.org/10.1016/0025-3227(93)90150-T

Cannariato, Kevin G, and James P Kennett, (1999). Climatically Related Millennial-Scale Fluctuations in Strength of California Margin Oxygen-Minimum Zone during the Past 60ky. Geology 27: 975–78.

Cavan, E. L., M. Trimmer, F. Shelley, and R. Sanders,(2017). Remineralization of Particulate Organic Carbon in an Ocean Oxygen Minimum Zone. Nature Communications 8: 14847. https://doi.org/10.1038/ncomms14847

Chaitanya, Akurathi Venkata Sai, Fabien Durand, Simi Mathew, Vissa Venkata Gopalakrishna, Fabrice Papa, Matthieu Lengaigne, Jerome Vialard, Chanda Kranthikumar, and R. Venkatesan. (2015). Observed Year-to-Year Sea Surface Salinity Variability in the Bay of Bengal during the 2009–2014 Period. Ocean Dynamics 65 (2): 173–86. https://doi.org/10.1007/s10236-014-0802-x

Chao, T. (1972) Selective dissolution of manganese oxides from soils and sediments with acidified hydroxylamine hydrochloride. Proceedings of the soil society of America 36, 746-753

Cheng, R. Lawrence Edwards, and Indra B. Singh. (2005). “Variability of Southwest Indian Summer Monsoon Precipitation during the Bolling-Allerod. Geology 33 (10): 813–16. https://doi.org/10.1130/G21498.1

Chester, R and Hughes, M.J.(1967). A chemical technique for the separation of ferromanganese minerals, carbonate minerals, and adsorbed trace elements from pelagic sediments. Chemical Geology 2, 246-262.

Chodankar, Anjali R, Virupaxa K Banakar, and Tadamichi Oba, (2005). Past 100 Ky Surface Salinity-Gradient Response in the Eastern Arabian Sea to the Summer Monsoon Variation Recorded by $\delta^{18}O_{\text{G. Sacculifer}}$. Global and Planetary Change 47 (2–4 SPEC. ISS.): 135–42. https://doi.org/10.1016/j.gloplacha.2004.10.008

Clark, Peter, Arthur Dyke, Jeremy Shakun, Anders Carlson, Jorie Clark, Barbara Wohlfarth, Jerry Mitrovica, Steven Hostetler, and Marshall McCabe. (2009). The Last Glacial Maximum. Science 325 (5941): 710–14. https://doi.org/doi: 10.1126/science.1172873

Cline, Joel D., and Francis A. Richards, (1972). Oxygen Deficient Conditions and Nitrate Reduction in the Eastern Tropical North Pacific Ocean. Limnology and Oceanography 17 (6): 885–900. https://doi.org/10.4319/lo.1972.17.6.0885

Codispoti, L. A., Jay A. Brandes, J. P. Christensen, A. H. Devol, S.W. A. Naqvi, Hans W. Paerl, and T. Yoshinari, (2001). The Oceanic Fixed Nitrogen and Nitrous Oxide Budgets: Moving Targets as We Enter the Anthropocene? Scientia Marina 65 (S2): 85–105. https://doi.org/10.3989/scimar.2001.65s285

Colin, C., L. Turpin, J. Bertaux, A. Desprairies, and C. Kissel.(1999). Erosional History of the Himalayan and Burman Ranges during the Last Two Glacial-Interglacial Cycles. Earth and Planetary Science Letters 171 (4): 647–60. https://doi.org/10.1016/S0012-821X(99)00184-3

Colodner, Debra, Julian Sachs, G. Ravizza, K. K. Turekian, and E. Boyle, (1993). The Geochemical Cycle of Re: A Reconnaissance. Earth and Planetary Science Letters 117: 205–21. https://doi.org/10.1016/0012-821X(93)90127-U

Crusius, John, and John Thomson, (2000). Comparative Behavior of Authigenic Re, U, and Mo during Reoxidation and Subsequent Long-Term Burial in Marine Sediments. Geochimica et Cosmochimica Acta, 64 (13): 2233–42. https://doi.org/10.1016/S0016-7037 (99)00433-0.

Crusius, John, Stephen Calvert, Thomas Pedersen, and David Sage, 1996. Rhenium and Molybdenum Enrichments in Sediments as Indicators of Oxic, Suboxic and Sulfidic Conditions of Deposition. Earth and Planetary Science Letters. 145 (1–4): 65–78. https://doi.org/10.1016/S0012-821X(96)00204-X

Danzeglocke, U., (2008). CalPal-2007online. http://www.calpalonline.de/, 2008-10-05.

Deplazes, Gaudenz, Andreas Lückge, Larry C Peterson, Axel Timmermann, Yvonne Hamann, Konrad a Hughen, Ursula Röhl, (2013). Links between Tropical Rainfall and North Atlantic Climate during the Last Glacial Period." Nature Geoscience 6 (2). Nature Publishing Group: 1–5. https://doi.org/10.1038/ngeo1712

DeSousa, S.N., M. DileepKumar, S. Sardessai, V.V.S.S. Sarma, and P.V. Shirodkar. (1996). Seasonal Variability in Oxygen and Nutrients in the Central and Eastern Arabian Sea. Current Science 71 (11): 847–51.

DeSousa, S.N., S.W. A. Naqvi, and G.V Reddy, (1981). Distribution of Nutrients in the Western Bay of Bengal. Indian Journal of Marine Science 10: 327–31.

Diaz, R. J., and R. Rosenberg, (2008). Spreading Dead Zones and Consequences for Marine Ecosystems. Science 321 (5891): 926–29. https://doi.org/10.1126/science.1156401.

Dickens, Gerald R., and Robert M. Owen. (1999). The Latest Miocene-Early Pliocene Biogenic Bloom: A Revised Indian Ocean Perspective. Marine Geology 161 (1): 75–91.

https://doi.org/10.1016/S0025-3227(99)00057-2.

Dileep Kumar, M., Biogeochemistry of the North Indian Ocean. Ind. Acad. Sci., (2006).

DOI: 10.1016/0016-7037(82)90119-3

Dixit, Yama, David A. Hodell, and Cameron A. Petrie. (2014). Abrupt Weakening of the Summer Monsoon in Northwest India ~4100 Yr Ago. Geology 42 (4): 339–42. https://doi.org/10.1130/G35236.1.

Domingues, Catia M., John A. Church, Neil J. White, Peter J. Gleckler, Susan E. Wijffels, Paul M. Barker, and Jeff R. Dunn,(2008). Improved Estimates of Upper-Ocean Warming and Multi-Decadal Sea-Level Rise. Nature 453 (7198): 1090–93. https://doi.org/10.1038/nature07080

Dutt, Som, Anil K. Gupta, Steven C. Clemens, Hai Cheng, Raj K. Singh, Gayatri Kathayat, and R. Lawrence Edwards. (2015). Abrupt Changes in Indian Summer Monsoon Strength during 33,800 to 5500years B.P. Geophysical Research Letters 42 (13): 5526–32. https://doi.org/10.1002/2015GL064015

Dutta, Koushik, Ravi Bhushan, and B. L. K. Somayajulu.(2001). ΔR Correction Values for the Northern Indian Ocean. Radiocarbon 43 (2): 483–88. https://doi.org/10.1017/S0033822200038376

Emerson, S R. (1998). The Geochemistry of Redox Sensitive Trace Metals, 1023–24.

Emerson, Steven R., and Sarah S. Huested. (1991). Ocean Anoxia and the Concentrations of Molybdenum and Vanadium in Seawater. Marine Chemistry 34 (3–4): 177–96. https://doi.org/10.1016/0304-4203(91)90002-E

Emery, W J, and J. Meincke. (1942). Global Water Masses: Summary and Review. Oceanologia 9 (4): 383–91.

Fagel, N., Debrabant, P., and Andrew, L., (1994). Clay supplies in the Central Indian Basin since the Late Miocene: climatic or tectonic control? Marine Geology, 122(1–2), 151–172. https://doi.org/10.1016/0025-3227(94)90209-7

Finney, B, and Mitch Lyle. (1988). Sedimentation at MANOP Site H (Eastern Equatorial Pacific) over the Past 400,000 Years: Climatically Induced Redox Variations and Their Effects on Transition Metal Cycling. Paleoceanography 3 (2): 169–89.

Fleitmann, D., Burns, S. J., Neff, U., Mudelsee, M., Mangini, A., and Matter, A., (2004). Palaeoclimatic interpretation of high-resolution oxygen isotope profiles derived from annually laminated speleothems from Southern Oman. Quaternary Science Reviews, 23(7–8), 935–945. https://doi.org/10.1016/j.quascirev.2003.06.019

Frakes, L. A, and J. E. Francis, (1988). A guide to phanerozoic cold polar climates from high latitude ice rafting in the cretaceous. Nature. 333: 547–549.

France-Lanord, C., Derry, L., and Michard, A., (1993). Evolution of the Himalaya since Miocene time: isotopic and sedimentological evidence from the Bengal Fan. Geological Society, London, Special Publications (Vol. 74). https://doi.org/10.1144/GSL.SP.1993.074.01.40.

Gadgil, S., (2003) The Indian monsoon and its variability. Annual Review of Earth and Planetary Sciences 31:1, 429-467. doi: 10.1146/annurev.earth.31.100901.141251.

Galy, Valier, Christian France-Lanord, Bernhard Peucker-Ehrenbrink, and Pascale Huyghe. (2010). Sr-Nd-Os Evidence for a Stable Erosion Regime in the Himalaya during the Past 12 Myr. Earth and Planetary Science Letters, 290 (3–4): 474–80. https://doi.org/10.1016/j.epsl.2010.01.004

Garzanti, Eduardo, Sergio Andó, Christian France-Lanord, Paolo Censi, Pietro Vignola, Valier Galy, and Maarten Lupker. (2011). Mineralogical and Chemical Variability of Fluvial Sediments 2. Suspended-Load Silt (Ganga-Brahmaputra, Bangladesh). Earth and Planetary Science Letters 302 (1–2): 107–20. https://doi.org/10.1016/j.epsl.2010.11.043

Gauns, M., Madhupratap, M., Ramaiah, N., Jyothibabu, R., Fernandes, V., Paul, J. T., and Prasanna Kumar, S., (2005). Comparative accounts of biological productivity characteristics and estimates of carbon fluxes in the Arabian Sea and the Bay of Bengal. Deep-Sea Research Part II: Topical Studies in Oceanography, 52(14–15), 2003–2017. https://doi.org/10.1016/j.dsr2.2005.05.009

Gerard Bond, Hartmut Heinrich, Wallace Broecker, Laurent Labeyrie, Jerry McManus, John Andrews, Sylvain Huon, Ruediger Jantschik, Silke Clasen, Christine Simet, Kathy Tedesco, Mieczyslawa Klas, Georges Bonani & Susan Ivy, (1992).Evidences of massive discharges of icebergs into the north atlantic ocean during the last glacial period. Nature 360: 245–249.

Ghienne, Jean François, Andre Desrochers, Thijs R.A. Vandenbroucke, Aicha Achab, Esther Asselin, Marie Pierre Dabard, Claude Farley, (2014). A Cenozoic-Style Scenario for the End-Ordovician Glaciation. Nature Communications 5:4485. https://doi.org/10.1038/ncomms5485

Gobler, Christopher J., and Hannes Baumann, (2016). Hypoxia and Acidification in Ocean Ecosystems: Coupled Dynamics and Effects on Marine Life. Biology Letters 12 (5): 20150976. https://doi.org/10.1098/rsbl.2015.0976

Goodbred, Jr., S.L., Kuehl, S.A., Steckler, M., and Sarker, M.H., (2003). Controls on facies distribution and stratigraphic preservation in the Ganges-Brahmaputra delta sequence. Sedimentary Geology, 155:301-316. https://doi.org/10.1016/S0037-0738(02)00184-7

Gomes, H. R., Goes, J. I., and Saino, T., (2000). Influence of physical processes and freshwater discharge on the seasonality of phytoplankton regime in the Bay of Bengal. Continental Shelf Research, 20(3), 313–330. https://doi.org/10.1016/S0278-4343(99)00072-2

Goswami, Vineet, Sunil K. Singh, and Ravi Bhushan. 2012. Dissolved Redox Sensitive Elements, Re, U and Mo in Intense Denitrification Zone of the Arabian Sea. Chemical Geology 291: 256–68. https://doi.org/10.1016/j.chemgeo.2011.10.021.

Govil, Pawan, and Divakar Naidu. (2011). Variations of Indian Monsoon Precipitation during the Last 32 Kyr Re Fl Ected in the Surface Hydrography of the Western Bay of Bengal. Quaternary Science Reviews 30 (27–28). Elsevier Ltd: 3871–79. https://doi.org/10.1016/j.quascirev.2011.10.004

Grasshoff, Klaus (1969). Chemical observations in the Red Sea and the inner Gulf of Aden during the International Indian Ocean Expedition 1964/65. PANGAEA, https://doi.org/10.1594/PANGAEA.603890.

H.G. Ostlund, R. Oleson, R. Brescher, (1980). GEOSECS Indian Ocean radiocarbon and tritium results Tritium Lab. Data Rep., 9, Univ. Miami, Miami, FL, p. 15.

Han, W., McCreary, J. P., and Kohler, K. E., (2001). Influence of precipitation minus evaporation and Bay of Bengal rivers on dynamics, thermodynamics, and mixed layer physics in the upper Indian

Ocean. Journal of Geophysical Research, 106, 6895. https://doi.org/10.1029/2000JC000403

Hays, J D, John Imbrie, and N J Shackleton, (1976). Variations in the Earth's Orbit : Pacemaker of the Ice Ages 194 (4270).

Helly, J. J., and Levin, L. A., (2004). Global distribution of naturally occurring marine hypoxia on continental margins. Deep-Sea Research Part I: Oceanographic Research Papers, 51(9), 1159–1168. https://doi.org/10.1016/j.dsr.2004.03.009

Howell, E. A., and Doney, S. C., (1997). Geochemical estimates of denitrification in the Arabian Sea and the Bay of Bengal during WOCE, a measure of denitrification CFC signal in the Bay of Bengal. Geophysical Research Letters, 24(21), 2549–2552.

Imbrie, J. Van Donk, N.G. Kipp (1973). Paleoclimatic investigation of a late Pleistocene Caribbean deep-sea core: comparison of isotopic and faunal methods. Quaternary Research, 3, pp. 10-38.

Ivanov-Frantskevich, G.N., (1961) Some peculiarities of hydrographyand water masses of the Indian Ocean. In: Oceanology researcharticles, I. G. Y. Program (Oceanology), vol 4, Acad. Sci. USSR, Moscow, pp 7–18

Ittekkot, V., Haake, B., Bartsch, M., Nair, R. R., and Ramaswamy, V., (1992). Organic carbon removal in the sea: the continental connection. (C. . Summerhayes, W. L. Prell, and K. C. Emeis, Eds.), Upwelling Systems: Evolution Since the Early Miocene. Geological society special publication. https://doi.org/10.1144/GSL.SP.1992.064.01.11

Jain, V., Shankar, D., Vinayachandran, P. N., Kankonkar, A., Chatterjee, A., Amol, P.,Neema, C. P., (2016). Evidence for the existence of Persian Gulf Water and Red Sea Water in the Bay of Bengal. Climate Dynamics. https://doi.org/10.1007/s00382-016-3259-4

Kabanova, Yu. G. (1963). Primary production and nutrients in the Indian Ocean. Trans. Inst. Oceanol. Acad. Sci. USSR 64: 257-264.

Kalvelage, Tim, Gaute Lavik, Phyllis Lam, Sergio Contreras, Lionel Arteaga, Carolin R. Löscher, Andreas Oschlies, Aurélien Paulmier, Lothar Stramma, and Marcel M. M. Kuypers, 2013. Nitrogen Cycling Driven by Organic Matter Export in the South Pacific Oxygen Minimum Zone. Nature Geoscience 6 (3): 228–34. https://doi.org/10.1038/ngeo1739

Kamykowski, Daniel, and Sara-joan Zentara (1990). Hypoxia in the world ocean as recorded as historical data set. Deep-SeaResearch 37 (12): 1861–74.

Karstensen, Johannes, Helmholtz Centre, Martin Visbeck, Helmholtz Centre, Groom View, and Johannes Karstensen, (2008). Oxygen Minimum Zones in the Eastern Tropical Atlantic and Pacific Oceans. Progress in oceanography 77 331-351 https://doi.org/10.1016/j.pocean.2007.05.009

Keeling, Ralph F., Arne Körtzinger, and Nicolas Gruber. (2010). Ocean Deoxygenation in a Warming World. Annual Review of Marine Science 2 (1): 199–229. https://doi.org/10.1146/annurev.marine.010908.163855

Kessarkar, Pratima M, V Purnachadra Rao, S W A Naqvi, and Supriya G Karapurkar. (2013). Variation in the Indian Summer Monsoon Intensity during the Blling-Allerd and Holocene. Paleoceanography 28 (3): 413–25. https://doi.org/10.1002/palo.20040.

Kessarkar, Pratima M., V. Purnachandra Rao, S. M. Ahmad, S. K. Patil, A. Anil Kumar, G. Anil Babu,

Sukalyan Chakraborty, and R. Soundar Rajan. (2005). Changing Sedimentary Environment during the Late Quaternary: Sedimentological and Isotopic Evidence from the Distal Bengal Fan. Deep-Sea Research Part I: Oceanographic Research Papers 52 (9): 1591–1615. https://doi.org/10.1016/j.dsr.2005.01.009.

Klinkhammer, Gary P, and Michael L Bender (1980). The Disiribution of Manganese in the Pacific Ocean. Science 46: 361–84.

Koschinsky, Andrea, and Peter Halbach, (1995). Sequential Leaching of Marine Ferromanganese Precipitates : Genetic Implications Geochimica et Cosmochimica Acta 59 (24): 5113–32. https://doi.org/10.1016/0016-7037(95)00358-4

Kumar, D. M., and Li, Y.-H. (1996)., Spreading of water masses and regenration of silica and 226Ra in the Indian Ocean. Deep-Sea Research II, 43(1), 83–110. https://doi.org/10.1016/0967-0645(95)00084-4

Kuypers, Marcel M.M., Lucas J. Lourens, W. Irene C. Rijpstra, Richard D. Pancost, Ivar A. Nijenhuis, and Jaap S. Sinninghe Damste, (2004). Orbital Forcing of Organic Carbon Burial in the Proto-North Atlantic during Oceanic Anoxic Event 2. Earth and Planetary Science Letters, 228, 3–4: 465–82. https://doi.org/10.1016/j.epsl.2004.09.037.

Levitus, Boyer (2005), www.nodc.noaa.gov/WOA05: Levitus and Boyer's Annual salinity and temperature online maps.

Lewis, Brent L, and George W Luther III, (2000). “Processes Controlling the Distribution and Cycling of Manganese in the Oxygen Minimum Zone of the Arabian Sea.” Deep Sea Research Part II: Topical Studies in Oceanography 47 (7–8): 1541–61. https://doi.org/10.1016/S0967-0645(99)00153-8.

Lisiecki, Lorraine E., and Maureen E. Raymo, (2005). A Pliocene-Pleistocene Stack of 57 Globally Distributed Benthic $\delta^{18}O$ Records. Paleoceanography 20 (1): 1–17. https://doi.org/10.1029/2004PA001071.

Lutz, M., Dunbar, R., and Caldeira, K. (2002). Regional variability in the vertical flux of particulate organic carbon in the ocean interior, Global Biogeochemical Cycles, 16(3), 1037. https://doi.org/10.1029/2000GB001383.

Manjunatha B., and Shankar R, (1996). Signature of Non steadsy state diagenesis in continental shelf sediments. Esturaine, Coastal and Shelf Science 42 (3): 361-369. https://doi.org/10.1006/ecss.1996.0024

Martin, John H., and George a. Knauer, (1984). Manganese Transport through Oxygen Minima. Earth and Planetary Science Letters 67 (1): 35–47. https://doi.org/10.1016/0012-821X(84)90036-0.

McKay, Jennifer L., T. F. Pedersen, and J. Southon, (2005). Intensification of the Oxygen Minimum Zone in the Northeast Pacific off Vancouver Island during the Last Deglaciation: Ventilation and/or Export Production? Paleoceanography 20 (4): 1–13. https://doi.org/10.1029/2003PA000979

McLennan, S. M. (2001). Relationships between the Trace Element Composition of Sedimentary Rocks and Upper Continental Crust. Geochemistry, Geophysics, Geosystems 2 (4): 1–30. https://doi.org/10.1029/2000GC000109

Meyers, Philip A. (1997). Organic Geochemical Proxies of Paleoceanographic, Plaeolimnologic, and

Plaeoclimatic Processes. Organic Geochemistry 27 (5): 213–50. https://doi.org/http://dx.doi.org/10.1016/S0146-6380(97)00049-1

Miller, Gifford H., Aslaug Geirsdottir, Yafang Zhong, Darren J. Larsen, Bette L. Otto-Bliesner, Marika M. Holland, David A. Bailey, (2012). Abrupt Onset of the Little Ice Age Triggered by Volcanism and Sustained by Sea-Ice/Ocean Feedbacks. Geophysical Research Letters 39 (2): 1–5. https://doi.org/10.1029/2011GL050168.

Milliman, J.D., (2001). River inputs. Encyclopedia of Ocean Sciences, pp. 2419–2427.

Milliman, J.D., Syvitski, J., (1992). Geomorphic/tectonic control of sediment discharge of sediment discharge to ocean: the importance of small mountainous rivers. Journal of Geology 100, 525–544.

Morrison, J.M., Codispoti, L.A., Gaurin, S., Jones, B., Manghnani, V., Zheng, Z., (1998).Seasonal variation of hydrographic and nutrient fields during the US JGOFS Arabian Sea Process Study. Deep Sea Research Part II: Topical Studies in Oceanography 45, 2053–2101.

Mudelsee, Manfred, and Maureen E. Raymo, (2005). Slow Dynamics of the Northern Hemisphere Glaciation. Paleoceanography 20 (4): 1–14. https://doi.org/10.1029/2005PA001153

Murray, J.W., Keith Stewart, Steven Kassakian, Marta Krynytzky, and Doug Dijulio, (2005). Oxic, Suboxic, and Anoxic Conditions in the Black Sea. The Black Sea Flood Question: Changes in Coastline, Climate, and Human Settlement, 1–21. https://doi.org/10.1007/978-1-4020-5302-3_1

Murty ,(1992).,Hydrography and circulation in the northwestern Bay of Bengal during the retreat of southwest monsoon_Proc_Ind_Acad_Sc.

North Greenland Ice Core Project members, (2004). High-resolution record of Northern Hemisphere climate extending into the last interglacial period. Nature, 431, 147-151.

Narvekar, J., and Prasanna Kumar, S., (2014). Mixed layer variability and chlorophyllabiomass in the bay of bengal. Biogeosciences, 11(14), 3819–3843. https://doi.org/10.5194/bg-11-3819-2014

Naqvi, S.W.A., P.V. Narvekar & E. Desa. (2006). Coastal biogeochemical processes in the North Indian Ocean. In: A. Robinson and K. Brink, editors, The Sea, Vol. 14, Harvard University Press, pp. 723-780.

Naqvi, S. W. A., Bange, H. W., Farías, L., Monteiro, P. M. S., Scranton, M. I., and Zhang, J, (2010). Marine hypoxia/anoxia as a source of CH_4 and N_2O, Biogeosciences, 7, 2159-2190, https://doi.org/10.5194/bg-7-2159-2010.

Nishimura, Mitsugu, Tetsuya Matsunaka, Yoshimune Morita, Takahiro Watanabe, Toshio Nakamura, Liping Zhu, Fumiko Watanabe Nara, Akio Imai, Yasuhiro Izutsu, and Kazuya Hasuike (2014). Paleoclimatic Changes on the Southern Tibetan Plateau over the Past 19,000years Recorded in Lake Pumoyum Co, and Their Implications for the Southwest Monsoon Evolution. Palaeogeography, Palaeoclimatology, Palaeoecology 396: 75–92. https://doi.org/10.1016/j.palaeo.2013.12.015

Nürnberg, Dirk, Jelle Bijma, and Christoph Hemleben, (1996). Assessing the Reliability of Magnesium in Foraminiferal Calcite as a Proxy for Water Mass Temperatures. Geochimica et Cosmochimica Acta 60 (5): 803–14. https://doi.org/10.1016/0016-7037(95)00446-7

Officer, C. B., R. B. Biggs, J. L. Taft, L. E. Cronin, M. A. Tyler, and W. R. Boynton,(1984). Chesapeake Bay Anoxia: Origin, Development, and Significance. Science 223 (4631): 22–27. https://doi.org/10.1126/science.223.4631.22

Olson, D B, G L Hitchcock, R A Fine, and B A Warren(1993). Maintenance of the Low Oxygen Layer in the Central Arabian Sea. Deep Sea Research Part II: Topical Studies in Oceanography 40 (3): 673–86. https://doi.org/10.1016/0967-0645(93)90051-N

Overpeck, Jonathan, David Anderson, Susan Trumbore, and Warren Prell,(1996). The Southwest Indian Monsoon over the Last 18000 Years. Climate Dynamics 12: 213–25. https://doi.org/10.1007/BF00211619

Owen, Robert M, Gerald R Dickens, (1994). Late Miocene-Early Pliocene mangenese redirection in the central Indian ocean: Expansion of intermediate water oxygen minimum zone. Paleoceanography, 9, 169-181

P. M. Grootes, M. Stuiver, J. W. C. White, S. Johnsen & J. Jouzel, (1993). Comparison of oxygen isotpe records from the GSIP2 and GRIP Greenland ice cores. Nature 366: 552–554.

Pattan, J. N., G. Parthiban, Anita Garg, and N. R.Cesar Moraes,(2017). Intense Reducing Conditions during the Last Deglaciation and Heinrich Events (H1, H2, H3) in Sediments from the Oxygen Minimum Zone off Goa, Eastern Arabian Sea. Marine and Petroleum Geology 84: 243–56. https://doi.org/10.1016/j.marpetgeo.2017.03.034

Paulmier, A., and D. Ruiz-Pino, (2009).Oxygen Minimum Zones (OMZs) in the Modern Ocean.Progress in Oceanography 80 (3–4): 113–28. https://doi.org/10.1016/j.pocean.2008.08.001

Paulmier, a., D. Ruiz-Pino, and V. Garcon, 2010. CO_2 Maximum in the Oxygen Minimum Zone (OMZ). Biogeosciences Discussions 7 (4): 6353–85. https://doi.org/10.5194/bgd-7-6353-2010

Pedersen, T. F., and N. B. Price, 1982. The Geochemistry of Manganese Carbonate in Panama Basin Sediments. Geochimica et Cosmochimica Acta 46 (1): 59–68. https://doi.org/10.1016/0016-7037(82)90290-3

Piotrowski, a.M., a. Galy, J.a.L. Nicholl, N. Roberts, D.J. Wilson, J.a. Clegg, and J. Yu. 2012. Reconstructing Deglacial North and South Atlantic Deep Water Sourcing Using Foraminiferal Nd Isotopes. Earth and Planetary Science Letters 357–358: 289–97. https://doi.org/10.1016/j.epsl.2012.09.036

Piotrowski, Alexander M., Steven L. Goldstein, Sidney R. Hemming, and Richard G. Fairbanks. (2004). Intensification and Variability of Ocean Thermohaline Circulation through the Last Deglaciation. Earth and Planetary Science Letters 225 (1–2): 205–20 https://doi.org/10.1016/j.epsl.2004.06.002

Piotrowski, Alexander M., Virupaxa K. Banakar, Adam E. Scrivner, Henry Elderfield, Albert Galy, and Aileen Dennis, (2009). Indian Ocean Circulation and Productivity during the Last Glacial Cycle. Earth and Planetary Science Letters,285 (1–2): 179–89. https://doi.org/10.1016/j.epsl.2009.06.007

Prasad, T. G., (1997)., Evaporation-Precipitation-Tropical Ind Ocean. Current science.

Punyu, V.R.; Banakar, V.K.; Garg, A. (2014) Equatorial Indian Ocean productivity during the last 33 kyr and possible linkage to Westerly Jet variability. Marine Geology, vol.348; 2014; 44-51. https://doi.org/10.1016/j.margeo.2013.11.010.

Rad, Ulrich Von, Hartmut Schulz, Volkher Riech, Maryke Den Dulk, Ulrich Berner, and Frank Sirocko, 1999. Multiple Monsoon-Controlled Breakdown of Oxygen-Minimum Conditions during the Past 30,000 Years Documented in Laminated Sediments off Pakistan. Palaeogeography, Palaeoclimatology, Palaeoecology 152 (1–2): 129–61. https://doi.org/10.1016/S0031-0182(99)00042-5.

Redfield, A.C. (1942). The processes determining the concentration of oxygen, phosphate, and other organic derivatives within the depths of the Atlantic Ocean Pap. Phys. Oceanogr. Meteorol. Volume 9, Issue 2, Pages 1-22.

Rahmstorf, S. 2002. Ocean Circulation and Climate during the Past 120,000 Years. Nature 419: 207–14. https://doi.org/10.1038/nature01090

Rajendran, A, M D Kumar, and J F Bakker, 1992. Control of Manganese and Iron in Skagerrak Sediments (Norheastern North Sea). Chemical Geology 98: 111–29.

Ramaiah, N., Fernandes, V., Paul, J. T., Jyothibabu, R., Mangesh, G., and Jayraj, E. A., (2010). Seasonal variability in biological carbon biomass standing stocks and production in the surface layers of the Bay of Bengal. Indian Journal of Marine Sciences, 39(3), 369–379.

Ramaiah, N., Fernandes, V., Paul, J. T., Jyothibabu, R., Mangesh, G., and Jayraj, E. A., (2010b). Seasonal variability in biological carbon biomass standing stocks and production in the surface layers of the Bay of Bengal. Indian Journal of Marine Sciences, 39(3), 369–379.

Rao, C. K., Naqvi, S. W. a., Kumar, M. D., Varaprasad, S. J. D., Jayakumar, D. a., George, M. D., and Singbal, S. Y. S. (1994). Hydrochemistry of the Bay of Bengal: possible reasons for a different water-column cycling of carbon and nitrogen from the Arabian Sea. Marine Chemistry, 47(3–4), 279–290. https://doi.org/10.1016/0304-4203(94)90026-4

Rashid, H, E England, L Thompson, and L Polyak. (2011). Late Glacial to Holocene Indian Summer Monsoon Variability Based upon Sediment. Terrestrail Atmosphere Ocean Sciences 22 (2): 215–28. https://doi.org/10.3319/TAO.2010.09.17.02(TibXS)1

Rashid, H., B. P. Flower, R. Z. Poore, and T. M. Quinn. (2007). A ~25 Ka Indian Ocean Monsoon Variability Record from the Andaman Sea. Quaternary Science Reviews 26 (19–21): 2586–97. https://doi.org/10.1016/j.quascirev.2007.07.002

Reichart, G J, L J Lourens, and W J Zachariasse, 1998. Temporal Variability in the Northern Arabian Sea Oxygen Minimum Zone (OMZ) during the Last 225,000 Years Paleoceanography 13 (6): 607–21.

Resplandy, L., M. Lévy, L. Bopp, V. Echevin, S. Pous, V. V. S. S. Sarma, and D. Kumar. 2012. Controlling Factors of the Oxygen Balance in the Arabian Sea's OMZ. Biogeosciences 9 (12): 5095–5109. https://doi.org/10.5194/bg-9-5095-2012

Roberson, A. L., J. Roadt, I. Halevy, and J. F. Kasting, (2011). Greenhouse Warming by Nitrous Oxide and Methane in the Proterozoic Eon. Geobiology 9 (4): 313–20. https://doi.org/10.1111/j.1472-4669.2011.00286.x

Rogers, Alex D, (2000). The Role of the Oceanic Oxygen Minima in Generating Biodiversity in the Deep Sea. Deep Sea Research Part II: Topical Studies in Oceanography 47 (1–2): 119–48. https://doi.org/10.1016/S0967-0645(99)00107-1

Ronald P. Kiene , Timothy S. Bates, (1990). Biological Removal of Dimethyl Sulphide from Sea Water. Nature 345: 702–5. https://doi.org/10.1017/CBO9781107415324.004.

Rudnick, R.L. and Gao, S. (2003) The Composition of the Continental Crust. In: Holland, H.D. and Turekian, K.K., Eds., Treatise on Geochemistry, Vol. 3, The Crust, Elsevier-Pergamon, Oxford, 1-64. http://dx.doi.org/10.1016/b0-08-043751-6/03016-4

Rutberg, Randye L, Sidney R Hemming, and Steven L Goldstein,(2000). Reduced North Atlantic Deep Water Flux to the Glacial Southern Ocean Inferred from Neodymium Isotope Ratios Nature 405 :935–38.

S N Murthy, Y V B Sarma, D P Rao, C S Murthy V. Water Charateristics, Mixing, Circulation in the Bay of Bengal during South West Monsoon.

Salzmann, Ulrich, Mark Williams, Alan M. Haywood, Andrew L.A. Johnson, Sev Kender, and Jan Zalasiewicz, (2011). Climate and Environment of a Pliocene Warm World. Palaeogeography, Palaeoclimatology, Palaeoecology 309 (1–2): 1–8. https://doi.org/10.1016/j.palaeo.2011.05.044

Sardessai, S., Ramaiah, N., Kumar, S. P., and de Sousa, S. N. (2007). Influence of environmental forcings on the seasonality of dissolved oxygen and nutrients in the Bay of Bengal. Journal of Marine Research, 65, 301–316.

Sarma, V V S S, (2002). An Evaluation of Physical and Biogeochemical Processes Regulating the Oxygen Minimum Zone in the Water Column of the Bay of Bengal Global biogeochemical cycles 16 (4): 1099–1010. https://doi.org/10.1029/2002GB001920.

Sarma, V. V. S.S . (2002). An evaluation of physical and biogeochemical processes regulating perennial suboxic conditions in the water column of the Arabian Sea. Global Biogeochemical Cycles, 16(4), 1082. https://doi.org/10.1029/2001GB001461

Sarma, V. V S S, B. Sridevi, K. Maneesha, T. Sridevi, S. A. Naidu, V. R. Prasad, V. Venkataramana, et al. 2013. "Impact of Atmospheric and Physical Forcings on Biogeochemical Cycling of Dissolved Oxygen and Nutrients in the Coastal Bay of Bengal." Journal of Oceanography 69 (2): 229–43. https://doi.org/10.1007/s10872-012-0168-y

Sarma, V. V. S. S., and Aswanikumar, V. (1991). VVSarma- Subsurface Chlorphyll Maxima In The North-Western Bob.pdf. Journal of Plankton Research. Oxford University Press.

Sarma, V.V.S.S., and V Aswanikumar. 1991. "VVSarma- Subsurface Chlorphyll Maxima In The North-Western Bob.Pdf." Journal of Plankton Research. Oxford University Press.

Schulte, Sonja, Frauke Rostek, Edouard Bard, Jürgen Rullkötter, and Olivier Marchal, (1999). Variations of Oxygen-Minimum and Primary Productivity Recorded in Sediments of the Arabian Sea. Earth and Planetary Science Letters 173 (3): 205–21. https://doi.org/10.1016/S0012-821X(99)00232-0

Schulz, Hartmut, Ulrich van Rad, and Helmut Erlenkeuser. (1998). "Correlation between Arabian Sea and Greenland Climate Oscillations of the Past 110,000 Years." Nature 393 (May): 54–57. https://doi.org/10.1038/31750

Selvaraj, K., V. Ram Mohan, and Piotr Szefer. (2004). "Evaluation of Metal Contamination in Coastal Sediments of the Bay of Bengal, India: Geochemical and Statistical Approaches." Marine Pollution Bulletin 49 (3): 174–85. https://doi.org/10.1016/j.marpolbul.2004.02.006

Sengupta, D., and N, B. R. G. (2006). Surface freshwater from Bay of Bengal runoff and Indonesian throughflow in the tropical Indian Ocean ., 1–7.

Sengupta, S, Anant Parekh, S Chakraborty, K Ravi Kumar, and T Bose. (2013). Vertical Variation of Oxygen Isotope in Bay of Bengal and Its Relationships with Water Masses 118: 6411–24. https://doi.org/10.1002/2013JC008973

Sengupta, S., Parekh, A., Chakraborty, S., Kumar, K. R., and Bose, T. (2013). Vertical variation of oxygen isotope in Bay of Bengal and its relationships with water masses, 118(October), 6411–6424. https://doi.org/10.1002/2013JC008973

Shackleton, N J, 1987. Oxtgen isotopes, Ice volume and Sea level.Quaternary Science 6: 183–90. https://doi.org/10.1016/0277-3791(87)90003-5.

Shackleton, N. J., M. A. Hall, and E. Vincent, (2000), Phase relationships between millennial-scale events 64,000–24,000 years ago, Paleoceanography, 15(6), 565–569, doi: 10.1029/2000PA000513

Shankar, D., P. N. Vinayachandran, and A. S. Unnikrishnan. 2002. The Monsoon Currents in the North Indian Ocean. Progress in Oceanography 52 (1): 63–120. https://doi.org/10.1016/S0079-6611(02)00024-1

Shankar, D., Vinayachandran, P. N., and Unnikrishnan, A. S. (2002). The monsoon currents in the north Indian Ocean. Progress in Oceanography, 52(1), 63–120. https://doi.org/10.1016/S0079-6611(02)00024-1.

Shankar, D., Shenoi S.S.C., Nayak, R.K., Vinayachandran, P.N., Nampoothiri, G., Almeida, A.M., Michael, G.S., Kumar, M.R., Sundar, D., Sreejith, O.P. (2005) Hydrography of the eastern Arabian Sea during summer monsoon 2002. J Earth Syst Sci 114:459–474. doi:10.1007/BF02702023.

Shenoi S.S.C, Shetye S.R, Gouveia A.D, Michael G.S., (1993) Salinityextrema in the Arabian Sea. In: Ittekkot V, Nair RR (eds) Monsoon biogeochemistry, Mitteilungen des Geologisch-Paläontologischen Instituts der Universität Hamburg, University of Hamburg, Germany, pp 37–49.

Shenoi, S. S. C. (2002). Differences in heat budgets of the near-surface Arabian Sea and Bay of Bengal: Implications for the summer monsoon. Journal of Geophysical Research, 107(C6), 1–14. https://doi.org/10.1029/2000JC000679

Shetye, S.R., A. D. Gouveia, S.S.C. Shenoi, D. Sundar, G. S. Michael, and G. Nampoothiri. (1993). The Westen Boundary Current of the Seasoanal Subtropical Gyre in the Bay of Bengal. Journal of Geophysical Research 98: 945–54.

Shetye, S.R., Gouveia, A.D., Shenoi S.S.C., (1994) Circulation and water masses of the Arabian Sea. Proc Indian Acad Sci (Earth Planet Sci) 103:107–123. doi:10.1007/BF02839532 (special issue: Biogeochemistry of the Arabian Sea).

Shibahara, Akihiko, Ken'ichi Ohkushi, James P. Kennett, and Ken Ikehara. (2007). Late Quaternary Changes in Intermediate Water Oxygenation and Oxygen Minimum Zone, Northern Japan: A Benthic Foraminiferal Perspective. Paleoceanography 22 (3): 1–13. https://doi.org/10.1029/2005PA001234

Sijinkumar, A. V., Clemens, S., Nath, B. N., Prell, W., Benshila, R., and Lengaigne, M. (2016). δ18O and salinity variability from the Last Glacial Maximum to Recent in the Bay of Bengal and Andaman Sea. Quaternary Science Reviews, 135, 79–91. https://doi.org/10.1016/j.quascirev.2016.01.022

Sinha, Ashish, Kevin G. Cannariato, Lowell D. Stott, Hong Chun Li, Chen Feng You, Hai

Sverdrup HU, Johnson MW, Fleming RH. (1942), The water masses and currents of the oceans. The oceans their physics, chemistry, and general biology. Prentice-Hall, New York, pp 605–761

Staubwasser, M., F. Sirocko, P. M. Grootes, and M. Segl. (2003). Climate Change at the 4.2 Ka BP Termination of the Indus Valley Civilization and Holocene South Asian Monsoon Variability.Geophysical Research Letters 30 (8): 3–6. https://doi.org/10.1029/2002GL016822

Stramma, Lothar, Eric D Prince, Sunke Schmidtko, Jiangang Luo, John P Hoolihan, Martin Visbeck, Douglas W R Wallace, Peter Brandt, and Arne Körtzinger,2012. Expansion of Oxygen Minimum Zones May Reduce Available Habitat for Tropical Pelagic Fishes,Nature Climate change 2: 33-37. https://doi.org/10.1038/NCLIMATE1304

Stramma, Lothar, Gregory C. Johnson, Janet Sprintall, and Volker Mohrholz. 2008. Expanding Oxygen-Minimum Zones in the Tropical Oceans Science , 320, 655-658. https://doi.org/10.1126/science.1153847

Stramma, Lothar, Sunke Schmidtko, Lisa A. Levin, and Gregory C. Johnson, 2010. Ocean Oxygen Minima Expansions and Their Biological Impacts. Deep-Sea Research Part I: Oceanographic Research Papers 57 (4): 587–95. https://doi.org/10.1016/j.dsr.2010.01.005.

Subramanian, V. (1993). Subramanian, 1993, Sediment Load-Ind Rivers.pdf. Current Science.

Subramanian, V., L. Van 't Dack, and R. Van Grieken. 1985. "Chemical Composition of River Sediments from the Indian Sub-Continent." Chemical Geology 48 (1–4): 271–79. https://doi.org/10.1016/0009-2541(85)90052-X.

Tamburini, F., Fo¨ llmi, K. B., Adatte, T., Bernasconi, S. M., Steinmenn, F., (2003). Sedimentary phosphorus records from the Oman Margin: new evidence of high productivity during glacial periods. Paleoceanography 18, 15-1– 15-14.

Thomson, J, N C Higgs, I Jarvis, D J Hydes, S Colley, and T R S Wilson, (1986). The Behavior of Manganese in Atlanic Carbonate Sediments. Geochimica et Cosmochimica Acta 50 (i): 1807–18.

Thomson, J, N C Higgs, I Jarvis, D J Hydes, S Colley, and T R S Wilson. 1986. The Behavior of Manganese in Atlanic Carbonate Sediments. Geochimica et Cosmochimica Acta 50 (i): 1807–18.

Tribovillard, Nicolas, Thomas J Algeo, Timothy Lyons, and Armelle Riboulleau, (2006). Trace Metals as Paleoredox and Paleoproductivity Proxies: An Update. Chemical Geology 232 (1–2): 12–32. https://doi.org/10.1016/j.chemgeo.2006.02.012.

Tripathy, G. R., Singh, S. K., and Ramaswamy, V. (2014). Major and trace element geochemistry of Bay of Bengal sediments: Implications to provenances and their controlling factors. Palaeogeography, Palaeoclimatology, Palaeoecology, 397, 20–30. https://doi.org/10.1016/j.palaeo.2013.04.012

Tyson, R. V., and T. H. Pearson, 1991. Modern and Ancient Continental Shelf Anoxia: An Overview. Geological Society, London, Special Publications 58 (58): 1–24. https://doi.org/10.1144/GSL.SP.1991.058.01.01

Ulloa, Osvaldo, Donald E Canfield, Edward F DeLong, Ricardo M Letelier, and Frank J Stewart, (2012). Microbial Oceanography of Anoxic Oxygen Minimum Zones. Proceedings of the National Academy of Sciences of the United States of America 109 (40): 15996–3. https://doi.org/10.1073/pnas.1205009109

Vinayachandran, P N, D Shankar, Siddharth Vernekar, and K K Sandeep. (2013). "A Summer Monsoon Pump to Keep the Bay of Bengal" 40.

Vinayachandran, P. N., Murty, V. S. N., and Ramesh Babu, V. (2002). Observations of barrier layer formation in the Bay of Bengal during summer monsoon. Journal of Geophysical Research: Oceans, 107(C12), SRF 19-1-SRF 19-9. https://doi.org/10.1029/2001JC000831

Vinayachandran, P. N., Shankar, D., Vernekar, S., and Sandeep, K. K. (2013). A summer monsoon pump to keep the Bay of Bengal, 40.

Vinayachandran, P. N., V. S. N. Murty, and V. Ramesh Babu. (2002). Observations of Barrier Layer Formation in the Bay of Bengal during Summer Monsoon. Journal of Geophysical Research: Oceans 107 (C12): SRF 19-1-SRF 19-9. https://doi.org/10.1029/2001JC000831

W. Dansgaard, S. J. Johnsen, H. B. Clausen, D. Dahl-Jensen, N. S. Gundestrup, C. U. Hammer, C. S.

Hvidberg, J. P. Steffensen, A. E. Sveinbjörnsdottir, J. Jouzel & G. Bond, Motohiro; Sonoda, and Naoto Chatani, 1993. Nature 366: 529–31.

Wang, Y. J. 2001. "A High-Resolution Absolute-Dated Late Pleistocene Monsoon Record from Hulu Cave, China." Science 294 (5550): 2345–48. https://doi.org/10.1126/science.1064618

Weijden, Cornelis H. van der, Gert Jan Reichart, and Hendrik Jan Visser, (1999). Enhanced Preservation of Organic Matter in Sediments Deposited within the Oxygen Minimum Zone in the Northeastern Arabian Sea. Deep Sea Research Part I: Oceanographic Research Papers 46 (5): 807–30. https://doi.org/10.1016/S0967-0637(98)00093-4

Wilde, Simon A., John W. Valley, William H. Peck, and Colin M. Graham, (2001). Evidence from Detrital Zircons for the Existence of Continental Crust and Oceans on the Earth 4.4 Gyr Ago. Nature 409 (6817): 175–78. https://doi.org/10.1038/35051550

Wilson, David J., Alexander M. Piotrowski, Albert Galy, and Josephine A. Clegg. 2013. Reactivity of Neodymium Carriers in Deep Sea Sediments: Implications for Boundary Exchange and Paleoceanography. Geochimica et Cosmochimica Acta 109. 197–221. https://doi.org/10.1016/j.gca.2013.01.042.

World Ocean Atlas, 2009 (www.nodc.noaa.gov)

Wyrtki, K., Oceanographic Atlas of the International Indian Ocean Expedition. National Science Foundation, Washington, D.C., pp. 531 (1971).

You Y, Tomczak M (1993). Thermocline circulation and ventilation in the Indian Ocean derived from water mass analysis. Deep-Sea Research Part I 40:13–56. doi:10.1016/0967-0637(93)90052-5

Young, Grant M, 2013. Precambrian Supercontinents, Glaciations, Atmospheric Oxygenation, Metazoan Evolution and an Impact That May Have Changed the Second Half of Earth History. Geoscience Frontiers 4 (3): 247–61. https://doi.org/10.1016/j.gsf.2012.07.003.

Zumft, W.G., 1997. Cell biology and molecular basis of denitrification. Microbiology and Molecular Biology Reviews 61, 533–616.

*****